UNIVERSITY OF PAVIA

Department of Brain and Behavioral Sciences

PhD in Biomedical Sciences - XXIX

Isolation and characterization of several Extracellular Vesicles Subtypes in Amyotrophic Lateral Sclerosis

Tutor :
Prof. Ceroni Mauro

Supervisor:
Dott.ssa Cristina Cereda

Ph.D
La Salvia Sabrina
Academic Year 2015/2016

Table of content

Aim of the work

Materials and methods

Results and Discussions

1. Extracellular Vesicles isolation and characterization

    1.1 Nanoparticle Tracking Analysis (NTA) confirmed extracellular vesicles dimensions
    1.2 MVs and EXOs markers confirmation by Western blot analysis
    1.3 qNano Analysis

2. Characterization of microvesicles by flow cytometry analysis

    2.1 Polystyrene/latex beads setting up and determination of positivity
    2.2 Higher levels of CD45 MVs in plasma of amyotrophic lateral sclerosis patients
    2.3 Imaging flow cytometry to compare two different dyes in Extracellular Vesicles
    2.4 Phenotyping immune Microvesicles by Imaging flow cytometry

3. Recognition of SOD1, TDP43 and FUS protein level in plasma derived MVs and EXOs from ALS patients

    3.1 Misfolded SOD1 protein level is higher in plasma derived MVs of ALS patients compared to healthy controls
    3.2 Misfolded SOD1 in CD45 + MVs distinguishes slow progression patients with high levels of plasma derived CD45 MVs

Conclusions
References

INTRODUCTION

1. AMYOTROPHIC LATERAL SCLEROSIS

Amyotrophic lateral sclerosis (ALS) is an adult onset, rapidly progressive neurodegenerative disorder, caused by the selective loss of upper and lower motor neurons in the cerebral cortex, brainstem and spinal cord. Neuronal degeneration leads to weakness, muscular atrophy, and spasticity that evolve to paralysis; the disease is fatal within 3-5 years of onset, generally due to respiratory failure[1]. The features of ALS were first described as a clinic-pathological entity by the French neurologist Jean Martin Charcot in 1862. "Amyotrophic" refers to the atrophy of muscle fibers, which are denervated as their corresponding anterior horn cells degenerate, leading to weakness of affected muscles and visible fasciculation[2]."Lateral sclerosis" refers to hardening of the anterior and lateral cortico-spinal tracts as motor neurons degenerate in these areas and are replaced by gliosis. ALS has recently been recognized as a multi-system disorder rather than a disease limited to motor neurons. Some ALS patients may show extrapyramidal features such as tremor, rigidity, propulsion, and impaired postural reflexes. In about one quarter of ALS patients, the disease is associated with subtle cognitive deficits. In addition, 3–5% of ALS patients are diagnosed with frontotemporal dementia (FTD), a dementia of non-Alzheimer's type with symptoms of behavioral changes, frontal executive deficit, and impaired handling of language[3].The pathological hallmark of ALS is denervation and atrophy of muscle due to loss of spinal motor neurons **(Figure 1)**.Swelling of the perikarya and proximal axons is also observed, as the accumulation of phosphorylated neurofilaments, Bunina bodies and Lewy body-like inclusions, and the deposition of inclusions of ubiquitinated material in these axons[4].

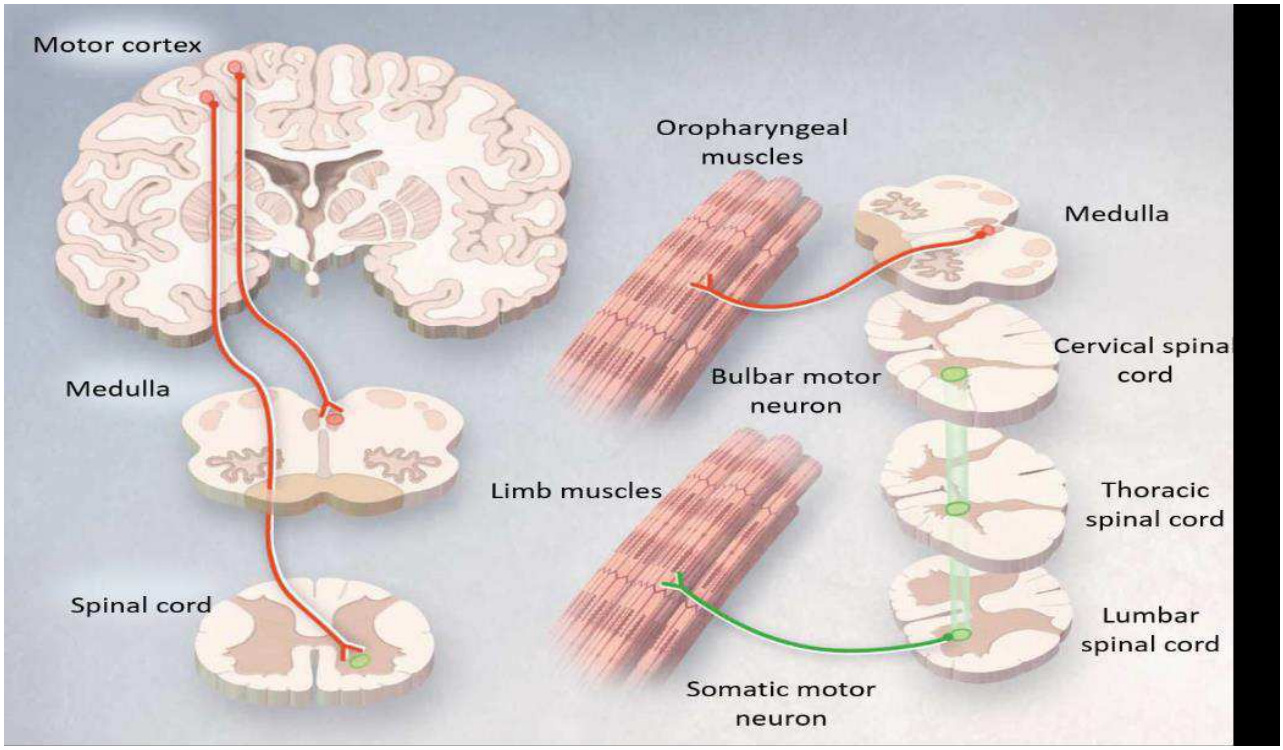

Figure 1. Degeneration of motor neurons in the motor cortex and degeneration of motor neurons in the brain stem and spinal cord selectively affected in ALS patients[5].

In addition, the activation and proliferation of astrocytes and microglia are also common in ALS. Unfortunately, there is no primary therapy for this disorder and the Riluzole, a presumed glutamate antagonist, is the only drug approved by the US Food and Drug Administration for the treatment of ALS, but the exact mechanism of action of Riluzole is as still unclear. It appears to prolong ALS survival by a few months on average, although when given at an early stage or to younger patients, it might prove more effective[3]. Symptomatic measures (for example, feeding tube and respiratory support) are the mainstay of management of this disorder[1].

1.1 Epidemiology

The incidence of sporadic ALS shows little variation in the Western countries, ranging from 1 to 2 per 100,000 person-years, with an estimated lifetime risk of 1 in 400. ALS is rare before the age of 40 years and increases exponentially with age thereafter. Mean age at onset is 58–63 years for sporadic ALS and 40–60 years for familial ALS, with a peak incidence in those aged 70–79 years. Men have a higher risk of ALS than women, leading to a male-to-female ratio of 1.2–1.5[6–8]. During recent decades, an increasing incidence of or mortality from ALS has been reported in Sweden, Finland, Norway, France, and the USA[3]. Geographic foci of the Western Pacific form of ALS, mainly in Guam and the Kii Peninsula of Honshu Island, Japan, have been reported, with prevalence 50–100 times higher than in other parts of the world. This form of ALS presents in three clinical forms, i.e., ALS, atypical Parkinsonism with dementia, and dementia alone, known collectively as the ALS-Parkinson's dementia complex (ALS-PDC). The cause of these aggregations remains elusive, and a decreasing prevalence of ALS-PDC was described recently[3].

1.2 fALS and sALS

ALS can occur sporadically, without any family history (sALS; 90-95% of patients), while a small percentage of ALS cases are considered familial (fALS; 5-10%). It can be inherited either as an autosomal dominant or recessive trait. Adult onset autosomal dominant inheritance is more common than juvenile onset caused by recessive transmission. X-linked dominant inherited ALS has been reported in one family[9]. Thanks to increased genome wide sequencing projects, more mutations have been discovered, adding more heterogeneity to the disease mechanisms. Among the genes reported in ALS pedigrees, there is strong evidence supporting a pathogenic role for the Cu / Zn superoxide dismutase 1 (SOD1) present in 20% of cases, trans active response DNA-binding protein of 43 kDa (TARDBP) in 3% of cases, fused in sarcoma (FUS) in 5% of cases and a newly identified hexanucleotide repeat expansion in chromosome 9 open reading frame 72 (c9ORF72) in 38 % of cases[10]. Gene mutations cause motor neuron death through different pathways: SOD1 mutations lead to oxidative stress; TARDBP, FUS and c9ORF72 induce disturbances in RNA machinery because their principal physiological functions include RNA processing, such as splicing, transport, and translation[11]. A single mutation can lead to different clinical presentations, suggesting that varying mechanisms influence outcome, and similar ALS phenotypes result from different mutations, implying that ALS is a syndrome of different causes that share similar pathophysiological pathways[11].

A genetic component is also thought to contribute to the pathogenesis of sporadic ALS, which accounts for the majority of ALS cases. A number of observations suggest a role for genetic factors in sALS. A meta-analysis of three twin studies gives an estimate of sALS heritability of 0.61 (95% CI 0.38–0.78)[12]. However, identification of gene defects in sALS cases has met with limited success so far. Several groups have reported on gene variants and association studies found in individuals with sporadic ALS. These studies linked sALS to particular genetic variants account for a small number of the total cases reflecting a complex pattern of inheritance with very low penetrance, a high degree of heterogeneity and/or the existence of environmental factors predisposing to ALS[13]. ALS is relentlessly progressive, as motor neuron injury gradually spreads. Most patients with ALS die within 3 to 5 years after symptom onset, but the variability in clinical disease duration is large, with some patients dying within months after onset and others surviving for more than two decades. Large differences in survival and age at disease onset exist even between individuals from one family, in whom ALS is caused by exactly the same mutation, suggesting the existence of otherfactors that modify the phenotype[1]. The clinical expressions of sporadic and familial ALS are very similar. Although ALS patients show some degree of heterogeneity as far as symptoms, age of onset, and disease duration are concerned, fALS cases are indistinguishable from sALS based on clinical and pathologic criteria. Thus, family history and genetics are the primary factors that discriminate between sALS and fALS. In the absence of family history, an early age of onset, atypical rapid or slow disease progression, pure lower motor neuron presentation or the presence of dementia may alert to a familial etiology[14]. All genes found mutated in fALS cases may also be mutated in sALS and first-degree relatives of patients with sALS have an increased risk of ALS and other neurodegenerative diseases[15]. Similar superoxide dismutase 1 (SOD1)-positive and TAR DNA-binding protein 43 (TDP43)-positive inclusions have been found in sALS and fALS[16,17].

2. NEUROINFLAMMATORY RESPONSE IN CNS

Neuroinflammation is a common traitof theneurodegenerative diseases such as Alzheimer's disease (AD), Parkinson's disease (PD), and Amyotrophic lateral sclerosis (ALS).It is common to observe an activation and proliferation of microglia in the neuronal environment defined microgliosi, and also an infiltration of T lymphocytes in the CNS site of degeneration; often this characteristic was regarded as a consequence of neuronal damage[18] but in these last years[19], it has increasingly been associated a potentially protective microglial’s role resulting in a increased neuronal survival.The release of specific molecules and microvesicles in the microenvironment may unbalance the microglia towards a phenotype rather than another influencing the inflammatory response as much as unregulated activated lymphocytes in the neural microenvironment.

2.1 CNS Resident Macrophages: Microglia

Microglia is present in nerve tissue permanently and is distributed in a different manner anatomically: perivascular macrophages they are located between the basal lamina of blood vessels and meningeal macrophages are located within the leptomeninges.

This "resting" form of microglia is composed of long branching processes and a small cellular bodyand in this form the long processes are able to occupy the entire space surrounding neuronsand check the entire area in order to discern the dangerous antigens presence. Microglia is characterized by a morphological change that is manifested in the retraction of the processes and a hypertrophy of

the body conversely activated microglia. Once activated microglia can show two different phenotype: proinflammatory phenotype is known as M1 activated microglia (classically) and it isusually released interleukin-(IL-) 1β, tumor necrosis factor α (TNF-α) and they are accompanied by an increase of reactive oxygen species,increase the expression of the enzyme NADPH and nitric oxide through upregulated expression of inducible nitric oxide synthase (iNOS). Lipopolysaccharide (LPS) is a potent stimulant of the phenotype M1, and it was observed that in cultured microglia thus active along with neurons leads to ROS and NO increased and a high increasing level of glutamate with consequences on neuronal survival[20]. Contrariwise inflammatory phenotype is called as M2 activated microglia (alternatively) in which it can be observed a rise of inflammatory cytokines such as interleukin-10 (IL-10) and a relative release of neurotrophic factors such as insulin-like growth factor-1 (IGF-1) and brain-derived neurotrophic factor (BDNF)resulting in a decrease in inflammation **(Table1)**.

	M1	M2
Cytokines Released	TNF- α; IL-1β;IL-6;IL-12;IL-23	IL-10;IL-4;IL-13;TGF- β
Arginine Metabolism	iNos → NO	Arginase→L-Ornithine
Other mediators	NO;ROS	Neurotrophics (GDNF,IGF-1)
Antigenicity	IL-1R,CCR7	IL-1Ra;CD150,CD14;CD163

Table 1. Phenotype Microglia classification based on antigenicity,cytokine,arginine metabolism, other released mediators

2.2 T lymphocyte cells

T cells are the protagonists of the adaptive response and can be classified based on the expression of surface molecules.Cytotoxic T cells (CTLs) express CD8 and induce apoptosis through the release of perforin,granzymes and exposure of Fas ligand; indeed Fas Ligand (CD95L) binds the receptor Fas (CD95) on host cells and leads to the activation of caspases and perforin causes pores in the membrane allowing granzymes to enter the host cell and act in it[21]. CD4 + T cells are known as helper T cells (Th) and it can be distinguished according to the cytokines that are released into the environment and the main function is to regulate the activity of other cells during the immune response, such as the microglia and macrophages**(Table2)**.

	Antigenicity	Cytokine profile	Effector function
Th1	CD4+	IL-2,	M1 macrophage activation
Th2	CD4+	IL-4, IL-10, IL-6, IL-13	Downregulation of M1 macrophage activation
Th17	CD4+	IL-17	M1 macrophage activation
Treg	CD4+CD25+FoxP3+	IL-4, IL-10, TGF-β	Damping of proinflammatory response
CTL	CD8+	TNF-α, IFN-γ	Elimination of infected cells

Table 2. Classification of T cell into subsets according to antigenicity,cytokine profile and effector function

For example, Th1 and Th17 through the release of their pro-inflammatory cytokines such as IL-2 and IL-17 can lead to M1microglial phenotype whereas Th2 cells releasing eg IL-4 (anti-inflammatory cytokine) can move to the M2 microglial phenotype[22]. Regulatory T cells (Tregs) are characterized by theexpression of CD4, CD25, CD62L, CD103, CD152, and by transcription factor FoxP3 and for each adaptive response is a specific level of cell regulation by Treg[22].

Extracellular vesicles are implied both in promoting and in inhibiting the immune response, depending on their cell of origin and on the signals present in the microenvironment. The effect of EVs on T cells was investigated by Mokarizadeh[23] in a rodent model in which EVs isolated from murine BM-SCs inhibited the proliferation of both syngenic and allogenic T lymphocytes. Additionally, they demonstrated that these microparticles were able to induce apoptosis in activated T cells and this inhibition was associated with an increased proportion of regulatory T CD4+/CD25+/FoxP3+cells. Extracellular vesicles secreted by DCs can either promote or inhibit immune response depending on the degree of maturation of their parent cells for instance EVs produced by mature DCs carry both antigenic material, MHC-peptide complexes, co-stimulatory molecules required for the initiation of immune responses by APCs[24].

3. PATHOGENESIS OF MOTOR NEURONS DEGENERATION IN ALS

The exact molecular pathway causing motor neuron degeneration in ALS is still unknown, but as with other neurodegenerative diseases, is likely to be a complex interplay between multiple pathogenic cellular mechanisms which may not be mutually exclusive[25,26]including indeed different factors. Despite this, sporadic and familial ALS are clinically and pathologically similar, suggesting a common pathogenesis. First of all ALS, appearing as a multisystemic disease, is based on the involvement of different tissues and cell typesaside from motor neuron, such as astrocytes,microglia, oligodendrocytes and muscles cells, among others, that are both targeted by the disease processes and actively participate to the final disease outcome[1]. Second, a number of genes have been identified so far that are definitely associated to ALS pathogenesis and that now cover a large fraction of the familial cases of the disease[27]. According to their known biological role, or to new acquired functions, because of gene mutations, they are apparently connected to different physiological processes, implying that diverse pathogenic mechanisms, not necessarily related, might be involved in ALS onset and progression. Cellular biological studies over the last two decades have led to the development of multiple interconnected pathogenic themes in ALS. Glutamate-mediated neurotoxicity is called excitotoxicity and has been considered as a possible pathogenic mechanism of ALS even before the identification of SOD1 as a causative gene. In this process excessive synaptic glutamate triggers calcium overload in postsynaptic motor neurons, possibly inducing mitochondrial dysfunction. Another process is based on the fact that MutSOD1 may associate or interact with the ER, the mitochondria, and the glial Nox2/Rac1 complex, thereby resulting in ER stress, mitochondrial dysfunction, and ROS overproduction, respectively. Mitochondrial impairment and dysregulation of calcium handling together with protein aggregates formation coupled to proteasome impairment and ER stress are major components of motor neuron injury that also lead to activation of the apoptotic cascade. Impaired axonal transport may contribute to energy deficit in the distal axon and the dying-back axonopathy that is observed in ALS. Disrupted axonal transport and loss of metabolic support from myelin sheaths that are formed by oligodendrocytes seem to contribute to motor axon vulnerability. Non-cell autonomous processes,

such as neuroinflammation and prion-like propagation of MutSOD1, might also damage motor neurons. Indeed, growing evidence suggests that a noxious property of SOD1 includes its prion-like propagation. This concept is supported by two notable characteristics of SOD1, namely cell-to-cell transmission and seeded aggregation. As an initiation event of intercellular transmission, both mutant and wild-type SOD1 aggregates can be released from injured cells and/or as part of exosomes[28]. MutSOD1 can be otherwise released via a main secretory pathway that is mediated by components of neurosecretory vesicles[23]**(Figure 2)**.

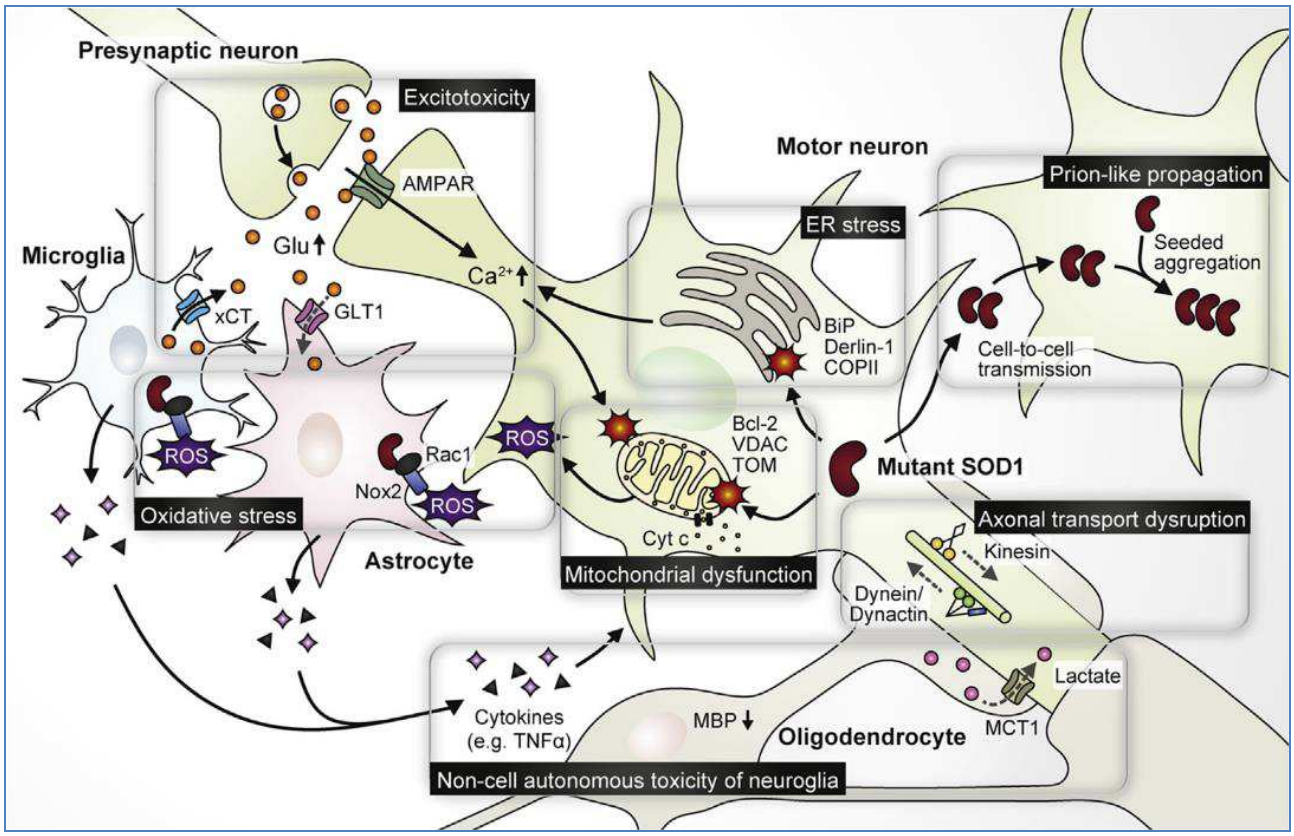

Figure 2. Overview of proposed neurotoxic mechanisms in SOD1-mediated ALS. Signalling and processes that are depicted by solid arrows are enhanced, while those that are depicted by dotted arrows are diminished in SOD1-mediated ALS (AMPAR, AMPA receptor; Glu, glutamate; xCT, cystine/glutamate transporter$_{24}$).

3.1 Oxidative stress

Reactive oxygen species (ROS) are generated by aerobic metabolism and have the potential to damage cells by oxidizing various biomolecules, such as proteins, lipids, and DNA. To prevent this noxious signalling, antioxidants engage in the removal of ROS. The collapsed balance between the generation and removal of ROS is defined as oxidative stress and is implicated in various diseases, including ALS. In fact, several oxidative stress markers are elevated in ALS patients[25]. Although SOD1 normally functions as an antioxidant enzyme by detoxifying superoxide (O2-), oxidative damage by MutSOD1 is predominantly attributed to a gain of toxicity via ROS upregulation rather than to a loss of enzymatic function. ROS are generated through several mechanisms, including NADPH oxidase activity. The mitochondrial respiratory chain also produces ROS and the MutSOD1 induced dysfunction of mitochondria, as described below, putatively enhances the

generation of ROS through changes in electron transport chain complex activity[26]. Glutathione (GSH) is a free-radical scavenger tripeptide, which is among the main regulators of the intracellular redox state. Its levels are lower in the motor cortex of ALS patients than in healthy volunteers in vivo[27] and decreasing GSH accelerates neurological deficit and mitochondrial pathology in the mutant SOD1-ALS mice model[28]. Furthermore, GSH depletion in cultured neurons induces the formation of cytoplasmic TDP-43 inclusions which are found in sporadic ALS patients[29]. Interestingly, even mutant C9orf72 repeats may be related to oxidative stress. Indeed, similarly to what happens when expressing mutant SOD1, motor neurons differentiated from patients' iPSC (induced Pluripotent Stem Cells) and expressing expanded C9orf72 repeat display a significant induction of catalase, which is indicative of oxidative stress and a significant change in levels of the mitochondrial transporter MTX3[30]. On the other hand, the relevance of ROS is due to the fact that it may also affect protein conformation and structure, leading to the accumulation of the abnormal protein inclusions that are extensively described in ALS mouse models and patient-derived tissue[31]. Cysteine-mediated aggregation of mutant SOD1 (mutSOD1) has been widely studied and wild type SOD1 (wtSOD1) also hyper-aggregates when oxidized[32]. Interestingly, recent evidence suggests that also wild-type and mutant TDP-43 aggregation is caused by incorrect disulphide bonds involving Cys residues in one of its RNA recognition motifs, and that aggregation is promoted by ROS[33]. The formation of misfolded protein aggregates can interfere and exacerbate other molecular mechanisms involved in motor neuron degeneration as mitochondrial dysfunction, axonal transport, ER stress and RNA metabolism. Mitochondria, not only represent the main site of ROS production, but are a known target of ROS because of their high dependence on membrane integrity and because they possess their own DNA and RNA that may be damaged by oxidation as well[31]. Aggregation of TDP-43[34] and FUS[35] proceeds through the stress granules (SGs) pathway. SGs are highly dynamic structures that are formed upon OS and contain RNA-binding proteins, transcription factors, RNA helicases and nucleases that work as sorting granules for mRNAs undergoing degradation, storage or translation[36]. SGs are found as a consequence of FUS mutation and mutated FUS is more rapidly directed to SGs after oxidative stress than wild type FUS[36]. Furthermore, TDP-43 is recruited to SGs in conditions of oxidative stress[37]. These SGs may simply sequester a subset of mRNAs thus inducing cell dysfunction or serve as nucleation site for larger protein aggregates as the ones found in ALS patients.

3.2 Protein toxicity: protein aggregation, degradation and prion-like domains

Protein toxicity covers a primary role in ALS pathogenesis; indeed, several proteins (both wild-type and mutant) are dysfunctional in both fALS and sALS, as evidenced by the formation of aggregates, abnormal cleavage events, or distinctive post-translational modifications (e.g., ubiquitination or hyper-phosphorylation).These changes occur both as primary consequences of mutations in the affected proteins and as secondary phenomena induced by the underlying disease process[38].

Protein aggregation and inclusion bodies. Accumulation of dense aggregates of ubiquitinated proteins, in association with eosinophilic aggregates described as "Bunina bodies" are characteristic of later stages of motor neuron disease and ALS pathology. Whether these deposits are toxic or reflect a cellular response to a more primary pathology remains unclear. Indeed, the possibility that some aggregates may reflect beneficial, compensatory events has also been considered[38]. Mutant

SOD1 spontaneously forms oligomers in vivo and in vitro[39]; aggregates of post-translationally modified wtSOD1 can also be detected in the spinal cords of many sALS patients[17]. Aggregated forms of SOD1 can disrupt a wide set of cellular functions, some of the adverse effects include: provocation of cellular hyperexcitability, disruption of mitochondrial function, induction of the unfolded protein response (UPR) and ER stress, impairment of molecular motors and axonal transport, and early disruption of the neuromuscular synaptic structures. Under normal conditions, TDP-43 is located in the nucleus, in most cases of sALS and fALS hyperphosphorylated, cleaved TDP-43 accumulates diffusely in the cytoplasm of neurons and glia, where it assembles into round and thread-like inclusions. The depletion of TDP-43 from the nucleus in these disorders has suggested that TDP-43–mediated toxicity may reflect either loss of its function in the nucleus, an acquired adverse effect of its pathological presence in the cytoplasm (gain-of-function), or both[38]. The pathobiology of TDP-43 and SOD1 inclusions are fundamentally different. Motor neuron death by mutant SOD1 is a consequence of the abundance of the protein: SOD1 KO mice demonstrate a late-life, slow motor neuropathy[40]. By contrast, both reduction and elevation of levels of wild type TDP-43 can be devastating, leading to frank motor neuron disease[41]. It thus seems unlikely that mutant TDP-43 toxicity bears a simple relationship to the dose of the protein or its RNA transcript. Mutant FUS, like SOD1 and TDP-43, is detected in diverse types of intracellular inclusions. Notably, FUS is a major component of stress granules (SGs); mutations in FUS that lead to intracellular retention of this protein increase its propensity to form these cytoplasmic structures[38]. Mutant FUS is also a major component of ubiquitin and p62-positive cytoplasmic inclusions in both fALS and FTLD patients. These aggregates are detected in both neurons and glia of the brain and spinal cord. The C9orf72 expansion produces both nuclear RNA foci and cytoplasmic protein inclusions. At autopsy, C9orf72 mutant brains show widespread intra-nuclear RNA foci[42] generated from both sense and antisense transcripts across the expanded GGGCC segment. Foci have been described in fibroblasts[43] and motor neurons derived from induced pluripotent cells generated from fibroblasts of C9orf72 ALS cases[44]. Notably, the expansion shows some instability; its size varies modestly between different cell types in the same individual. In addition to these intra-nuclear RNA foci, histopathological studies have documented that these cases have at least three types of protein inclusions. Two of these are TDP-43–positive inclusions and distinctive spheroidal inclusions that are positive for a p62. Several components of these p62-positive inclusions have been identified, including RNA-binding motif 45 (RBM45) and heterogeneous nuclear ribonucleoprotein A3 (hnRNPA3). Unexpectedly, neurons from cases with the C9orf72 intronic expansion also possess a third type of inclusion: intracytosolic aggregates composed of dipeptide repeat proteins encoded by the intronic hexanucleotide repeat that are produced through non-canonical, repeat-associated non-ATG–mediated (RAN-mediated) translation[38]. These atypical peptides reflect translation of amino acids from all possible reading frames of the GGGGCC expanded domains[45,46]. Some RAN-produced peptides, such as those containing repeated arginines, are neurotoxic in flies and mammalian neurons in vitro[47]. Proteins degradation and misfolded proteins are generated in various cellular compartments, including the cytoplasm, nucleus and ER, are efficiently removed by quality control systems composed of the ubiquitin (Ub)-proteasome system (UPS), chaperone mediated autophagy (CMA) and macroautophagy[48].Compared with proliferating cells, post-mitotic neurons are more sensitive to the accumulation of cytotoxic proteins because they cannot dilute toxic substances by cell division. Moreover, protein quality control is intrinsically challenging in neurons because of their cellular structure with dendrites and axons in which protein aggregates need to be packaged into autophagic vacuoles and send to the cell body, rich in lysosomes, for degradation[48].

Although young neurons can manage to clear cytotoxic proteins, this task becomes increasingly more difficult throughout the course of aging during which the components of the UPS, CMA and macroautophagy are downregulated in expression and activity[49]. In the affected neurons of many neurodegenerative diseases, pathogenic protein aggregates can further downregulate the activities of proteolytic pathways[48]. The inability to metabolize abundant misfolded proteins will also impair the routine turnover of other proteins, this may induce ER stress and the UPR[38].

Prion-like domains in ALS proteins. The possibility that a pattern of dissemination of pathology and then motor neuron death in ALS might be prion-like was first suggested due to the observation that ALS usually begins focally and spreads in a pattern that implicates contiguous pools of motor neurons[38]. Cell-to-cell spread and propagated misfolding of both mutant[50] and wild type[51] SOD1 have been reported. Moreover, TDP-43 and FUS have low complexity, glycine-rich domains that enhance aggregate formation. Indeed, both proteins emerge in an in silico screen for proteins that harbor domains comparable to known yeast prion peptides[52].

More recently, two heterogeneous nuclear ribonucleoproteins (hnRNPA1 and hnRNPA2B1) with prion-like domains have been genetically linked with fALS[53]. Interestingly, the ribonucleoprotein hnRNPA3 is reported to bind the C9orf72 fALS-associated C9orf72 repeat and accumulate in cytoplasmic inclusions unique to C9orf72 patients[54].

Many prion-like domains containing DNA/RNA-binding proteins are components of ribonucleoprotein granules (RNP granules), which maintain RNA homeostasis during cellular stress[55] and stress granules (SGs), a form of RNP granule that rapidly assembles in response to a range of stressors, are particularly relevant to ALS pathology[38]. The interaction and self-assembly of the prion-like domains of cytosolic RNA-binding proteins facilitates the rapid assembly of stress granules, allowing the sequestration of RNA into these inclusions[56]. In response to stress, mutant form of TDP-43[37] and FUS[56] incorporate rapidly into persistent SGs or form small oligomeric aggregates that interact with the granules. An abnormally strong interaction of the mutant prion-like domains may prevent the disassembly of these granules, resulting in the persistent sequestration of mRNAs and inhibition of their translation. Alternatively, their incorporation into granules might facilitate the conversion of prion-like domains to amyloid states, seeding larger, fibrillary oligomers and inclusion bodies[38].

3.3 Exotoxicity and Glutamate response

Glutamate is the principal excitatory neurotransmitter of the central nervous system (CNS). Excessive release of glutamate from presynaptic neurons or delayed clearance from the synaptic cleft results in the sustained activation of postsynaptic receptors[56]. This then provokes the Ca^{2+} overload in the postsynaptic cells and probably subsequent toxic events, such as mitochondrial dysfunction[26]. This glutamate-mediated neurotoxicity is called excitotoxicity and has been considered as a possible pathogenic mechanism of ALS even before the identification of SOD1 as a causative gene[57]. Glutamate transporter 1 (GLT1; also known as EAAT2) is expressed on astrocytes and has a significant role in glutamate reuptake. The selective loss of GLT1 has been reported in ALS and is considered to be a causative mechanism of excitotoxicity[58]. There are multiple hypotheses regarding the mechanism of GLT1 reduction, including alternative RNA editing,

cleavage by caspase-3, altered miRNA expression, and defects in neuron-astrocyte communication[59]; however, the importance of GLT1 reduction in SOD1-related ALS pathogenesis remains controversial[60]. Another possible cause for excitotoxicity is the excessive glutamate efflux. It has been reported that glutamate release from spinal cord nerve terminals is promoted in SOD1 G93A mice[61]. Microglia also contribute to fatal excitotoxicity through its release of glutamate mostly by a cystine/glutamate antiporter that releases glutamate in exchange for the capturing of extracellular cysteine[62]. Excessive extracellular glutamate is supposed to increase Ca^{2+} level in postsynaptic neurons by the overactivation of Ca^{2+} permeable glutamate receptors. As an additional effect, astrocytes that express MutSOD1 lose the ability to regulate the composition of neuronal ionotropic a-amino-3-hydroxy-5methylisoxazole-4-propionic acid (AMPA) receptors, thereby resulting in the reduction of their important subunit glutamate receptor 2 (GluR2)[63]. The lack of the GluR2 subunit heightens Ca^{2+} permeability of AMPA receptors, which increases the vulnerability of motor neurons to excitotoxicity. Cytosolic Ca^{2+} level in motor neurons might be also raised by the release of stored Ca^{2+}. Inositol 1,4,5-triphosphate (IP3)-mediated Ca^{2+} efflux from the ER regulates various signalling pathways[64], and its defects have been reported to be involved in the neuronal toxicity. One of the inositol 1,4,5-triphosphate receptors (IP3R) subtypes, IP3R2 is upregulated in the blood samples from ALS patients and the neuronal overexpression of IP3R2 shortened the lifespan of SOD1 G93A mice[65]. However, the precise mechanism of disturbances in neuronal calcium homeostasis in the ALS context is still unclear.

3.4 Mitochondrial abnormalities

Another target organelle for the mutSOD1 is the mitochondria[72]. In mutSOD1 transgenic mice, cardinal mitochondrial functions, such as respiratory chain activity and Ca^{2+} buffering capacity, are diminished by the time of disease onset[67-66]. Moreover, mutSOD1 selectively accumulates on the cytosolic face of spinal cord mitochondria, even at the pre symptomatic stage, which implies that mitochondrial SOD1 aggregates contribute to disease initiation[68]. Mitochondrial homeostasis can be disrupted through the interaction of mutSOD1 with several target proteins. Primary targets are Bcl-2 and its binding partner, voltage-dependent anion channel 1 (VDAC1), both of which are integral membrane proteins that are embedded in the outer mitochondrial membrane. MutSOD1 binds to Bcl-2 and converts it into a toxic conformation that exposes the BH3 death domain, through which metabolite transfer via VDAC1, such as ADP influx into the mitochondria, is inhibited4[69]. Interestingly, over-oxidized WTSOD1 has also been reported to form a toxic complex with Bcl-2 in lymphoblasts from a subset of SALS patients[32]. In contrast, others argue that mutSOD1 directly binds and inhibits VDAC1[70]. Another possible target is the translocase of the outer mitochondrial membrane (TOM) complex. Although interactions between the mutSOD1 protein and the TOM complex were not detected, the mitochondrial protein import was partially impaired and was accompanied with an increase in several components, TOM20, TOM22, and TOM40, in SOD1 G93A transgenic rats[55]. Mitochondrial dysfunction may trigger apoptosis by its release of cytochrome c (Cytc) from the mitochondrial intermembrane space. It has been reported that the double knockout of Bcl-2-associated X protein (BAX) and Bcl-2-homologous antagonist/killer (BAK) in SOD1 G93A transgenic mice prevented motor neuron injury and extended survival significantly, which suggests that mitochondrial apoptotic pathways have an important role in neurodegeneration[71]. Moreover, mitochondria play an important role in the intracellular calcium

homeostasis as a calcium buffer, accumulating or releasing calcium depending on the cytosolic levels. Abnormalities in mitochondrial calcium homeostasis were reported in ALS patients and in mutant SOD1 animals[24]. Excessive intracellular calcium levels induce motor neuron death through several mechanisms including: generation of reactive oxygen species (ROS); release of cytochrome c from the mitochondria; glutamate excitotoxicity [24]. All these mechanisms may have a special role in motor neurons because these cells contain less mitochondrial density per volume compared to non-neuronal cells, thus making neurons more deficient in mitochondrial calcium bufferingproperties[24]. In addition, ALS patients show a deficiency in calcium binding proteins calbidin and paralbumin in cortical motor and spinal motor neurons. These two proteins regulate intracellular calcium levels and their deficiency may result in neuronal loss[24]. Endoplasmic Reticulum stress Endoplasmic Reticulum (ER) stress occurs when proteins with an aberrant conformation accumulate in the ER lumen due to a disruption in protein quality control or an overload of newly synthesized polypeptides in the ER. The unfolded protein response (UPR) copes with ER stress by inducing several adaptive responses to reduce the amount of misfolded proteins. However, failure in UPR or prolonged ER stress results in apoptotic cell death. The involvement of ER stress in the pathogenesis of ALS has been suggested in both SOD1-related ALS and SALS cases[73]. Moreover, a longitudinal analysis that uses mutSOD1 transgenic mice revealed that the vulnerability of motor neurons in ALS is closely related to chronic ER stress and that vulnerable (fast-fatigable) motor neurons express ER stress markers even at presymptomatic stages and long before resistant (fast fatigue-resistant or slow) motor neurons[74]. Several targets for mutSOD1 both inside and outside the ER have been proposed. In the ER lumen, mutant SOD1 aggregates bind to an ATP-dependent chaperone BiP[75]. ADP-bound BiP binds to substrates while its co-chaperone, SIL1, catalyses the conversion of an ADP- to an ATP-bound state of BiP, thereby facilitating its release of substrates[76]. A recent compelling study suggests that the expression level of SIL1 in motor neurons determines their vulnerability by modifying the intensity of UPR signalling[77]. The authors speculated that, in vulnerable motor neurons, a reduced SIL1 level impairs the ability of BiP to process misfolded proteins, which exacerbates ER stress. Further research should elucidate the precise mechanism of neurotoxicity that is caused by the reduction of SIL1. Cytosolic mutSOD1 interacts with Derlin-1, which serves as a critical component of ER-associated degradation (ERAD), a machinery for eliminating misfolded proteins from the ER[22]. This interaction inhibits ERAD and induces ER stress, which ultimately elicits apoptosis through the activation of an ER stress sensor, inositol-requiring enzyme 1 (IRE1) and its downstream effector, apoptosis signal-regulating kinase 1 (ASK1). Notably, in addition to many of the reported ALS related mutants, wtSOD1, under zinc-depleted conditions, interacts with Derlin-1[78]. This indicates the possibility that SOD1-Derlin-1 interaction may be involved in the pathogenesis of SOD1 mutation-negative ALS. Additionally, disrupted ER-Golgi trafficking can also produce ER stress possibly through the interaction of the MutSOD1 with coat protein II complex[79].

3.5 Endoplasmic Reticulum stress

Endoplasmic Reticulum (ER) stress occurs when proteins with an aberrant conformation accumulate in the ER lumen due to a disruption in protein quality control or an overload of newly synthesized polypeptides in the ER. The unfolded protein response (UPR) copes with ER stress by inducing several adaptive responses to reduce the amount of misfolded proteins. However, failure in

UPR or prolonged ER stress results in apoptotic cell death. The involvement of ER stress in the pathogenesis of ALS has been suggested in both SOD1-related ALS and SALS cases[73]. Moreover, a longitudinal analysis that uses mutSOD1 transgenic mice revealed that the vulnerability of motor neurons in ALS is closely related to chronic ER stress and that vulnerable (fast-fatigable) motor neurons express ER stress markers even at presymptomatic stages and long before resistant (fast fatigue-resistant or slow) motor neurons[74].

Several targets for mutSOD1 both inside and outside the ER have been proposed. In the ER lumen, mutant SOD1 aggregates bind to an ATP-dependent chaperone BiP[75]. ADP-bound BiP binds to substrates while its co-chaperone, SIL1, catalyses the conversion of an ADP- to an ATP-bound state of BiP, thereby facilitating its release of substrates[76]. A recent compelling study suggests that the expression level of SIL1 in motor neurons determines their vulnerability by modifying the intensity of UPR signalling[77]. The authors speculated that, in vulnerable motor neurons, a reduced SIL1 level impairs the ability of BiP to process misfolded proteins, which exacerbates ER stress. Further research should elucidate the precise mechanism of neurotoxicity that is caused by the reduction of SIL1. Cytosolic mutSOD1 interacts with Derlin-1, which serves as a critical component of ER-associated degradation (ERAD), a machinery for eliminating misfolded proteins from the ER[22]. This interaction inhibits ERAD and induces ER stress, which ultimately elicits apoptosis through the activation of an ER stress sensor, inositol-requiring enzyme 1 (IRE1) and its downstream effector, apoptosis signal-regulating kinase 1 (ASK1). Notably, in addition to many of the reported ALS related mutants, wtSOD1, under zinc-depleted conditions, interacts with Derlin-1[78]. This indicates the possibility that SOD1-Derlin-1 interaction may be involved in the pathogenesis of SOD1 mutation-negative ALS. Additionally, disrupted[21].ER-Golgi trafficking can also produce ER stress possibly through the interaction of the MutSOD1 with coat protein II complex[79].

3.6 Inflammatory dysfunction and contribution of non-neuronal cells

Although ALS is not primarily a disorder of autoimmunity or immune dysregulation, there is considerable evidence that inflammatory processes and non-neuronal cells may play a part in pathogenesis of ALS. The motor neuron death process provokes a neuro-inflammatory reaction that recruits and activates astrocytes and microglia that produce inflammatory cytokines such as interleukins, cyclooxygenase- 2 (COX-2), tumor necrosis factor alpha (TNFα) and monocyte chemoattractant protein-1 (MCP-1), monocyte colony-stimulating factor (MCSF) and transforming growth factor 1 (TGF-1). Some cytokines can trigger microglia to produce copious reactive oxygen and nitrogen species through assembly of NADPH oxidase (NOX), induction of nitric oxide synthase (iNOS), and transcriptional upregulation of lipid-oxidizing enzymes such as COX2. Toxicity induced by ALS-derived astrocytes to motor neurons has been demonstrated in vitro using human astrocytes and motor neurons derived from induced pluripotent stem cells[38] with the involvement of signalling via prostaglandin receptors[80]. Pro-inflammatory mediators including monocyte chemoattractant protein 1 and IL-10 are present in the CSF of patients with ALS and biochemical indices of immune-response activation are present in the blood[81]. Compelling evidence of an association between inflammation and a progression of the disease arises also from studies in murine models of FALS both mutant SOD1 transgenic mice and rats. Several authors reported an increase in the expression of proinflammatory factors before the onset of the disease with sustained

microglial activation throughout the active phase of the disease progression. This was confirmed by Beers et al. who studying double transgenic mice carrying mutant SOD1 and lacking CD4 showed development of a more aggressive ALS phenotype, still reversible by bone marrow transplantation[84]. An interesting result was reported by Zachau et al.[185] who identified the overexpression of CD45+ leukocyte derived MVs in the CSF of an 80-year-old patient with ALS symptomatology (400 times higher) compared to four healthy controls. The increased number ofMVs may contribute to the ALS inflammatory process by formation of immune complexes enabling prion-like propagation of misfolded proteins in neural cells[85]. However the impact of microglia, which can be neuro-protective as well as toxic, is determined by many factors including the phenotype of incoming reactive T cells[38]. Reduced counts of CD4+ CD25+ regulatory T (TREG) cells and monocytes (CD14+ cells) are detected early in ALS, suggesting recruitment of these cells to the CNS early in the neurodegenerative process. TREG cells interact with CNS microglia, attenuating neuro-inflammation by stimulating secretion of anti-inflammatory cytokine[82]. Jenny S. Henkel et al. demonstrated that when the ALS patients were separated based on the rate of disease progression into rapidly versus slowly progressing ALS patients, the percent of CD4+ CD25high TREGs were reduced in rapidly progressing patients compared with slowly progressing patients and reduced compared with control volunteers[83] **(Figure 3)**.

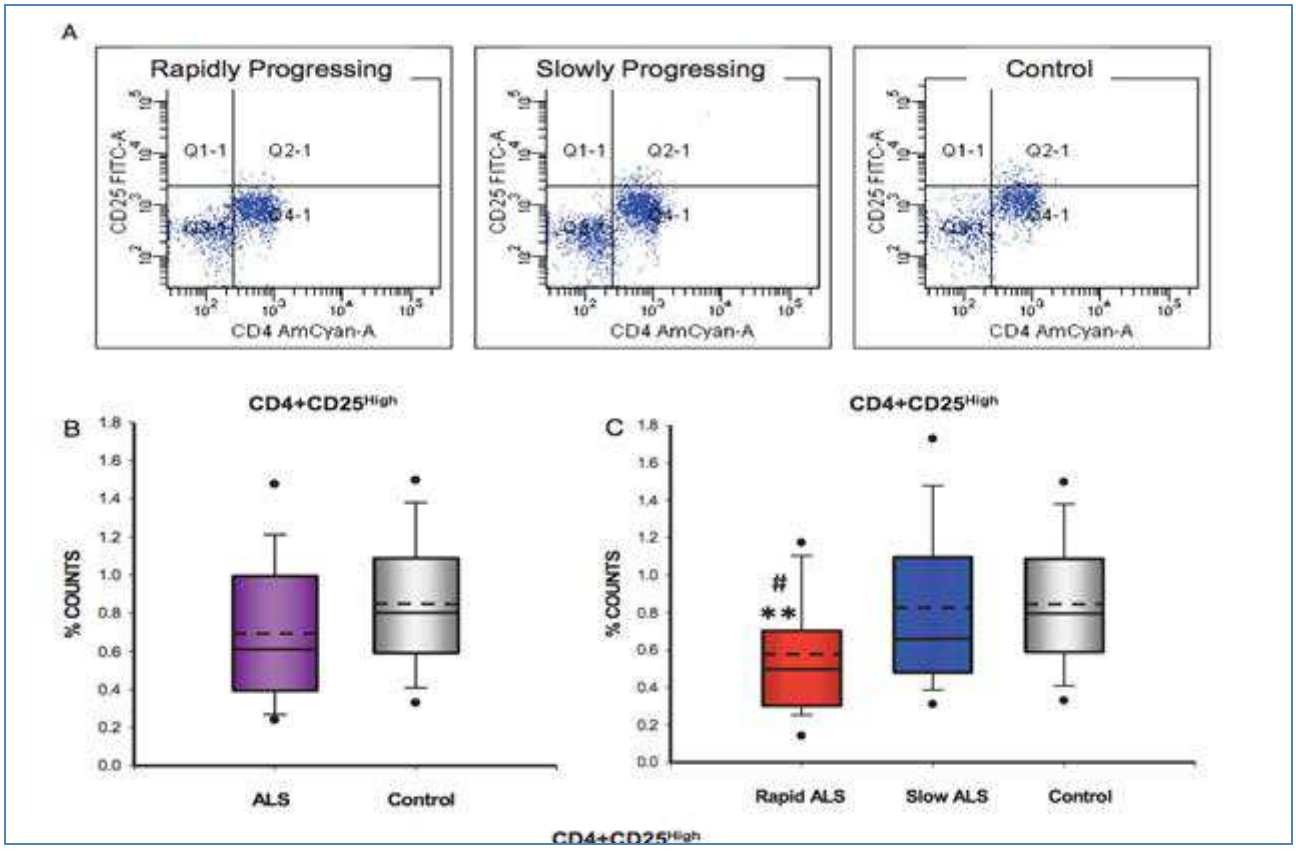

Figure 3. CD4+ CD25high regulatory T-lymphocytes (Tregs) are reduced in rapidly progressing ALS patients[83].

4. SOD1

4.1 Physiological role of SOD1

Copper, zinc- superoxide dismutase-1 (SOD1) is a member of the human SOD family of proteins, which also includes SOD2 and SOD3. While all three proteins function as anti-oxidizing enzymes that catalyse the dismutation of superoxide radicals (O2−) to hydrogen peroxide (H2O2), they are distinct proteins with unique characteristics[87]. SOD1 (Molecular Weight: 32 kDa) is highly abundant,comprising ~ 1% of total protein in the cell[88], and resides mainly in the cytosol with some degree of localization in the mitochondrial inner membrane space[89].Other key differences amongst the SOD proteins include their quaternary structures and mechanism of superoxide dismutation: SOD1 is a homodimer while SOD2 and SOD3 are homotetrameric proteins; SOD1 and SOD3 catalyse the dismutation of O2− through the alternate reduction and re-oxidation of Cu2+, whereas SOD2 utilizes manganese (Mn) as a redox active transition metal for this purpose. In SOD1 the conversion of toxic superoxide radicals to hydrogen peroxide and oxygen is mediated by a copper atom at the active site instead other post-translational modifications, such as Zn2+ coordination[90] and disulphide oxidation, help create a mature and structurally stable protein organized with an eight-stranded Greek key beta-barrel structural motif. SOD1 has pro-oxidant activities, including peroxidation, the generation of hydroxyl radicals, and the nitration of tyrosine. SOD1 catalysis plays a key role in signal transduction, a function that is largely under-appreciated compared to its role as an anti-oxidizing enzyme. For example, the catalytic product of SOD1 H2O2 is able to modulate a variety of signal transduction pathways, including but not limited to gene expression, cell proliferation, differentiation and death[91,92]. Another function that have been proved to be mediated by SOD1 is related to a role in signalling as secreted secondary messenger. Although SOD1 is predominately localized to the cytoplasm, multiple reports have demonstrated that SOD1 can be secreted[93,94,95]. The presence of extracellular SOD1 can in turn increase intracellular calcium levels100, a phenomena shown to have neuroprotective effects.

4.2 SOD1 pathogenic role in ALS

Although only 2% of patients with ALS have a mutation in SOD1, the discovery of this mutation20 was a landmark in ALS research because it provided the first molecular insights into the pathogenesis of the disease. Currently, 171 mutations have been identified within SOD1 that are linked to ALS (http://alsod.iop.kcl.ac.uk/)[97]. Approximately 20–25% of FALS cases and 6% of all ALS cases are caused by mutations in SOD15. The majority of these mutations (>80%) result in aminoacid substitutions while the remaining lesions are a combination of insertions, polymorphisms, and deletions. FALS-linked mutations are not localized to one portion of SOD1, but rather span the entire protein. Mutations in the gene for superoxide dismutase 1 may lead to the production of toxic hydroxyl radicals (OH-) or promote the use of other abnormal substrates such as peroxynitrite (ONOO-), ultimately leading to the aberrant nitration of tyrosine residues (Tyr) in proteins. Therefore, it has been hypothesised that SOD1 mutations may cause disease by a toxic gain of function, not by the loss of the scavenging activity of SOD1[96,102].

Several groups have reported the mutation-induced conformational changes of SOD1 as the cause of SOD1 toxicity. The mutated SOD1, but not the wild type SOD1 contains an exposed N-terminal short region, which provokes endoplasmic reticulum stress by targeting an ER resident protein,

Derlin-1[98]. Another study reported that mutSOD1 has an increased propensity to expose its hydrophobic surfaces when compared to WTSOD1 and that the varying hydrophobicity across MutSOD1 correlates with aggregation propensity[99].These reports indicate that suppressing the conformational alterations and/or masking the exposed surfaces of mutSOD1 would be beneficial to attenuate toxicity by soluble or aggregated mutant SOD1 species. Activity such as this in intracellular molecular milieu can be attributed to the chaperon system, whose disruption results in cytotoxicity. In fact, several chaperons have been implicated in the pathogenesis of ALS, including protein disulphide isomerase (PDI) and the macrophage migration inhibitory factor (MIF). Intracellular protein aggregation is common among many neurodegenerative diseases. In ALS, SOD1 inclusions are found in fALS patients with SOD1 mutations as well as in MutSOD1 transgenic mice[100,101]. These observations lead to a question shared by many aggregation-prone neurotoxic proteins, such as tau in Alzheimer's disease and a-synuclein in Parkinson's disease; which form of the proteins exerts toxicity, soluble or aggregated? Some evidences suggest that the soluble form confers toxicity in the context of SOD1-mediated ALS and this is supported for example by observations that the level of solubility of the mutSOD1 correlates with cytotoxicity and that the decreased aggregation of mutSOD1 in transgenic mice fails to ameliorate devastating phenotypes[23,108].Conversely, others have reported that the aggregation propensity of various mutSOD1 correlates with the disease severity[103,104]. Soluble species can diffusely spread throughout the cytosol, making it possible for these compounds to exert toxic effects through undesirable interactions with numerous targets. Misfolded SOD1, resulting from mutations or aberrant post-translational modifications, causes the protein to engage in aberrant interactions. Misfolded SOD1 can be both secreted and taken up from the extracellular environment through different vesicular trafficking mechanisms. Then extracellular misfolded SOD1 is able to activates microglia by binding to the CD14/TLR4 receptor, thereby elevating nitric oxide synthase (iNOS) activity as well as secretion of superoxide anion ($O2^-$) and pro-inflammatory cytokines (TNFα and Il-1β). This mode of microglia activation leads to motor neuron death[105,106]. Indeed, the expression and up take of misfolded SOD1 leads to ER stress, which elevates the pro-apoptotic protein and induces mitochondrial damage[107,51]. Thus, the combination of MutSOD1 uptake and intracellular expression in in neurons could exacerbate ER stress and tilt the scale from the unfolded protein response (UPR) coping mechanism toward apoptosis in vivo. The presence of misfolded SOD1in the axon results in axonal transport inhibition through a mechanism involving the phosphorylation of p38 MAPK and the kinesin motor. All of these aberrant functions compromise the integrity of the motor-neuron, and potentially contribute to both fALS and sALS pathogenesis **(Figure4)**. Nevertheless, the role of SOD1 aggregates in the ALS aetiology remains unclear. Accordingly, protein aggregates cannot be disregarded, as they may also exert toxic effects by sequestering important cellular components.

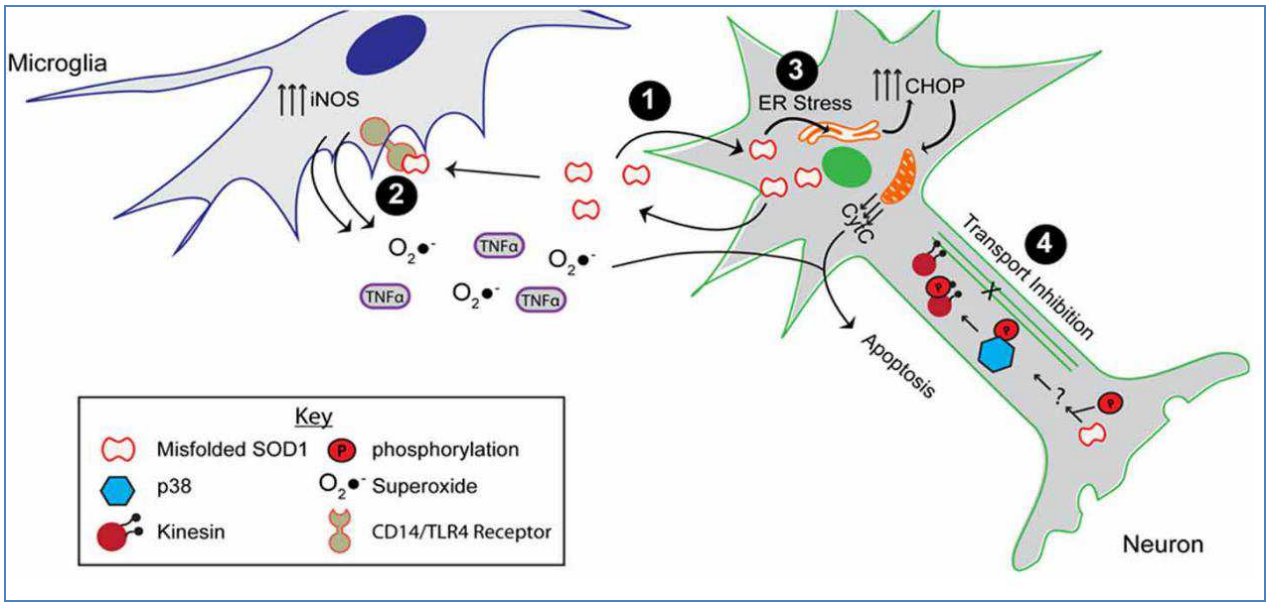

Figure 4. The toxic properties shared by ALS-linked mutant SOD1 and modified WT SOD1 that are gained by this enzyme and are able to lead to important cellular impairments[83].

4.3 Emerging role of misfolded SOD1 in ALS

Mutant SOD1 exhibits an altered tertiary structure, evidenced by enhanced hydrophobicity compared to SOD WT[108]. While X-ray crystallography has failed to reveal significant structural differences between WT and mutant SOD1proteins[109], solution-based structural studies indicate that fALS-linked mutations induce some degree of SOD1 unfolding, or "misfolding". Here the term "misfolding" refers to the structural loosening of SOD1 due to a mutation and/or altered post-translational modification within a soluble form of the protein inducing the exposition of linear sequences or conformational epitopes that are otherwise buried in the intact, native protein. A direct consequence of mutation-induced misfolding of SOD1 is aggregation, which refers to their reversible assembly of misfolded SOD1 species into an insoluble structure **(Figure 5)**.

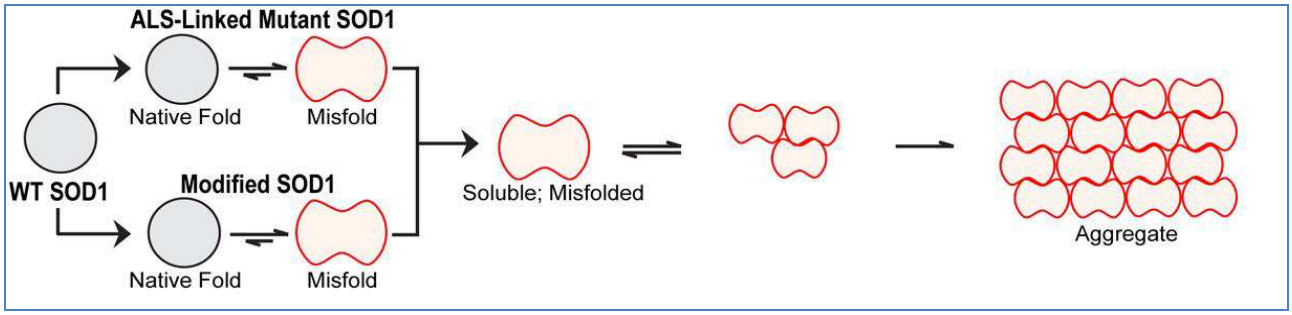

Figure 5. Misfolded and aggregated SOD1[101].

SOD1 aggregation has been extensively investigated in vivo, both in ALS human post-mortem tissues and in mutant-SOD1 transgenic mice. The enhanced aggregation propensities of fALS-linked SOD1 mutants have also been comprehensively examined in cell culture and in other in vitro assays Cereda et al. found that an increased expression of total SOD1 protein seems evident in peripheral blood mononuclear cells (PBMCs) of sALS patients that could have two fates in the

physiopathological mechanisms of ALS: to remain soluble and able to exert its function(s) in the nucleus or to aggregate in the cytoplasm[111]. Nevertheless, the hypothesis of enhanced accumulation of soluble SOD1 in the nucleus as a possible ‘‘defensive’’ mechanism deserves further in-depth investigation since it may lead to novel therapeutic approaches based on the pharmacological targeting of SOD1 sub-cellular distribution as well as on the modulation of its solubility.

Although it remains unclear whether SOD1 aggregation is a causative or protective factor in disease progression, several recent reports demonstrate that misfolded SOD1 species can spread from cell to cell in a prion-like fashion [112,113,114]. Munch et al. demonstrated that the uptake of aggregated ALS-linked SOD1 mutants in cultured neuronal cells seeded aggregation of endogenous mutant-SOD1 and Ayers et al.[115] demonstrated that aggregates composed of ALS-causing SOD1 mutants are taken up by cells in an in vivo model with injection of spinal cord homogenates prepared from paralyzed mice expressing mutant SOD1 into spinal cord of genetically vulnerable SOD1 transgenic mice. These endogenous SOD1 aggregates persisted well after (>30 days) the original aggregates dissipated from cell division, consistent with a prion-like propagation of aggregated SOD1118.More recently, uptake of both misfolded mutant-SOD1 as well as aggregated mutant-SOD1 was shown to induce aggregation of the native WT SOD1 protein[114]. This latter report demonstrated how misfolded SOD1 can alter the conformation of otherwise normally folded SOD1[115].

Scientists tried to find correlations between the effect of misfolded SOD1 and the role of other pathogenic proteins involved in ALS development. Mackenzie et al.[116]reported that TDP43 was present in its pathological form in sALS cases suggesting its direct role in the pathogenesis of the disease, but it was present in its wild type form in all SOD1 mutated ALS patients. The significance of this result is the implication that the pathological processes underlying motor neuron degeneration in sALS are different from those associated with SOD1 mutations. Pokrishevsky, Grad e Cashman published important research studies from this point of view[117,118]. In 2012 they reported that SOD1 misfolding is observed with cytosolic accumulation of mutant FUS or TDP43 in FUS-fALS and TDP43-fALS, respectively, as well as of TDP43 WT in sALS. However, SOD1-fALS, wherein motor axons display prominent inclusions of misfolded SOD1, is not associated with cytosolic accumulation of FUS or TDP43. So researches proposed that SOD1 misfolding could constitute a critical molecular event in the unified pathogenesis of fALS and sALS, distal to FUS or TDP43 cytosolic accumulation. Misfolded mutant and SOD1 WT can template the misfolding of natively folded SOD1 WT and propagate from cell to cell in vitro. Stochastic induction of a competent template by mutant SOD1, FUS, or TDP43 could trigger the propagation of SOD1 misfolding in fALS and sALS. In sALS, cytoplasmic accumulation of TDP43 WT, as a local response to injury or cell stress, may also induce a productive template of misfolded SOD1, or may be a toxic consequence of SOD1 misfolding[119].Recently these researchers even showed for the first time that TDP-43 or FUS-induced misfolded human SOD1 WT and this acquires the prion-like property of intercellular transmissibility and induction of endogenous human SOD1 WT misfolding in recipient cells[118]. The intercellular transmission of human mutant or misfolded wild-type SOD1 is likely to occur through release of naked aggregates by dying cells, which are taken up by macropinocyotosis and can trigger seeded aggregation or through the release of disease-associated exosomes containing intraluminal and surface-associated misfolded SOD. Following uptake of exosomes from the extracellular environment, the release of misfolded SOD1 into the recipient cells

might occur through direct fusion of exosomal membrane with the plasma membrane, or by intraluminal fusion of the exosomes with the endosomal membrane following endocytosis. This work indicates that the propagation of SOD1 misfolding is an active and independent process, which can occur in the absence of TDP-43 or FUS pathology[118].

5. Mutated proteins involved in SOD1 related in ALS

As previously showed, in the last decade several new causative genes, such as TDP-43, FUS, and C9ORF72, have provided unexpected insights into the pathogenesis of ALS. They appear to commonly exert toxicity through abnormal RNA metabolism or processing. TDP43 is a member of the heterogeneous nuclear ribonuclear protein (hnRNP) RBPs family that have different functions in RNA metabolism and homeostasis[120]. Mutations in the genes encoding several hnRNPs as hnRNPA1, hnRNPA2/B[121], and Matrin[31,25]cause fALS or motor neuron disease as part of a multisystem disorder. TDP43 also shares significant structural and functional homology with fused in sarcoma (FUS), an RBP that is part of the FET family of RNA/DNA-binding proteins that includes Ewing sarcoma breakpoint region 1 (EWSR1) and TATA box binding protein-associated factor 15 (TAF15)[129]. Nonsense or missense mutations in FUS, EWSR1, and TAF[15] are associated with fALS[123,124]. TDP-43 and FUS contain two RNA recognition domains-structures that are common to many RNA-interacting proteins, including those that are involved in mRNA transport. TDP-43 and FUS may form part of such RNA transport complexes and, when mutated, could thereby contribute to motor neuron injury through loss of axonal mRNA transport[125128]. Alternatively, decreased nuclear expression and function of these proteins could disrupt various aspects of RNA processing, including pre-mRNA splicing, nuclear mRNA export, mRNA sorting to distinct cytoplasmic compartments, and/or processing of noncoding RNAs[122]. Convincingly, the C9ORF72 repeat expansion is also hypothesized to drive repeat-associated non-ATG (RAN) translation that results in toxic peptides1. Immunohistochemistry studies identified ubiquitin-positive inclusions that contain TDP-43 and those that contain FUS in post mortem tissues of all patients with SALS or SOD1 mutation-negative FALS but not in any SOD1-related patients with FALS that were examined[116]. These observations imply that the toxic mechanisms of SOD1 might be exclusively confined to FALS cases with SOD1 mutation. In contrast, a handful of papers suggest a role for WTSOD1 in the pathogenic mechanism by other causative gene products. First, other ALS-related genes can induce the misfolding and/or aggregate formation of WTSOD1. SOD1-immunoreactive inclusions were detectable in the spinal cords of FALS patients with and without SOD1 mutations[17]. Another report demonstrated that mutant TDP-43 and FUS, and wild-type TDP-43, but not wild-type FUS triggered misfolding of WTSOD1 in neural cells[117]. Notably, it is well known that fluctuations in the abundance of TDP-43 can induce cellular dysfunction. Therefore, an excess of even native TDP-43 has detrimental effects[41]. While the implication of wtSOD1 in SOD1 mutation-negative patients with FALS remains controversial, several reports have suggested shared toxic mechanisms by which SOD1 mutations and other gene mutations act. One recent report demonstrated that conditioned medium that was harvested from astrocytes that carry either the mutant SOD1 or TDP-43 possessed the ability to induce motor neuron death through voltage-sensitive sodium (Na+) channels in a nitroxidative stress dependent manner, thereby indicating a shared, non-cell autonomous process[126]. Moreover, C9ORF72 expansion was implicated in the exertion of neuronal degeneration via pathways that are somewhat similar to

mutSOD[126]. While comparing transcripts between induced pluripotent stem cells (iPSCs) that were derived from patients with C9ORF72 expansion and an SOD1 A4V mutation, several genes were found to be commonly upregulated. For instance, a motor protein kinesin KIF14 and an oxidative stress-related catalase CAT were both upregulated. Until now, there have been only a limited number of studies to support or contradict the implications of wtSOD1 in patients with fALS with mutations in other genes. A lack of established animal models with ALS-associated gene mutations, except for SOD1, may be a great barrier to elucidating the role of these related genes. Considering that nearly all ALS associated mutants target motor neurons, it is possible that multiple causative gene products share the same targets as mutSOD1 and, perhaps, even exploit wtSOD1 to attack them.

6. EXTRACELLULAR VESICLES PART A :

6.1 Lipid content of extracellular vesicles

Extracellular vesicles are typically enclosed by a single phospholipid bilayer. However there might be exceptions to this rule. A recent cryoelectron microscopy study of human ejaculate extracellular vesicles has demonstrated the presence of vesicular structures with double or even more multiple membrane by layers as well[127]. Since extracellular vesicles are membrane enclosed structures, lipids are universal and obligate components of EVs and the smaller an EV is, the larger proportion of it's total mass is contributed by membrane lipids. Another basic consideration worth keeping in mind is that phospholipid bilayers form closed compartments spontaneously [128].

Planar phospholipid membranes have edges exposed to water. The closed structure is stable because it avoids the exposure of the hydrophobic hydrocarbon tails to water, which would be energetically unfavorable. Therefore, membrane fragments form vesicular structures. This is worth keeping in mind in the extracellular vesicle field. Any membrane fragment, no matter whether it comes from a necrotic cell or if it comes from a ruptured extracellular vesicle, will seal and form a vesicle that mimics an intact extracellular vesicle. The lipid membrane composition of extracellular vesicles strongly resembles that of the plasma membrane of the cell. The major molecule of components include phospholipids, glycolipids, cholesterol, integral and peripheral proteins[129]. However there are also differences between the plasma membrane of the cell and the membrane of extracellular vesicles. The plasma membrane is characterized by an asymmetrical distribution of lipids. Phosphatidyl serine and phosphatidyl ethanolamine are sequestered in the inner membrane leaflet. In contrast, in extracellular vesicles, membrane phospholipid asymmetry is lost and phosphatidyl serine is also detectable in the outer membrane leaflet.

Also there is another difference[130],because of the curvature extracellular vesicles may transiently expose the hydrophobic core of their membrane to the aqueous phase, thus presenting lipid packing defects and the presence of phosphatidyl serine, also in the outer membrane leaflet of extracellular vesicles; for this reasone it’s usuful use flouorochrome-labelled phosphatidyl serine binding proteins such as labelled annexin V or lactadherin. Furthermore Milk fat globule-EGF factor 8 protein (MFGE8) known as lactadherin, is more common to detect extracellular vesicles and while

Annexin V require the presence of calcium ions for phosphatidyl serine binding, the latter does not require it[131].

Transmembrane or lipid bound extracellular proteins are expected to be present in EV isolates. These include tetraspanins such as CD63, CD9, and CD81, integrins and cell adhesion molecules, growth factor receptors, heterotrimeric G proteins and the previously mentioned phosphatidyl serine binding proteins. There are differences between the lipid contents of the plasma membrane of the cell and the membrane of the smallest size extracellular vesicles, which are commonly referred to as exosomes. Most lipid classes were found to be elevated in exosomes, and the relative amounts of glycosphingolipids, cholesterol, sphingomyelin, and phosphatidyl serine were found to be more than 15 times higher in exosomes than in the plasma membrane of the cell. Furthermore there are differences in the lipid membranes of different size based extracellular vesicle subpopulations. In the intermediate size vesicles, often referred to as microvesicles, microparticles or ectosomes, the lipid composition is similar to that of the plasma membrane. But phosphatidyl serine and phosphatidyl ethanolamine are homogeneously distributed across the bilayer membrane. In contrast, the smaller size vesicles, exosomes are highly enriched in glycosphingolipids, sphingomyelin, cholesterol and phosphatidyl serine. The sphingomyelin to phosphatidyl choline ratio is approximately three to one, and exosomes are reported to contain a greater quantity of ceramide. There are differences also in the lipid packing densities of size based extracellular vesicle sub populations. The smallest size vesicles are the ones which are characterized by the highest lipid packing density. Their membrane is more liquid ordered than that of the other EVs, those with intermediate and large sizes. Lipid rafts are liquid ordered membrane subdomains enriched in cholesterol, saturated fatty acids, and sphingomyelin.They are characterized by tight lipid packing density. Rafts are also known to be resistant to non ionic detergents at low temperature[132].Exosomes are often also enriched in cholesterol, saturated phospholipids and sphingomyelin, suggesting that exosome membranes contain lipid raft like domains. Detergents are known to lyse lipid membranes. Since extracellular vesicles are membrane enclosed structures, they are sensitive to detergent lysis[133].

The major researcher use detergent lysis to differentiate detergent sensitive extracellular vehicles from less sensitive protein aggregates, such as immune complexes, during flow cytometry. Using the fluorochrome conjugated annexin V, it is able to detect extracellular vehicles in rheumatoid arthritis synovial fluid for istance. Upon addition of triton, these vesicles disappear. However if it is used a fluorochrome conjugated antibody to IGM, and even if it is taken to add triton the events do not disappear[132].

Since these are not particular events, these are protein aggregates immune complexes[133].Therefore if it is investigated complex biological fluids in which to have high number of immune complexes or other protein aggregates, it is advisable to take away to try to under resistant events from the total event count once we determine the EV number. Differential detergent lysis combined with tunable resistive pulse sensing to distinguish size base extracellular vesicles sub populations. In this experiment, they are isolated large, intermediate sized and small vesicles from the condition media of 40 different cell lines. The percentages of extracellular vesicles remaining intact in the presence of detergent and they are illustrated as colored bars[134].

Notably both large and intermediate size vesicles behave quite similarly in the presence of SDS. Both lies at 0.01%. In contrast the smaller size vesicle prove to be more resistant to detergent lysis, an order of magnitude higher concentration of SDS was required to lies them. And if it is looked at the trison X100 lysis, deoxycholate lysis or twin 20 lysis, they can always see the same pattern. The smallest size vesicles require the highest concentration to get lysed[134].In this way it is demostrated the differential sensitivity of different size base extracellular vehicles sub populations to detergents using flow cytometry and the large and intermediate sized vesicle require much lower concentration of SDS to get lysed compared to the smaller size vesicles[134].

6.2 Role of lipid Evs for uptake

There is a lot of different ways that EVs can find their way into cells and that's lots of different paths infact actually lipid rafts are very studied in extracellular vesicle uptake for this reason: for example lipid raft-mediated endocytosis, macro-pinocytosis, caveolin-dependent endocytosis, and membrane fusion, and phagocytosis[135]. EV uptake is reduced when EV producing cell are pre treated with compounds which avoid the biosynthesis of glysphingolipids and sphingolipids of EVs have been shown to have an important role in binding and endocytosis, possibly through cholesterol rich microdomains[135]**(Figura6).**

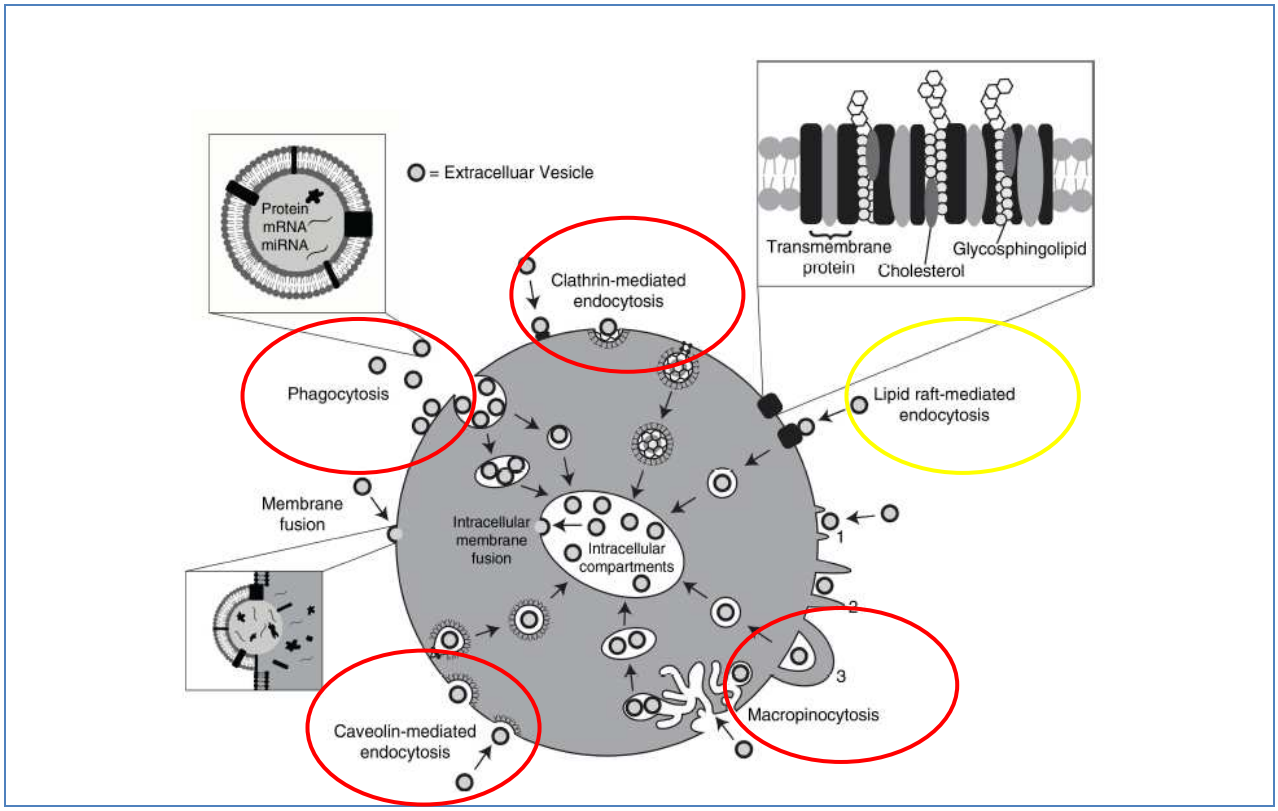

Figura6 . Pathways shown to participate in EV uptake by target cells. EVs have been shown to be internalized by cells through phagocytosis, clathrin- and caveolin-mediated endocytosis. There is also evidence to support their interaction with lipid rafts resulting in EV uptake[135].

The second role of EV lipids is related to membrane rigidity and stability. Sphingomyelin and cholesterol increase overall rigidity and stability. And GM3 ganglioside increases the stability of

EVs and prevents their recognition by blood components and uptake by the reticuloendothelial system. EV lipids play very important roles in EV biogenesis. Cholesterol depletion by methyl-B-cyclodextrin induces EV release. Ceramyte formed by the action of neutral sphingomyelinase 2 on sphingomyelin, triggers budding of exosomes into bodies. And these lysobisphosphatidic acid and phosphatidic acid are involved in the biogenesis of EVs. There are numerous lipid dependent biological functions of EVs for istance EV-bound prostaglandins activate signaling pathways in rat basophil leukemia cells[136]. Eicosanoids are transferred between cells by EVs[137] and EV lipids impact Notch[138]signaling and induce cell death in pancreatic tumor cells. But there are further lipidevendent functions of EVs: EV-bound lysophosphatidylcholine was shown to play a role in the maturation of dendritic cells[139]and trigger lymphocyte chemotaxis. Seminally will interact with sperm cells and transfer to them cholesterol which is fundamental for the capacitation process[140.] And finally, EV sphingomyolin has a pro-angiogenic character that can promote endothelial cell migration, tube formation, and neovascularization[141] .An interesting aspect of extracellular physical biology is that secretary phospholipase A2 enzyme can use extracellular vesicles as a substrate and may impair EV quantification if present in sufficient amounts in biological fluids .In an aqueous environment, cylindrical lipids such as phosphotidyl choline and sphingomyelin produce stable planar monolayers. In contrast, conical lipids such as phosphotidyl ethanolamine and phosphotidyl syrine and inverted conical lipids such as lipophosphotidylcholine produce monolayers with negative and positive curvatures, respectively. Curvature sorting of membrane components begins in the parent cell during budding of membranes[142].It largely determines the shape, size, and composition of EVs and influences their biological roles. This mechanism is highly non specific and this implies that several structure of components are shared among different kinds of vesicles. Budding toward the lumen of endosomes may require acid an inverted cone under luminal surface and phosphatidylinositol three phosphate[142].Cholesterol is required for budding of highly cured vesicles with 40 to 50 nanometer in diameter. And cholesterol and sphingomyelin are important for stabilizing membranes during fusion and phosphothidil ethanolamine greatly stimulates fusion efficiency.The first step is stalk formation : two adjoining membranes merge their outer leaflets producing a negatively curved monolayer regionfacilitated by cone-shaped fatty acids. Next the stalk widens and generates a fusion pore lined by a positively curved monolayer region favored by inverted cone-shaped lipids[142].

6.3 Role of Annexin V in the plasma membrane

Plasma membrane of a living cell is a highly organized three-dimensional system composed of lipids, proteins and glycans, so that the two leaflets forming it are of quite different composition. The major part of electrically neutral phosphatidylcholine (PC) and sphyngomielin (SM) is located in its outer leaflet, whereas most of phosphatidylethanolamine (PE) and practically all anionic lipidsphosphatidyl serine(PS) and phosphatidic acid (PA) face the cytosolic milieu[143,144].Such asymmetry creates a strong distribution of electrostatic charge between two membrane surfaces that is maintained due to the action of specific lipid-translocating proteins. Its maintaining is of great biological importance allowing correct assembly of membrane proteins and interaction with intracellular structures[145,146].

The labeled annexin V is currently the most frequently used probe to visualize the early-stage apoptosis in microscopy and to characterize the apoptotic cell populations by flow cytometry .The principle of annexin V assay is presented in **(Figure 7)**.

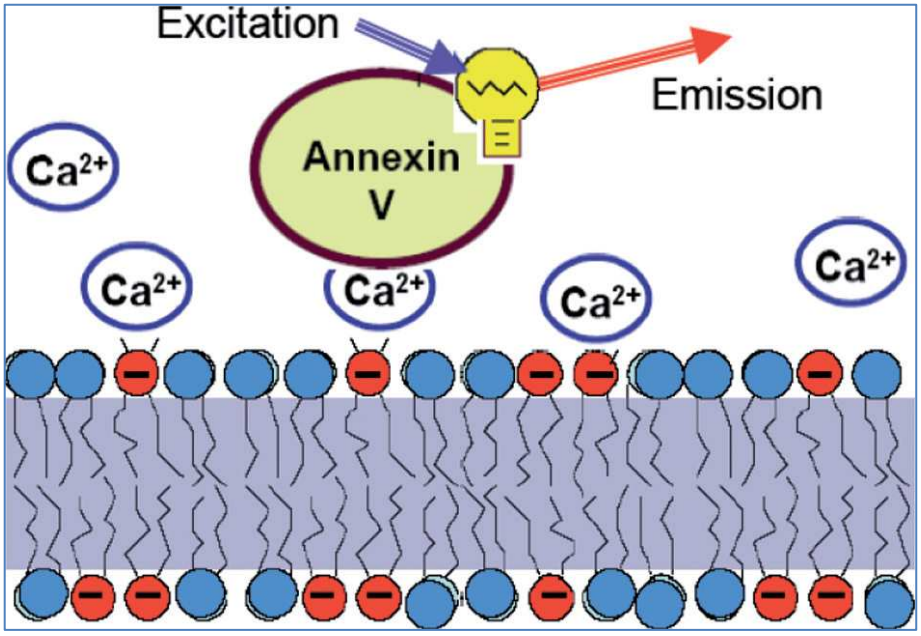

Figure 7. The principle of apoptosis detection method based on annexin V with the aid of Ca^{2+} ion. This protein interacts with high affinity with PSheads exposed on the membrane surface. Annexin V can be labeled with fluorescent dye that allows visualization of cell with exposed PS.

Operating in physiological conditions, this 36 -κDa calcium-binding protein binds with relatively high affinity (Kd ~10,7,8 M) to the surface of cells that expose negatively charged PS, and due to attached fluorescent dye these cells become labeled. Same process happens when Annexin binds the surface of extracellular vesicles therefore, despite it is not a selective marker for all extracellular vesicles, remains still the most frequently used which still allows a vesicular division. The years of successful application of annexin V binding assay still allowed revealing its important disadvantages:

1. The link with the Annexin requires the presence of millimolar (usually ~2.5 mM) concentrations of Ca^{2+} ions, since only with their complexation the protein binds to PS with high affinity. This is not always desirable or even tolerable. For instance, the isolation of blood cells requires adding Ca^{2+} chelators for suppressing blood clotting, and after that the chelators have to be washed-out and Ca^{2+} ions added again for apoptosis assay. Also, false positive results may appear because most animal cells have a Ca^{2+}-dependent scramblase that can move PS to the cell surface.

2. The complete annexin V binding requires incubation times from tens of minutes up to one-two hours. This makes its application problematic for kinetic analysis of the process that develops on the same scale of hours and this does not allow catching its earliest steps of PS exposure occurring in minutes[147]. The annexin V binding is limited by its slow diffusion and slow formation of its high-affinity complexes.

3. The false positive results may result due to annexin V binding to negatively charged aldehyde adducts that may appear on cell surface in stress conditions[148] and in some apoptosis-independent pathologies, such as Barth syndrome[149].Therefore an increased binding of annexin-V does not necessarily reflect an apoptotic state of the cell[150].

4. As a protein, annexin V can itself be a subject of enzyme degradation. This limits its application in vivo and also requires controlled suppressing of protease activity if the cells from solid tissues are prepared by separation with the aid of proteases [151].

5. The labeled recombinant annexin V is expensive and moderately unstable. Therefore the assay with its use is not convenient for high throughput screening needed e.g. in drug discovery[152]

6.4 Membrane Phospholipids

6.4.1 Localization of Various Phospholipids in the PM

The PM is mainly constructed of phospholipids. The phospholipids form a bilayer (5 nm in thickness) by utilizing their amphipathic characteristics, with the polar head groups facing the water and the hydrophobic fatty acyl chains facing each other on the interior of the bilayer. Many different types of phospholipids can be accommodated into a single bilayer, and the lipid composition is expected to influence the physiological functions of the membrane **(Figure 8**).

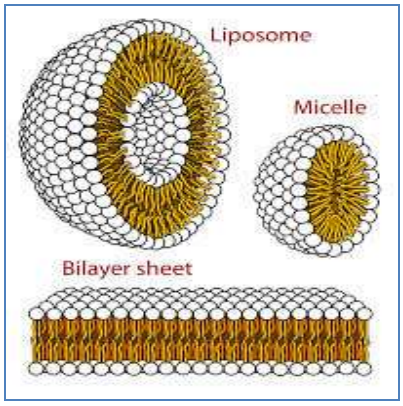

Figure 8: Phospholipid shape and the associated mechanism of membrane recognition and deformation. The shape of a lipid molecule is classified into three categories: cylindrical, conical, and inverted conical.

The phospholipid composition also varies in each cell type and membrane[153,154].The four primary phospholipids found in eukaryotic membranes are phosphatidylcholine (PC), phosphatidylethanolamine (PE), phosphatidylserine (PS), and sphingomyelin (SM). In addition, two less abundant species, phosphatidylinositol (PI) and phosphatidic acid (PA) can also exist in the membranes.

The various types of lipids show asymmetric distribution in the inner and outer leaflets of thePMlipid bilayer. PC and SM are predominantly localized in the outer membrane, whereas PE is primarily found in the inner membrane[155,156].Furthermore, PS is exclusively found in the inner leaflet of the PM along with PI and several phosphoinositides, including PI 4-phosphate [PI(4)P], PI 4,5-bisphosphate [PI(4,5)P2], and PI 3,4,5-trisphosphate [PI(3,4,5)P3][157,158].

The distribution of PS and phosphoinositides causes the electrostatic properties of the membrane to vary[159,160].Membranes of the early secretory pathway [e.g., endoplasmic reticulum (ER) and cis-Golgi] have a weakly charged cytosolic leaflet due to the scarcity of PS and phosphoinositides. In contrast, membranes of the late secretory pathway (e.g., endosome and PM) have a highly charged cytosolic leaflet because of their abundance of PS and phosphoinositides. The electrostatic nature of PS allows it to act as a partial substitute for phosphoinositides in membranes, especially during the interaction with cationic motifs. Membrane-deforming domains, such as BAR, F-BAR, and I-BAR, are one such example of cationic motifs that adapt to curved anionic membrane surfaces using electrostatic interactions **(Figure 9)** :

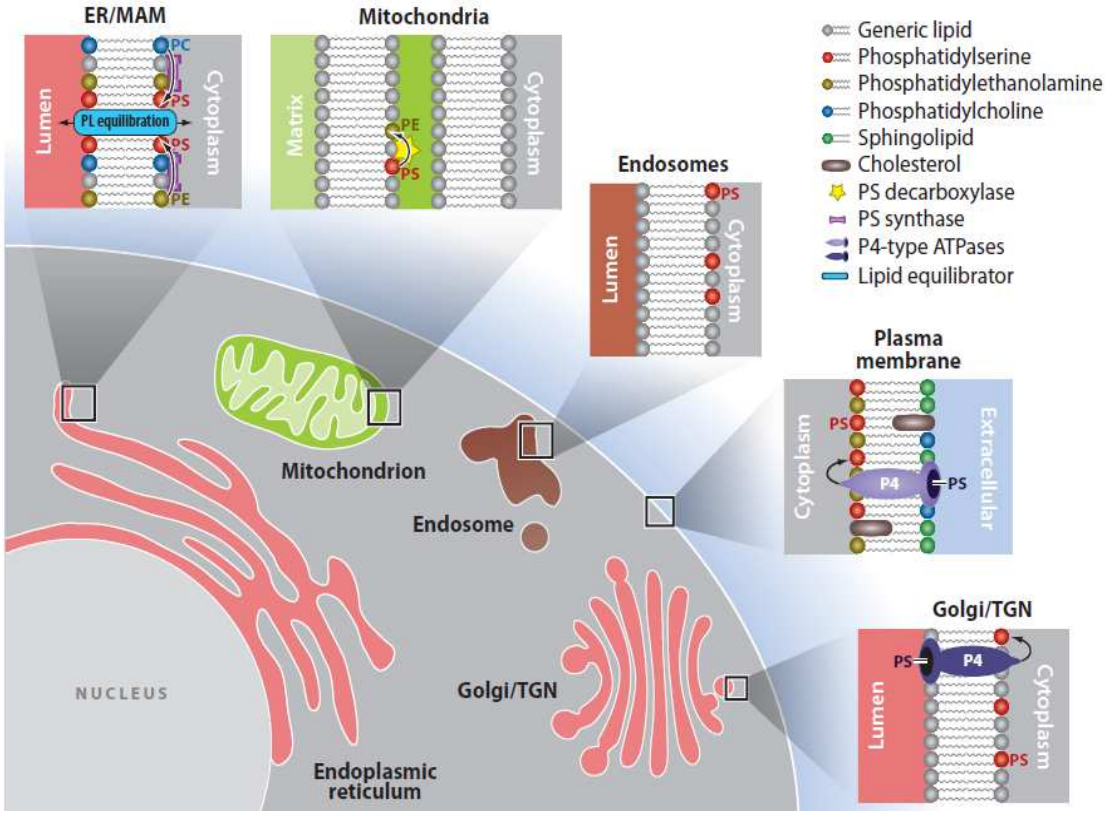

Figure 9 . Phosphatidylserine topology, synthesis, and transport across bilayers in mammalian membranes. The topology of phosphatidylserine (PS; red headgroup) is illustrated where known. PS is produced in the mitochondrial-associated membranes (MAMs) of the endoplasmic reticulum (ER) from phosphatidylethanolamine (PE; light brown headgroup) or phosphatidylcholine (PC; blue headgroup) by PS synthases. PS is decarboxylated to PE by PS decarboxylase on the outer leaflet of the mitochondrial inner membrane. Phospholipids (PLs) are translocated to the inner (luminal) leaflet of the ER by a nonspecific equilibrator mechanism, similar to a scramblase. P4-type ATPases in the late Golgi complex/trans-Golgi network (TGN) and plasma membrane actively transport PS to the cytoplasmic leaflet to create or maintain PS asymmetry. The topology of cholesterol (dark brown oblong) and sphingolipids (dark green headgroup) at the plasma membrane is also shown. Unspecified lipids are represented by a gray headgroup.

Therefore, phosphoinositides, rather than PS, are the preferred phospholipids for many proteins, likely owing to their stronger charge. This preferential interaction has made phosphoinositide a major player in controlling the construction of fine membrane structures utilized for a variety of cellular functions, including cell migration, membrane trafficking, and cell proliferation[158].

6.4.2 Roles of the Phospholipid head group and fatty acid tail

Phospholipids constituting the majority of lipid bilayers have a variety of polar head groups, differing in size and charge. For example, the polar heads of PE are smaller than those of PS, PC, and SM, whereas phosphoinositides have very large polar heads because of the presence of the phosphate- bearing inositol ring The size of the polar head group causes each of these lipid types to form different structures and PE is defined as a conical-shaped lipid and by itself forms a structure with negative curvature, similar to the inverted hexagonal phase of tubes, with the head groups on the inside and the hydrophobic tails on the outside. In contrast, PI and phosphoinositides have an inverted conical shape and form structures with positive curvatures. PC, PS, and SM are cylindrical-shaped lipids, which preferentially form flat bilayer structures. In the eukaryotic PM, PC and PS are the most common constituents of the outer and inner leaflets, respectively. PC and PS alone form flat or gently curved planar membranes in vitro, but PE, cholesterol, and phosphoinositides cannot form bilayers without other lipids. Furthermore, the presence of these lipids causes

destabilization of the planar membranes formed by PC and PS, which seems to be required for vesicle budding, fusion, and other shape changes involving biological membranes[161]. Therefore, local accumulation of these lipids in specialized areas of the PM can modulate the membrane shape with their physical properties, electrostatic nature, and through the recruitment of membrane-binding proteins.

Lipid geometry also depends on the acyl chains, particularly the presence of double bonds that produce a kink in the middle of the chain[162]. For example, the oleoyl chain consists of 18 carbons with one double bond (C18:1) and occupies a larger volume than a palmitoyl chain (C16:0) that consists of 16 carbons without any double bond. Thus the size of the polar heads and species of acyl chain influence the lipid packing of membranes. Furthermore, cholesterol, while not a phospholipid, is also abundant in the PM and is a particularly unique component because it is amphipathic, with a polar hydroxyl group and a hydrophobic planar steroid ring. These properties allow it to intercalate between the phospholipids, with its hydroxyl group near the polar head groups and its steroid ring parallel to the acyl chains of the phospholipids, thus improving lipid packing. The PM contains phospholipids with relatively high-saturated fatty acids as well as high levels of cholesterol allowing for tight lipid packing. In contrast, the ER is characterized by loose lipid packing due to the abundance of unsaturated phospholipids and scarcity of cholesterol.

PI and phosphoinositides contain high levels of polyunsaturated fatty acids, predominantly consisting of 1-stealyl and 2-arachidonyl acyl chains. An arachidonyl chain (C20:4) has four double bonds, and therefore, its acyl chain bends sharply. The large polar head group and abundance of arachidonic acid in phosphoinositides cause them to disturb lipid membrane packing and, in regions of the membrane where phosphoinositides are concentrated, larger spots of lipid-packing defects may be formed. Indeed, brain PI(4,5)P2 [dominantly 1-stearyl-2-arachidonyl PI(4,5)P2]was found to be a potent modifier of lipid bilayer when gramicidin A channels' sensitivity to changes in lipid bilayer properties was measured[163].Furthermore, cytosolic proteins seem to interact electrostatically with loosely packed lipids more easily than closely pace lipids In contrast to the loose-packing nature of individual phosphoinositide molecule, phosphoinositides mixed with other phospholipids

in a global cellular membrane are known to form phosphoinositideenriched microdomains[164,165]. These microdomains are thought to be further stabilized or reinforced in the presence of phosphoinositide-clustering proteins.Thus cytosolic proteins are probably more suitable toaccess and interact with phosphoinositides that are concentrated at these “hot spots.”

6.4.3 Electrostatic Interactions Between Phosphoinositides and Cytoskeletal Proteins

Phosphoinositide binding at cationic-charged regions rich in basic amino acid residues has been observed for a variety of cytoskeletal proteins[166]Importantly, a lot of actin regulatory proteins contain basic amino acid residues that can in fact interact with phosphoinositides, mainly PI(4,5)P2. Although the net charge of PI(4,5)P2 is less than that of PI(3,4,5)P3, the contribution of PI(3,4,5)P3 to the surface charge of the membrane is presumably low because of the lower amount of PI(3,4,5)P3 found in the membrane compared with PI(4,5)P2. PI(4,5)P2 has been shown to interact with multiple actin regulatory proteins, including vinculin[167,168], talin-actinin[169], cofilin[170], gelsolin[171] Ezrin-Radixin-Moesin (ERM), and other actin regulatory proteins. The binding of phosphoinositides to the actin regulatory proteins regulates the rearrangement of cortical actin filaments, which support the membrane deformation to construct filopodia and lamellipodia. Furthermore, this binding also activates G-actin nucleation-promoting factors (NPFs), including neural Wiskott-Aldrich syndrome protein (N-WASP) and WASPhomologous verprolin homology protein 2 (WAVE2), both of which are known to be ubiquitously expressed in the cell[172]. These data suggest that inositol lipid signaling influences the remodeling of the actin cytoskeleton and membrane morphology through changes in the levels of PI(4,5)P2 at the PM. Indeed, increased expression of PI(4)P5K induces massive actin filament formation[173]while expression of synaptojanin, a phosphoinositide phosphatase, causes disruption of actin filaments[174]. Taken together, it appears that an increase in the level of PI(4,5)P2 tends to promote actin filament formation, whereas a decrease in the level of PI(4,5)P2 leads to actin depolymerisation [175].Notably, PI(4,5)P2 is unexpectedly concentrated in lipid rafts[176] where Rho- and ADP-ribosylation factor (Arf)-GTPases facilitate PI(4,5)P2-synthesizing PI 5-ki-nases by inducing the recruitment of these kinases to these sites in the PM. Thus actin assembly can be initiated with remarkable efficiency at these PI(4,5)P2-rich rafts through the enhanced recruitment and activation of WASP and ERM proteins, leading to the promotion of the actin polymerization and actin filament assembly[177] Thus PI(4,5)P2- regulated rearrangement of actin filaments in compartmentally restricted areas of the PM seems to concentrate all of the factors necessary for micro-structure formation.

6.4.4 Phosphoinositide-binding domains

A variety of membrane-associated proteins have phosphoinositide- binding domains with binding pockets for particolar phospholipids. These domains recognize phosphoinositides with structural specificity Among them, the PH domain was the first phosphoinositide-binding domain reported and is conserved among a large number of proteins in the human proteome[178]. The other phosphoinositide-binding domains are PX[179] Fab1, YOTB, Vac1p, and EEA1 (FYVE)[180], ENTH [181], AP180 NH2-terminal homology (ANTH) some of PDZ such as those found in Syntenin, PTP-BL, CASK, and Tiam-1[182],Tubby[183]Dock homology region 1 (DHR-1)[184]GOLPH3 [185], some of C2 such as those found in synaptotagmin and PLAs[186], band 4.1, Ezrin, Radixin, and Moesin (FERM)[187]and glucosyltransferase, Rab-like GTPase activator, and myotubularin (GRAM) domains[188].

The PH domains that recognize PI,P2, PI,P3, or PI, P2 are involved in functions important during a variety of events in the PM. For example, once the PI,P3 hot spots are formed in the PM by the activation of PI 3-kinase, Akt/PKB is recruited to the PM through the PH domain and is activated. Akt/PKB is a serine/threonine kinase that binds to PI,P3 through its NH2-terminal PH domain and is activated by phosphorylation at Thr-308 and Ser-473.

Lipid specificity is also observed for the other phosphoinositide- binding domains. The ENTH domain specifically binds to PI,P2 . PIP is enriched in early endosomes and acts as a recruiter of PIP-binding proteins to this site, and the FYVE domains of early endosome antigen 1 (EEA1) and hepatocyte growth factor-regulated tyrosine kinase substrate (Hrs) show exclusive, high-affinity binding to PIP. However, the FYVE domain of protrudin localizes to endosome and binds to PI,P2, PI,P2, and PI,P3. The PX domains of SNX3, NADPH oxidase component, and p40phox also bind to PIP rather than PI(3,4)P2[189]On the other hand, the p47phox PX domain binds both lipids, but binds more strongly to PIP2.

Several of the phosphoinositide-binding domains have the capability to deform liposomes into tubules and small vesicles. For example, the ENTH domain deforms PI(4)P2-containing liposomes to small vesicles by inserting its NH2-terminal amphipathic helix into the membrane.

Furthermore, the BAR, F-BAR, and I-BAR domains preferentially bind to PI,P2 and PI,P3, allowing them to deform PI(,5)P2/PI,P3-enriched membranes into vesicles and tubular-like structures, although they can generally bind negative-charged phospholipids, such as PS. Some BAR and F-BAR domain-containing proteins are accompanied by an extra lipid-binding domain, such as PH and PX domains. The presence of neighboring PH and PX domains may help to target the protein to sites where a particular phosphoinositide exists. The membrane deforming activity of BAR, F-BAR, and I-BAR domains is highly dependent on lipid-binding ability, and lipid-binding deficient mutants lose membrane-deforming activity.

6.5 GENERAL PRINCIPLES FOR MEMBRANE CURVATURE FORMATION

The mechanisms of membrane deformation can be classified into three categories: lipid metabolism, protein scaffolding, and binding protein insertion/interaction[190].

6.5.1 Lipid Metabolism

The shape of each lipid molecule, cylindrical, conical, or inverted conical, is different. Enrichment of inverted conical or conical lipids is thought to drive membrane deformation. This enrichment can be achieved by increased lipid metabolism, which is mediated by the synthesis and/or transport of new lipid molecules to the membrane. The metabolism-mediated mechanisms include the enzymatic conversion of precursor lipids to usable forms as well as the addition of the head group onto the lipid backbone. The production of phosphoinositides with relatively large head groups might by itself be enough to induce membrane curvature, but the low concentration of phosphoinositides in the PM indicates that this is not the primary method used to alter global membrane curvature[191,192].However, phosphoinositides do appear to afford such effects locally in concentrated areas of the PM, such as clathrin-coated pits, caveolae, and near membrane receptors. Another metabolic mechanism employed to alter membrane curvature utilizes the hydrolysis of the

acyl chain, which removes one of the two acyl chains in the lipid molecule. For example, PA is normally a conical lipid, but lysophosphatidic acid (LPA) is an inverted conical lipid. Therefore, conversion of PA to LPA is assumed to induce curvature formation. It was proposed that PA-hydrolyzing activity of endophilin was one of such example. However, the activity was the contaminant from the source of the protein purification, and indeed the membrane deformation was mediated by the BAR domain of endophilin[193]. The transport of lipid molecules to induce membrane curvature can be mediated by flippases, which induce lipid asymmetry between hemi-layers during cytokinesis and cell migration[194] During apoptosis, type IV P-type ATPases (P4-ATPases) and CDC50 family proteins form a putative phospholipid flippase complex used for the translocation of PS and PE[195], exposing PS to the outer leaflet of the PM, which normally does not contain PS. Furthermore, the lipid scramblase, transmembrane protein 16F (TMEM16F), can also perform Ca^{2+}-dependent scrambling of membrane phospholipids, resulting in the exposure of PS to the cell surface leading to apoptosis[196].However, the full mechanism of such enzymatic regulation and its precise effects on membrane curvature are still unclear.

6.5.2 Indirect protein scaffolding

Membrane deformation using the scaffold-mediated mechanism was first found for caged vehicles, such as clathrincoated pits, which can be pinched off to form clathrincoated vesicles. Clathrin coats are involved in clathrin-mediated endocytosis from the PM to form endosomes. Clathrin coats are not membrane-binding proteins, but they are connected to the membrane through adaptor proteins (APs) or cargo proteins[197].On the other hand, COPI/II coats are involved in vesicle transport between the ER and the Golgi apparatus. Some components of COPI/II coats directly bind to the membrane, but GTPases such as Arf play important roles for COPI/II assembly on the membrane [198].In both cases, the formation of rigid lattice scaffolds, involving both the APs/cargo proteins as well as the secondary binding proteins, is thought to be the structural determinant of such caged vesicles. The membrane curvature formation can also be just friggere by the assembly of proteins on the membrane without specific membrane binding properties. This mechanism is recently proposed as protein “crowding” for curvature formation[199] In this case, the assembly of proteins on the membrane with some anchoring to the membrane can bend the membrane. However, the existence of crowding mechanism in vivo is still unclear. The protein assembly of, for example, AP protein complex at the clathrin- coated pit might be considered to be such example[200].

Classically, the actin polymerization is thought to be a major source of force generation for membrane curvature formation, for protrusive structures such as lamellipodia and filopodia. The actin filaments exist in high density beneath the plasma membrane, and thus can be thought to be a mechanism for indirect protein scaffolding for membrane curvature formation. The elongating barbed ends of polymerizing actin filaments are thought to push membrane by their filling of the space between the filaments and fluctuating membrane, where the filling by actin filaments functions as “ratchet” for membrane protrusion[200].

6.5.3 Binding Protein Insertion/Interaction

There are two mechanisms of membrane deformation that occur through the direct binding of the proteins to the membrane. One utilizes the electrostatic interactions between the lipid-binding domains on the protein surface and the negatively charged lipids at the membrane. Two wellknown classes of proteins with structural folds conducive to this type of electrostatic interaction are the BAR domain containing proteins (BAR proteins) and the endosomal sorting complexes required for transport (ESCRT) proteins. The recently identified BAR proteins are thought to deform membranes primarily by electrostatic interaction follone by the recruitment of other membrane-modifying proteins. The ESCRT proteins utilize their electrostatic interactions with the membrane to function in membrane budding, which is essential for releasing virus vesicles to the outside of the cells as well as the biogenesis of membrane organelles containing vesicles, otherwise known as the multivesicular body[201] The details of ESCRT-mediated membrane changes are described in depth in other reviews [202].

Direct protein insertion into the membrane is another mechanism used to alter membrane curvature. This mechanism of membrane deformation was first characterized for proteins containing an amphipathic helix, whereby the cylindrical helix is laid down on the membrane, exposing the hydrophilic surface to the cytosol[203]. Although the exposure of this surface prevents the penetration of the helix into the membrane, like that of a transmembrane protein, the hydrophobic surface alone is still inserted into the hemilayer of the membrane, thereby enlarging the area of the inner leaflet of the bilayer and causing membrane deformation. If the hydrophilic surface is positively charged, the helix interacts with anionic phospholipids in the cytosolic layer of the membrane, while inserting the other side into the hydrophobic interior, which is the case for the ENTH domain of epsin and the N-BAR domain of amphiphysin and endophilin. The positively charged, unstructured amino acids in the NH2-terminal region of the ENTH domain, in combination with the structure region of the domain, interact specifically with the head group of PI(4,5)P2. The interaction of ENTH domain and PI(4,5)P2-containing membrane then turns the last 17 residues into an amphipathic helix, which is then inserted into the membrane[204].

Furthermore, if the hydrophilic surface of the helix does not have a strong charge, then the helix has a tendency to function as a sensor for membrane curvature, capturing the vesicles for intracellular vesicle transport. Such a sensor function has been found in the amphipathic lipid packing sensor (ALPS) motif of the ArfGAP1, which is involved in COPI coat disassembly[205]. ALPS motifs have been found in proteins associated with the nuclear envelope (Nup133), the ER (Atg14L), and the cis-Golgi (ArfGAP1, GMAP-210) and thus seem to be involved in the events of the early secretory pathway[206]. The ALPS motif of Arf- GAP1 is unstructured in solution, but inserts its bulky hydrophobic residues between loosely packed lipids, and forms an amphipathic helix on highly curved membranes.[207,208] This helix appears to favor insertion at sites of lipid packing defects that arise in the external leaflet of a liposome when its curvature increases. Furthermore, the ALPS/ArfGAP1 helix differs from classical amphipathic helices, as there is an abundance of serine and threonine residues on its polar face[209]. Thus ALPS motifs favor curvature and lipid-packing defects rather than curvature and electrostatic interactions. These ALPS motifs are characterized by their secondary amphipathic helix structures and are not related to a specific amino acid sequence[210]. In addition to amphipathic helices, proteins with stretches of hydrophobic residues are also known to form loop/ wedge-shaped insertions into the membrane, inducing deformation. Caveolins and

reticulons are examples of such membrane-embedded proteins that, after interacting with the membrane, undergo oligomerization to generate curvature.Furthermore, self-assembly of caveolin and reticolo can induce membrane remodeling to create plasma membrane invaginations and tubulate the ER[211] .A similar protein structure is also found in flotilin, which is a scaffold protein involved in a less-characterized clathrin-independent endocytic pathway[212].There are two additional important examples for membrane deformation mediated by membrane insertion. One is the eps15 homology (EH) domain-containing proteins 2 (EHD2) protein. The EHD2 protein is known to oligomerize,and this oligomerization and the insertion appear to be essential for membrane deformation[213]The C2 domain from several proteins, such as synaptotagmin, Doc2a/b, and group IVA cytosolic phospholipase A2 (cPLA2), induces and/or senses membrane curvature likely through membrane insertion, which occurs in Ca^{2+}-dependent manner[214]. The roles and mechanisms of C2 domain-mediated membrane deformation are discussed in other reviews[215].

6.6 THE BAR DOMAIN SUPERFAMILY

6.6.1 Identification of BAR Proteins

BAR proteins are classified as having a BAR (N-BAR), FBAR, or I-BAR domain depending on their sequence. However, all BAR proteins are composed of a helix bundle, where three helices of one monomer form into a dimer, producing a six-helix bundle that displays various degrees of intrinsic curvature.

Thus the structural classification of these three BAR domain subfamilies is less important. However, the important distinction between BAR proteins is in the degree of curvature innate to each BAR domain, which allows a cell to generate a large range of varying curvature when utilizing a scaffolding mechanism. In all BAR domains, the positively charged residues are enriched at a particular surface of the dimer, identifying it as the membrane contact site [216].With the exception of the I-BAR proteins, the membrane contact surface is found on the concave side (or the inside of the arc-shaped protein dimer). Considering only the dimer of the BAR domains, most BAR domains are thought to fit with negatively charged lipid membranes through their positive concave face. Furthermore, they induce membrane tubulation in vitro. Importantly, the membrane tubules formed by the BAR proteins are topologically the same as those found in the membrane invaginations of in vivo plasma membranes.

The amphipathic helix, in conjugation with the concave structure, is important for its ability to sense and induce membrane curvature. Hence, the N-BAR module plays a dual role in regulating membrane curvature. Insertion of NH2-terminal amphipathic helices into membranes causes changes in lipid packing and effectively creates local membrane curvature. Thus the NH2-terminal amphipathic stretch plays pivotal roles in membrane tubulation and shallow helical fold insertion into the membrane. The scaffolding and loop/wedge insertion mechanism are independent of each other; however, both are thought to work simultaneously to induce membrane curvature. In addition, the amphipathic helix can also function as a sensor for membrane curvature as it acts as an anchor for the membrane and can sense high levels of positive curvature as in case of ALPS motif. Moreover, a high concentration of BAR domains with amphipathic insertions has been shown to induce vesiculation of liposomes[217,218]. In terms of physical chemistry, each lipid molecule is thought

to adapt itself to an energetically lower state. It might be reasonable to assume that the lower state is achieved by the vesiculation of the tubulated membrane. It is likely that the high degree of membrane curvature generated by a hydrophobic insertion can make phase separation of membrane lipids by clustering specific lipids, which probably leads to the formation of boundaries between lipid clusters on the membrane[219] This boundary might function as cutting line for vesiculation or scission of the membrane[220.] It is proposed that shallow hydrophobic insertions are sufficient for vesicle formation, driving membrane fission, whereas crescent-like protein scaffolds, such as BAR domains without amphipathic helix or loop insertion support formation of membrane tubules, hence disfavoring fission.

6.6.2 Clathrin-Mediated Endocytosis

The most extensively studied function of BAR domains involves clathrin-mediated endocytosis (CME)[220,221].CME is initialized by clathrin-coated pit formation, which is the proposed site of sequential recruitment and detachment of the BAR proteins[222].It is hypothesized that first, an F-BAR protein with shallow curvature, FCHo1/2, is recruited, which initiates the assembly of the clathrin-coated pits[223] .

CME is initialized by clathrin-coated pit formation, which is the proposed site of sequential recruitment and detachment of the BAR proteins[222] . It is hypothesized that first, an F-BAR protein with shallow curvature, FCHo1/2, is recruited, which initiates the assembly of the clathrin-coated pits[224].Then, F-BAR proteins, such as FBP17 and PACSINs, are recruited, followed by BAR domains with significant curvature, such as endophilin and amphiphysin. The FCHo1/2 proteins are unique among the BAR proteins because they do not have the SH3 domain found in other BAR proteins, but instead, FHCo1/2 has a motif for binding to epsin and other mole-cules, providing the scaffold for additional protein binding at the clathrin-coated pits[225].The other BAR proteins, including those recruited at the clathrin-coated pits after FCHo1/2, have the SH3 domain that can bind to donami and N-WASP. Dynamin is an essential protein that causes the mechanical scission of the clathrin-coated pits into clathrin-coated vesicles and has been shown to cooperate with BAR proteins during membrane scission[226]. Furthermore, the sequential recruitment of BAR proteins at the clathrin-coated pits is also observed in yeast [227]and while a dynamin-like molecule does exist in yeast, it is not essential for scission of clathrin-coated pits. Instead, WASP-homolog-mediated actin polymerization plays an essential role during this process228. However, detailed understanding of how this sequential recruitment is regulated is currently limited.

It is known that PI(4,5)P2 plays a crucial role in CME. Clathrin-coated pit formation is initiated in PI(4,5)P2-enriched membranes, and PI(4,5)P2 is essential for the early steps in CME, namely, nucleation, cargo selection, and coat assembly, whereas the latter steps, such as scission and uncoating, depend on PI(4,5)P2 elimination. A lot of proteins associated with clathrin-coated pits bind directly to PI(4,5)P2, but clathrin does not. The clathrin-binding proteins, such as epsin and AP180, have ENTH and ANTH domains, respectively, that interact with PI(4,5)P2. Classical BAR domain-containing proteins, such as endophilin and amphiphysin, also bind to PI(4,5)P2 and can deform PI(4,5)P2-containing membranes[229]. However, it should be noted that BAR domains generally do not recognize PI(4,5)P2 specifically, rather bind to membrane with electrostatic interactions. Furthermore, dynamin also binds to PI(4,5)P2 through its PH domain. After the early

steps of CME are complete, endophilin is thought to recruit the PI(4,5)P2 phosphatase synaptojanin, which depletes PI(4,5)P2 from the clathrin-coated pits, thereby inducing clathrin uncoating and scission[230]. Thus the CME process is closely regulated by PI(4,5)P2.

Furthermore, the BAR proteins appear to finely regulate actin polymerization during CME, depending on the membrane size and structure. The first example, demonstrating the dependency of actin polymerization on the size of the membrane, indicated that actin polymerization by Toca-1 and FBP17 in combination with N-WASP was affected by the diameter of the liposome[231].The curvature-dependent formation of actin filaments was also observed when actin polymerization was induced by the BAR-PX domain of SNX 9 on phosphoinositide-coated silica beads of a defined curvature[232].In this case, the actin filaments were found to be elongated toward the neck of constricting clathrin- coated pits.

Therefore, actin polymerization was found to push the membrane in analogous ways during both filopodia, lamellipodia, and clathrincoated pit formation, presumably under the regulation of a diverse set of BAR domain proteins[233]. Along with the BAR proteins, N-WASP is thought to induce actin polymerization at the clathrin-coated pits,[234]. However, N-WASP-mediated actin polymerization by itself is not required for endocytosis in cultured cells under normal conditions without membrane tension. Notably, this actin polymerization is required for endocytosis under membrane tension, presumably to support the membrane during scission[235]indicating a context specific need for N-WASP-mediated polymerization. In addition to N-WASP, other actin regulatory proteins, such as WAVE, formin, VASP, and Cobl, can also function downstream of the BAR proteins[236].

6.6.3 Other invagination/endocytotic structures

The involvement of BAR domain proteins in the formation of other membrane structures is less clear. Caveolae are flask-shaped invaginations that are enriched in cholesterol, sphingolipids, and PI(4,5)P2,[237]The major structural component of caveolae is the integral membrane protein caveolin, a membrane-embedded protein that undergoes oligomerization to generate curvature[238].Caveolins have transmembrane domains that contain an amphipathic helix inserted into the bilayer[232] This helix also binds cholesterol and could cause the raftlike lipid composition of the caveolae[232] .Recent work has identified a protein familyassociated with caveolae, which includes cavin1[238]. Cavin proteins interact with caveolin in mature caveolae, and the deletion of cavin results in the loss of caveolae[239].Thus this cavin complex may function as a scaffold for caveolin and other components of caveolae.

With regard to F-BAR-domain proteins, PACSIN2 was shown to be present in caveolae and appears to be important for morphogenesis of the caveolae structure[240].Indeed, depletion of PACSIN2 results in the loss of morphologically defined caveolae. Similar to the BAR proteins in the clathrin-coated pits, PACSIN2 binds to donami and N-WASP through its SH3 domain[241].There is an Asn-Pro-Phe (NPF) motif in PACSIN2 that can bind to EHD2[242] which is thought to stabilize the caveolae through the association with actin filaments[243]likely induced by PI(4,5)P2 Thus it is clear that PACSIN2 plays an important role in the formation of caveolae. Another F-BAR protein, NOSTRIN, is also reported to be localized at caveolae, although it is not clear specifically how

NOSTRIN functions in this membrane structure[243]Among the variety of endocytotic pathways that internalize numerous cargoes, several appear to proceed independently of the canonical protein clathrin. The clathrin-independent carriers (CLIC) and GPI-enriched endocytic compartments (GEEC) pathways play major roles in such uptake[244].GTPase regulator associated with focal adhesion kinase- 1 (GRAF1) protein, which contains an NH2-terminal BAR domain, a PH domain, a Rho-GAP domain, a prolinerich domain, and a COOH-terminal SH3 domain, is shown to be important in coordinating small G protein signaling and membrane remodeling to facilitate internalization of CLIC/GEEC pathway cargoes[245].In this pathway, GRAF1 localizes to PI(4,5)P2-enriched sites in the membrane via its NH2-terminal BAR and PH domains, and deforms the membrane to facilitate endocytic intermediate formation.

6.6.4 Membrane Protrusions

The protrusive structures found on membrane surfaces had previously been believed to be organized solely by the power of actin polymerization[246].Therefore, it was surprising that membrane deformation was found to be, at least in part, mediated by BAR proteins. Currently, there are two classes of BAR proteins with protrusion forming ability, proteins containing an I-BAR, and some of the FBAR domain-containing proteins, which comprise only a small population of the entire BAR protein superfamily. The I-BAR domain, which has a kink in the helix, was first found in IRSp53 and then later discovered in MIM[247]The kink produces the surface of the inverted membrane, to the opposite direction than do classical BAR domains. The I-BARs can deform membranes in vitro into protrusion-like shapes, consequently clarifying the role of I-BAR domain in negative curvature formation. However, it is still uncertain whether such membrane deformations are actually taking place in vivo, although several researchers have concluded that I-BAR proteins are localized at and involved in the formation of filopodia and lamellipodia[248]In other words, it is still unknown whether protrusions forming independently from actin filaments actually exist in the natural cellular environment. As Ahmed et al.[249] pointed out, the artificial filopodia induced by the I-BAR domain in cell culture and the “genuine” filopodia observed in vivo show distinctively different dynamics: the former is relatively stable and less motile with a lifetime of more than 10 min, compared with the latter with a lifetime of 79–142s. Importantly, the full-length IRSp53 has the scaffolding ability to generate actin-mediated forces, which may explain the differences in the filopodia dynamics. The relative contribution of curvature- sensing, -generating, and scaffolding is currently unknown, and further studies are necessary to provide additional insight into the mechanism of IRSp53-mediated filopodium formation. Another class of BAR domains with protrusion-forming activity was found in srGAP proteins that were classically called as Slit-Robo GTPase activating proteins. The srGAP family of proteins consists of four family members, srGAP1, 2, 3, and 4, which have from the NH2 terminus an F-BAR domain, a Rho-GAP, and an SH3 domain. Although each family member contains a GAP domain, there are differences in GTPase activity between the proteins. All four family members display spatially and tem-porally distinct patterns of expression in the central nervous system[250] and have been shown to regulate cell migration and neuronal morphology in mammalian cells. Surprisingly, the overexpression of the F-BAR of srGAP2 did not cause invagination, but instead led to outward protrusions along the cell surface[251].As well, srGAP1 and srGAP3 induce filopodia formation, although they are less potent than srGAP2. And incubating this domain with liposomes caused deformations of the membrane similar to those created by the

IRSp53 I-BAR domain in vitro. These data were unexpected because F-BAR domains, in general, had been believed to induce positive membrane curvature. However, it is plausible that the F-BAR domain of srGAP functions like I-BAR, although there is no reported structure for the F-BAR domain of those proteins to corroborate this hypothesis. Thus this family of Rho-GAP is now defined as inverse F-BAR (IF-BAR), which is functionally distinct from other F-BAR domains. Recent studies show that the F-BAR-containing srGAP family of proteins can regulate dendritic spine morphogenesis. Dendritic spines, small bulbous protrusions found on neuronal dendrites, are postsynaptic structures that receive inputs from axons. Spine formation, remodeling, and shape change are associated with the brain's ability to store and process information in response to an experience. With the use of primary cultures of neurons, both srGAP2 and sr- GAP3 were shown to promote dendritic spine maturation, presumably by facilitating dendritic filopodia formation at the site of developing spines[252].The overexpression of the GAS7 F-BAR domain has also been reported to induce cellular protrusions, which are suggested to be related to neurite extension[253] However, the mechanisms of these relationships remain unclear because the structures have not been solved yet.

6.6.5 How Is the BAR Domain Superfamily Regulated?

The BAR domain superfamily is unique in its structural characteristics and its structure-membrane curvature interactions. Therefore, because of their numerous biological functions, it is important to understand how the BAR domain superfamily is regulated. A large number of cytosolic proteins are known to be activated and transduce signals upon phosphorylation or the addition of a charge to the protein. Recently, the BAR domains of ACAP4 have been reported to be activated by phosphorylation during membrane association in a manner dependent on epidermal growth factor (EGF) stimulation[254].However, when we consider the increase of negative charge brought by phosphorylation, the consequence might be the opposite, because an addition of negative charge may enhance repulsion from anionic lipids of the membrane. Drosophila syndapin/ PACSIN is also reported to be phosphorylated, but in this case, the phosphorylation inactivates the membrane tubulation ability[255] .Mammalian PACSIN1 and PACSIN2 are also reported to be phosphorylated, which results in defective neuronal morphologies and/or functions[256] Because phosphorylation introduces a strong negative charge, it is assumed that the electrostatic membrane interactions are destroyed, thereby leading to weaker membrane affinity. Autoinhibition is a widely used mechanism for the regulation of multidomain proteins. For example, N-WASP is regulated by the intramolecular interaction between the VCA and the CRIB motif[256] This interaction is released by the binding of PI(4,5)P2 and Cdc42, thereby freeing the VCA to associate with the Arp2/3 complex. WAVE is also regulated by protein complex formation, where the VCA region is exposed through phosphorylation and binding of the small GTPase Rac[257] However, among the BAR proteins, such autoinhibition has not been reported. Only one curious example is PACSIN1, in which the SH3 domain is proposed to interact with the F-BAR domain intramolecularly; however, the lack of a 1:1 stoichiometry for the F-BAR and the SH3 domains in the crystal structure indicates that this is a weak interaction[258]that would not be surprising if the regulation of BAR proteins depended on molecule-molecule interactions (i.e., interactions with other proteins or lipids). This type of mechanism is known to be utilized in the regulation of SH3 binding proteins. In this process, if IRSp53 is phosphorylated by Par1b kinase or an unidentified kinase downstream of GSK3, then the binding of the SH3 domain is hindered by the binding of 14–3-3 protein [259]). However, to date, no

regulatory mechanism controlling the membrane deforming ability of the BAR proteins has been discovered. So far, it is not clear how BAR domain assembly, which is required for forming a stable membrane micro-structures, is regulated. Membrane bending due to thermal fluctuationmay be sufficient for triggering BAR domain assembly. This initial BAR assembly likely results in the assembly of several additional molecules, which may lock the membrane into the conformational structure formed by the protein domains. In this case, BAR proteins are pure sensors of membrane curvatures, of which no particular regulation might be required. However, this theory has not yet been tested directly. If BAR proteins are actively engaged in the formation of membrane curvature, then it is still unclear how the membrane deforming ability of the BAR proteins is regulated, even 9 years after the structural determination of the amphiphysin BAR domain.

6.6.6 Bar proteins and disease

The members of the BAR protein superfamily play crucial roles in the formation of fine membrane micro-structures, such as membrane protrusions, filopodia, lamellipodia, and endocytotic invaginations. Therefore, defects in the function of these proteins are likely related to a variety of diseases. Cell culture and animal model knockout studies are powerful tools used to determine the physiological role of a protein in vivo. Here, we describe several BAR protein mutations connected to disease pathology as well as the phenotypic consequences of lacking one or more BAR protein in a mouse model. Multiple F-BAR proteins affect immune cell function through their effects on membrane cytoskeleton remodeling. For example, an alternatively spliced form of CIP4 localizes in the phagocytic cup ofRAWmurine macrophage cells, indicating a potential function in phagocytosis[259].Furthermore, CIP4 is necessary for integrin-dependent T cell trafficking, and CIP4-deficient T lymphocytes cause impaired T-cell-dependent antibody response, impaired contact hypersensitivity, and defective adhesion to immobilized VCAM1 and ICAM1 in endothelial cells, leading to impaired transendothelial migration[260].The membrane-deforming ability of the BAR proteins was pioneered by the study of amphiphysin with mutation defective in muscle formation. Amphiphysin is necessary for the organization of the excitation-contraction coupling machinery (t tubule), which is long invagination in muscles, but it is not necessary for synaptic vesicle endocytosis in Drosophila[261].In mammals, mutation of amphiphysin 2 (Bin1) causes autosomal recessive centronuclear myopathy by interfering with the remodeling of t tubules and/or endocytic membranes[262]In this case, two missense mutations affecting the BAR domain disrupt the membrane tubulation properties in transfected cells[263].

The endocytosis and exocytosis of neurotransmitters and their receptors are crucial for a large number of neuronal functions. Dynamin, endophilin, and PACSIN1/Syndapin I are essentially involved in such processes, presumably through their functions in scission, subsequent uncoating of cargo, and/or recycling. PACSIN1 is crucially involved in the morphogenesis of neuronal cells in cooperation with N-WASP and dynamin[263].Furthermore, PACSIN1 knockout mice suffer from seizures, a phenotype consisten with excessive hippocampal network activity[264] as well as defects in presynaptic membrane trafficking processes. At the molecular level, it appears that PACSIN1 plays an important role in the recruitment of all dynamin isoforms and is a central player in vesicle-membrane fission reactions[265] Thus PACSIN1 acts as a pivotal membraneanchoring factor for the dynamins during regeneration of synaptic vesicles.

Unlike PACSIN1, triple knockout of all three mouse endophilin proteins did not cause defects in endocytotic vesicle scission, but led to defects in the uncoating of clathrincoated vesicles, thereby reducing the dynamics of synapse transmission[266].This defect is likely caused by the loss of the ability of endophilin to bind to and recruit synaptojanin, the PI(4,5)P2 phosphatase that functions to uncoat these vesicles[267]. However, further studies are needed to elucidate the precise mechanisms involved in this process[267].Interestingly, CIP4 appears to function in the formation of neurite, although it is unclear how CIP4 functions in endocytosis or other processes in neurons. CIP4-null neurons are specifically precocious in forming neurites (stage 1–2 transition), but not in polarization (stage 2–3 transition), indicating that CIP4 expression inhibits neuritogenesis. If CIP4 is a negative regulator of neuritogenesis, then the CIP4-null neurons would be expected to form longer neurites than those of the wild-type controls, and this is indeed the case. The CIP4-null cortical neurons extend axons 1.5 times longer than the controls at 1 day in vitro[336] .One additional link between CIP4 and neuronal health is through the huntingtin gene, which CIP4 can bind to, thus potentially affecting the symptoms and progression of Huntington's disease[269].As described above, srGAPs which have Rho-GAP activities are important multifunctional adaptor proteins involved in various aspects of neuronal development, including axon guidance, neuronal migration, spine maturation, and synaptic plasticity. Therefore, the defects of srGAP genes are thought to link to some neurodevelopmental disorders, such as mental retardation, schizophrenia, and seizure. The srGAP3 protein, alternative name of mental-disorder associated GAP protein (MEGAP), is reported to be disrupted and functionally inactivated by a translocation breakpoint in a patient who shares some characteristic clinical features, such as hypotonia and severe mental retardation, with the 3psyndrome (caused by deletions affecting many genes at the terminal end of chromosome 3p)[270] Loss of srGAP3 was found to result in reduced density of spines and be linked to impaired learning and memory[271] Its knockout mice lead to mismigration of postnatal neural progenitors and blockage of the cerebral aqueduct, inducing lethal hydrocephalus[272]or schizophrenia-related behaviors[273]. On the other hand, srGAP2 is implicated in a severe neurodevelopmental syndrome causing early infantile epileptic encephalopathy[278]. Interestingly, there are human specific splicing isoforms of srGAP2, which might be involved in human specific brain development[273].Intriguingly, the role of PACSIN1/Syndapin I also extends to cilia formation in the sensory hair cells of the inner ear in zebrafish, where it is required for formation of both microtubule-dependent kinocilia and F-actin-rich stereocilia[279]Furthermore, two less characterized F-BAR domaincontaining proteins, FCHSD1 and FCHSD2, are also reported to be involved in hair cell stereocilia function through regulation of actin polymerization[281].

7. EXTRACELLULAR VESICLES : PART B

7.1 Classification of extracellular vesicles

The extracellular space of multicellular organisms contains solutions of metabolites, ions, proteins and polysaccharides. However, it is clear that this extracellular environment also contains a large number of mobile membrane-limited vesicles for which they are defined as "extracellular vesicles" (EVs). Within the past decade, extracellular vesicles have emerged as important mediators of intercellular communication, being involved in the transmission of biological signals between cells

in both prokaryotes and higher eukaryotes to regulate a diverse range of biological processes. The transfer of membrane components between donor and acceptor cells was first demonstrated in 1973[282].EVs include exosomes, shedding microvesicles (MVs)/ectosomes and apoptotic bodies .The common feature is all the three Evs subtypes is a lipid bilayer membrane that surrounds a specific cargo of biomolecules, e.g., proteins, RNA, or cellular debris but their size and buoyant densities vary significantly[283]. Exosomes are thought to be around 30–150 nm in diameter and have a buoyant density of 1.10–1.14 g/mL with a cup-like morphology when observed under the transmission electron microscopy4 Contrary to exosomes, ectosomes (MVs) are large vesicles ranging from 100–1000 nm in diameter ubiquitously assembled at and released from the PM through outward protrusion or budding[284].

Apoptotic blebs are protrusive blisters formed when cellular plasma membrane delaminates from the cortical cytoskeleton, covering the entire surface of apoptotic cells. The formation of apoptotic blebs is a physical process that results from an increase in hydrostatic pressure following cellular contraction[285]. This dynamic cyclic process of bleb formation and retraction can occur over sustained periods during the progression of programmed cell death[286]. Apoptotic blebs become packed with cellular organelles and chromatin to form the basis of fragmentary membrane-clad apoptotic bodies. Some in vitro studies have reported that inhibition of apoptotic blebbing significantly impaired corpse clearance by monocytes and macrophages[287,288].Apoptotic bodies are the final consequences of cellular fragmentation. They are 50-5000 nm extracellular vesicles that contain intact organelles, DNA, and histones[289].

7.2 Pathway involving various types of vesicles

The evolution of multicellular organisms from unicellular ones required that cells develop methods to “communicate” with neighboring and distant cells within the organism[290].

This intercellular communication was critical for the evolution of organs and groups of specialized cells within organs (tissues), as well as the regulation of proliferation, apoptosis, and differentiation of specialized cells (tissue homeostasis). Cells communicate by releasing soluble factors (e.g., hormones, growth factors, lipid mediators, cytokines, nitric oxide, etc.) that activate other cells locally or distantly through receptors or nonreceptor mechanisms. Recently, extracellular vesicles (EVs) are proposed as a novel mode of intercellular communication for both short and longer-range signaling events[291,292].Many forms of intercellular communication are involved in homeostasis and normal physiology so it is highly likely that toxicant-induced changes in intercellular communication are frequent and central to toxic manisfestations in the whole organism. There are thus two different pathways vesicular : a classical secretory pathway compared to non-classical secretory pathway.

The Golgi Apparatus is composed of flattened fluid-filled sacs that controls the flow of molecules in a cell as the case of proteins. Carbohydrates are added to the protein to complete its production. This finished product, glycoprotein, is pinched off' the Golgi apparatus, and is transported by a vesicle of the cell membrane. When these vesicles reach the cell membrane, they bind to a receptor on the surface and excrete the protein, where it can then undergo its function. In parallel as we can observe above, another way to release directly vesicles from the plasma membrane can take place

by ectosomes's secretion through an outward budding. In both cases, these vesicles take up into a ricipient cell by endocytosis and accumulate in early endosomes. The latter can be defined as a vesicular collection bags for intracellular comunication. Non-classical secretory pathway includes exocytic pathway and degradative pathway. The first begins with the formation of a multivesicular body (MVB) full of intraluminal vesicles (ILV) that is directed to the PM and these vesicles take the name of exosomes in the moment in which they are released. The secondo one occors when MVB fuses with the lysosomes and degradative enzymes become active. This step is important to eliminate ubiquitinated proteins and to reduce activated growth factors quickly.

7.2.1 Biogenesis of exosomes

The biogenesis and secretion of exosomes is believed to be mediated via a ceramide and/or ESCRT-dependent pathway. The ceramide-dependent pathway is based on the formation of lipid rafts in which sphingomyelin is converted to ceramide by sphingomyelinases. These ceramide-enriched domains have structural imbalances between monoleaflets causing the membrane to bend inward.In the ESCRT-dependent pathway, components of the ESCRT machinery are sequentially recruited to the endosomal membrane, which starts with Hrs, and bind to phosphatidylinositol-3-phosphate (PI(3)P) and the 3,5-bisphosphate (PI(3,5)P2) through lipid binding domains (e.g., FYVE, GLUE), and to the ubiquitinated protein (ESCRT-0). ESCRT-I and -II drive budding of ILVs, during which cargo is transported into the lumen, and ESCRT-III is recruited by Alix to complete budding and drive vesicle scission (spiral formation and pulling). DUBs deubiquitinate the protein and Vps4 recycles the ESCRT machinery. The now formed MVB is transported to the PM and through fusion, the ILVs are released into the extracellular environment.Exosomal luminal cargo predominantly consists of mRNA, miRNA and gDNA fragments, and a myriad of different proteins depending on the cell of origin. Generally, proteins involved in MVB formation, tetraspanins, membrane transport and fusion, transmembrane proteins, cytoskeletal components and proteins of cytosolic origin are part of exosomes. In addition, biomolecules associated with various diseases, including cancer, neurodegenerative diseases, such as Parkinson's, Alzheimer's and transmissible spongiform encephalopathies (prion disease), and inflammatory disorders have been identified in exosomes.Several other intracellular effectors may be involved in exosome release, although it is unknown if their role is related to the biogenesis of ILVs in MVBs or to their secretion.

Overexpression of diacyl glycerol kinase α (DGKα) in T cells inhibits activation-induced secretion of CD63/LAMP1-positive exosomes bearing Fas-ligand[292,293]and its inhibition leads to increased exosome release. Further analyses suggested that DGKα acts as a negative regulator of the formation of MVBs15, which then explains the decrease in exosome secretion when the protein is overexpressed. During HIV-1 viral release in human cell lines, in addition to increasing viral production and release, citron kinase (a RhoA effector) enhanced the release of vesicles bearing HSC70, CD82, and LAMP1 17suggesting that citron kinase is involved in the exocytosis of late endosomal compartments.

Finally, genetic approaches in the worm C. elegans have proposed the V0 subunit of V-ATPase as a possible mediator of the fusion of MVBs with the PM. Using EM, Liegeois[293,294] noted that cuticle

mutants appeared to specifically accumulate MVBs at the PM and identified the V0 subunit as the mutated gene responsible for this phenotype. This suggests that the V0-ATPase is required for the fusion of MVBs at the apical epidermal PM, leading to the production of the cuticle. Because several isoforms exist in mammalian cells, it is still unclear whether the V0 ATPase is involved in exosome secretion.

7.2.2 Biogenesis of ectosomes

Ectosomes are relatively heterogeneous, both in size and in their composition. In contrast to exosomes, the release of ectosomes does not require exocytosis . In cells where the process is greatest (dendritic cells[297], macrophages, microglia), the release is visible within a few seconds after stimulation by ATP from the P2X7 receptor and proceeds for several minutes, accompanied by retraction and the rearrangement of the cell's shape[295,296].An increase in the concentration of free Ca^{2+} acts as a cytosolic second messenger to sustain the release of ectosomes [399-400].However, the activation of protein kinase C by phorbol esters has also been shown to induce strong ectosome release responses [401].

Like exosomes, ectosome membranes are not identical to the PM of the cell of origin, but rather specific changes are induced upon nucleation and budding of the PM that cause this discrepancy. Although ectosomes contain similar types of cargo as exosomes, the molecular composition of ectosomes is less well defined compared with exosomes. Several studies have highlighted the fact that ectosomes contain a diverse population of proteins including matrix metalloproteinases (MMPs)[401,402]glycoproteins, e.g., GPIb, GPIIb-IIIa and P-selectin[403,404] integrins, e.g., Mac-1[405] receptors, e.g., EGFRvIII[406,] and cytoskeletal components such as β-actin and α-actinin-4[371].The formation of ectosomes at the PM primarily involves membrane constituents and their rearrangement, the cytoskeleton, and recruited proteins involved in membrane abscission. Upon nucleation, the interaction between cytoskeletal proteins and the PM is gradually lost, both by a local increase in cytosolic Ca^{2+} and protein degrading enzymes that induce disassembly of the cytoskeleton (e.g., calcium-activated calpains). In this way, an initial delamination of the PM from the cortical cytoskeleton occurs. Concomitantly, lipid translocases, enzymes that are involved in the exchange of lipids between the inner and outer leaflet of the membrane bilayer to maintain membrane asymmetry, are activated to induce changes within the bilayer such as exposure of phosphatidylserine on the outer leale and thus favoring budding and membrane abscission. This process is called a translocase-dependent mechanism.

To complicate matters further, changes in the PM organization may occur via translocase-independent mechanisms, as determined in B lymphocytes[408]and indeed annexin V-negative ectosomes derived from platelets and endothelial cells have also been detected [409,410].

Interestingly some elements of the ESCRT Complex are involved during the process bludding as TSG-101,Alix, ESCRT I highlighting how these processes are interconnected among themselves and have yet to be completely clarified[411,412].The ectosomes's formation is a rather different than

exosomes, so this process mostly involves plasma membrane in which the cytoskeleton undergoes arrangements and many proteins are are activated in order to get this type of vesicular release.

8. EXTRACELLULAR VESICLES : PART C

8.1 Extracellular vesicles role in neurological disorders

EVs present a central role in tissue and organ homeostasis and have been implicated indirectly to have a role in cellular senescence thanks to their constitutively secretion in physiological conditions. This theory has been confirmed by Hayflick and colleagues who identified cellular senescence about 5 decades ago leading to the hypotheses that cellular senescence may be either beneficial or detrimental to the cells and cellular enviroment[413]. Although historically the primary role attributed to exosomes has been the removal of unnecessary proteins from the cells, now we know that their principal function is their role in cell–cell communication[414]. In addition, they participate in several different functions and in a large variety of pathways such as immune response, pregnancy, tissue repair, and blood coagulation, among others.

EVs may have a significant undiscovered role in the normal physiological conditions. The release of EVs in cancer, neurodegenerative or other diseases alludes to a biological function. Whether it is a protective or pathogenic signal remains elusive. In a protective role, the cells may get rid of pathogenic or oncogenic proteins/RNA through EVs so as to minimize the damage within[413]. Furthermore, RNAs are transported by EVs from cell to cell and can modulate gene expression in the recipient cell. Alternatively, the EVs could be used as amplifiers to spread pathogenic molecules between cells. After transfer, mRNAs are translated leading to a new set of proteins in the target cell and miRNAs inhibit the expression of resident proteins[415]. In the immune system, antigen presenting cells (APCs) secrete exosomes bearing MHC-peptide complexes, which can activate T-cells, suggesting a role of exosomes in the adaptive immune response. On the other hand, tumor exosomes can induce anti-tumor responses but are also able to facilitate tumor development by suppressing immune responses, stimulating tumor growth, invasion, angiogenesis, and metastasis[416]. In the mammalian nervous system, cortical neurons release exosomes from somato-dendritic compartments. Synaptic glutamatergic activity mediates the rise in post-synaptic calcium levels triggering exosome secretion. As neuronal exosomes carry AMPA receptor subunits, they might play a role in synaptic plasticity by regulating the number of AMPA receptors in the post-synaptic membrane[417]. Exosomes thus may be implicated in trans synaptic communication in vertebrates and invertebrates. Current studies suggest a model where active neurons signal to oligodendrocytes and demand the delivery of supportive biomolecules via exosomes. Oligodendrocytes can then utilize these vesicles to locally transfer metabolites, protective proteins, glycolytic enzymes, mRNA and miRNA to axons, which may maintain axonal integrity[418].

Instead intercellular transfer of exosomes may be relevant for pathology in several neurodegenerative diseases, since pathogenic proteins such as prions, β-amyloid peptide, superoxide dismutase SOD1, α- synuclein and tau are released from cells in association with EVs[418]. These vesicles are assumed to spread the pathogenic proteins throughout the tissue leading to a maximal diffusion of the toxic misfolded or mutated protein from one cell to surrounding environment. This mechanism is able to induce the activation of CNS cells such as oligodendrocytes, astrocytes and microglia cells that in turn activate a pathological reaction leading to a development of immune response and to an impairment of the normal neuroprotective system **(Figure 10)**.

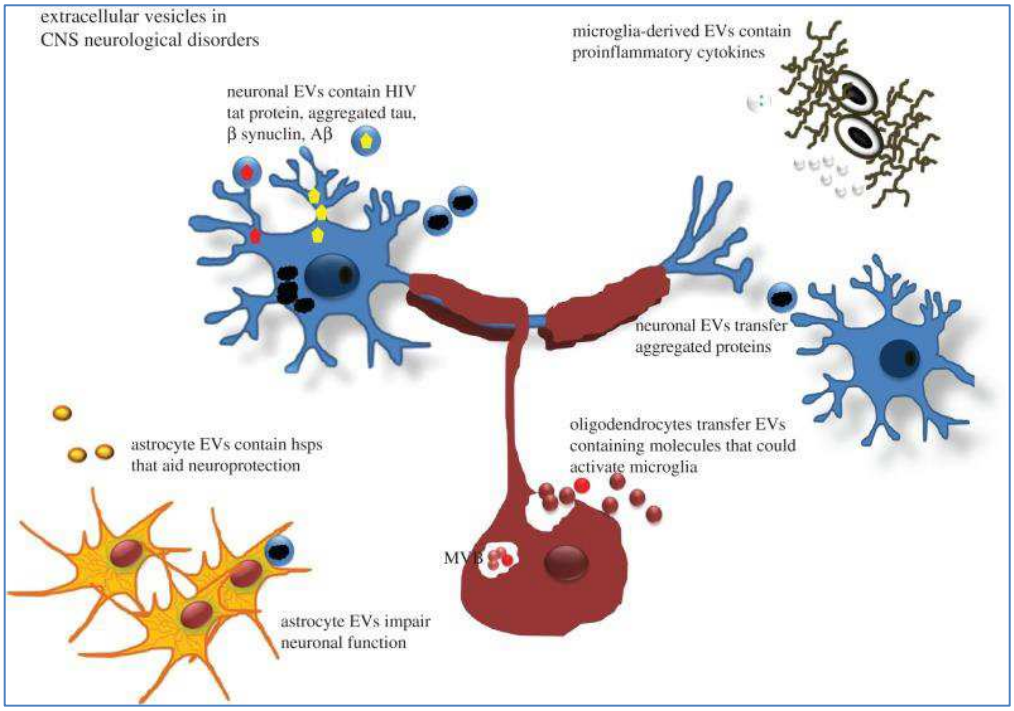

Figure 10.Extracellular vesicles in neurological disorders as mediators of pathogenic proteins spread in CNS[419]

Even though EV mediated signalling remains a grey area, it can be concluded that the exact role of EVs will depend on the precise conditions and functional state of the biological system in which they are released[420].

8.2 Diagnostic and Prognostic Potential of Extracellular Vesicles in Peripheral Blood

Given the importance of exosomes in normal and patho-biological conditions, extracellular vesicles are being studied more and more for their potential therapeutic uses in different kind of tissues such as brain and heart. For example, they are evaluated as biomarkers for the diagnosis and disease follow-up both in tumors, neurodegenerative and cardiovascular diseases and infective diseases. They are studied in their role from immunomodulators to suppressor able to stimulate or inhibit the immune system, as vectors for drug delivery and as therapeutic agents per se. Recent researches focus on EVs function in pregnancy as promoters of utero-placental angiogenesis and maternal tolerance to foetus and in their capacity of tissues regeneration[420].

Numerous studies have established that EVs can be detected in a multitude of biological fluids, such as saliva, urine, blood, ascites, breastmilk and cerebrospinal fluid[421,422]. In this context, blood is an immense source of EVs, and serum is estimated to contain approximately 3X 10^6 exosomes per microliter.

The use of EVs analysis encompasses several advantages over the traditional procedures of many soluble molecules in blood, such as hormones and cytokines. One significant advantage is the inherent protection of the EV cargo of proteins and RNA from degradation, thus rendering them intact and functional[422], otherwise, they would be rapidly degraded in blood[421]. This has proven to be particularly significant for the use of miRNA as valuable biomarkers because most RNA in blood exists as cargo of EVs. Regarding another aspect of stability, EVs appear to have a relatively long half-life in blood[421]. Therefore, EVs can likely be transported from any location of the body to the blood stream, thus making them easily accessible for analysis, compared with biopsies. This also has a significant advantage for the patient because the collection of a blood sample is a minimally invasive procedure associated with much less discomfort than a biopsy. Another advantage of EVs is related to the great dynamic range of molecules present in the bloodstream. It can often become an issue to detect relevant biomarkers because these diagnostic molecules frequently constitute a small part of the total number of molecules in a blood sample[422]. This is also the case for EV-associated proteins, which for exosomes denote <0.01% of the plasma proteome.

8.3 Overview of the techniques used to analyse extracellular vesicles (EVs) present in blood

The characterization of EVs in peripheral blood can be based on several of their biochemical and biophysical properties. These properties include size, cargo, density, morphologic findings, lipid composition and protein phenotype. Currently, a wide range of techniques facilitates EVs analysis. Some techniques have existed for years and are being further developed to embrace the challenges of this type of analysis. Other techniques have emerged as a consequence of the increasing interest within the field. First of all, it is evident that EVs isolation is essential and with no standardized protocols yet, this is a major focus in the field of EV research[423] The isolation includes numerous sequential centrifugation steps with increasing centrifugal force, thus using size and density properties of the EV subsets to separate these from other components of blood. Several methods exist to characterize the protein composition of EVs, related to either a surface marker phenotype or the proteins present in the EVs cargo. The analytical technique called Western blotting (WB) or immunoblotting is a widely accepted method used to detect specific protein markers in EVs. In general, WB is applied to validate the presence or absence of EV protein markers in purified samples based on the availability of specific antibodies. A major advantage of WB is the possibility of detecting intravesicular and membrane associated proteins with the same technology. The results obtained by WB are semi quantitative and can be correlated to the presence of a uniformly expressed protein. Flow cytometry is another powerful technique for multi parametric analysis of single biological particles and remains the most extensively used technique for enumeration and phenotyping of EVs in clinical samples. By suspending particles in a hydro dynamically focused fluid stream passing a laser beam, this technique allows simultaneous analysis of the physical

characteristics, including size and granularity, and expression of multiple antigens of up to thousands of particles per second[424] **(Figure 11).**

Figure 11. Overview of the techniques used to analyze extracellular vesicles (EVs) present in blood samples from a clinical and diagnostic perspective[425] (LOD=limit of detection).

Thanks to all these advantages, these techniques are the most important used in this thesis project for EVs isolation and characterization. The development of techniques for the determination of the amount and size distribution of EVs in a blood sample is greatly valuable because of the observation that an increased production of EVs has been detected in several pathologic conditions. In addition, knowing the size of the EVs present can be informative because it can indicate which vesicle type is the most dominant type in an unprocessed sample and provide information about the quality of an isolation procedure. Other analysis are based on the study of EVs RNA cargo that is known to contribute to the potential diagnostic and prognostic value of these vesicles.

9. EXTRACELLULAR VESICLES ROLE IN ALS

It has been yet realized that neurodegenerative disorders have a common molecular and cellular mechanism involving protein aggregation and formation of inclusion bodies in selected areas of the nervous system leading to neuronal cell death which is one of the major causes and hallmark of neurodegeneration. Indeed, sorting of proteins correctly folded inside the cells and degradation of toxic ones is important for the health of neurons. At the moment, there is experimental evidence supporting propagation of pathological conformations in both SOD[112,113,115,]and TDP-43[426].

The mechanisms responsible for the intercellular transmission of propagated SOD1 misfolding are not fully elucidated, but different theories have been developed that suggest the uptake of misfolded WTSOD1 through both exosome dependent and independent means. Extracellular transport vesicles have been suggested as a possible mechanism for the progression of neurodegenerative disease pathology, especially between living neural cells. Grad et al. analysis shows that misfolded human WTSOD1 can be released from mouse motor neuron-like cells on exosomes and is subsequently taken up by neighbouring cells. In this case misfolded SOD1 is localized to the outer surface of the exosomal membrane51, as opposed to native SOD1, which normally resides in the exosomal lumen. The surface localization of misfolded SOD1 allows for its recognition and subsequent deactivation by potential pharmacological and immunological therapeutics. As an alternative mechanism of transmission, aggregates of mutant and misfolded WTSOD1 can be released from dying cells and efficiently taken up by neighbouring cells via the process of macropinocytosis. Exosome independent uptake of SOD1 is not aggregate-specific as aggregated forms are taken up as efficiently as non-aggregated forms. However, the process does show specificity, as an irrelevant cellular aggregate, such as glutathione S-transferase, is not taken up in the same manner as SOD1, suggesting the involvement of receptors in this process **(Figure 12).**

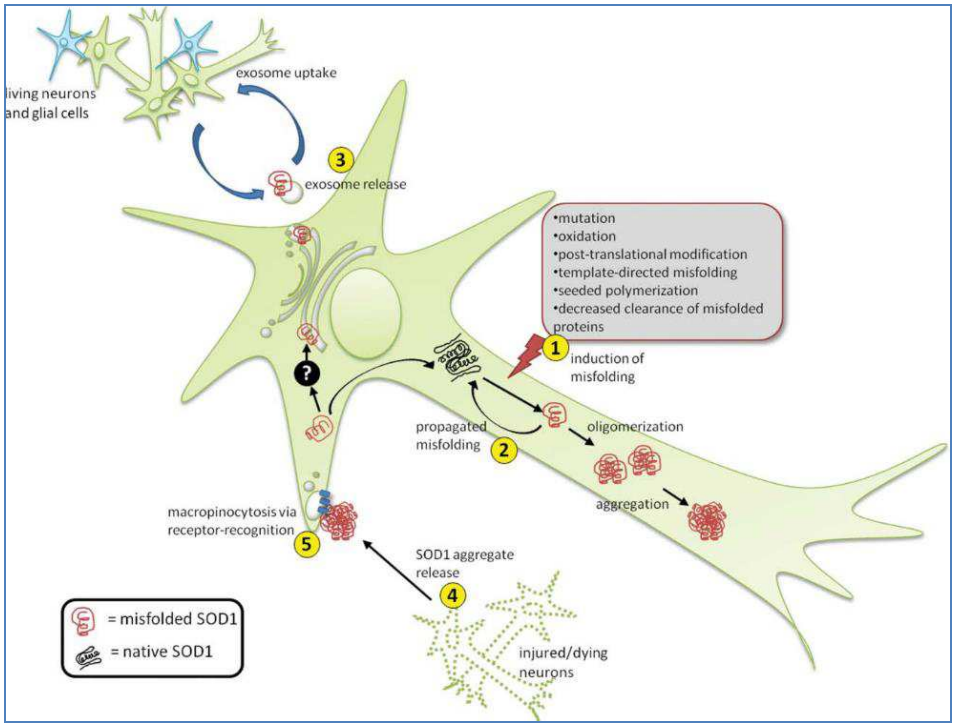

Figure 12. Propagation and transmission of misfolded SOD1 can be based on exosome dependent and independent pathway[427].

The presence of misfolded mutant SOD1 often compromises the secretory pathway[428] because mutant SOD1 oligomers accumulate in the Endoplasmic Reticulum-Golgi compartments as a precursor to its secretion[429], a trafficking step often reserved for cargo heading for degradation to the lysosome or secretion directly into the extracellular space by late endosomes. Such a route is not routinely taken by a normally soluble cytosolic protein. Taken together, it is clear that SOD1 in its pathological form can be involved into the vesicle-mediated secretory system to ensure its survival not only within the cell, but also its transmission to other cells in order to perpetuate new rounds of toxic protein misfolding. Although experimental evidence supports prion-like propagation and

transmission of misfolded SOD1, it remains poorly understood how misfolded SOD1 avoids degradation by the proteostatic machinery of the cell, incorporates itself into the secretory pathway such that it remains associated with the surface of extracellular vesicles, and what specific receptors, if any, control the uptake of misfolded WTSOD1 presented on exosomes or vesicle-free aggregates. Along with other pathological proteins, misfolded SOD1 is targeted for degradation through ubiquitination, but can escape this process through oligomerization and aggregation. Larger multimeric forms of protein are known to become more thermodynamically stable and thus less sensitive to protease recognition and degradation. Due to this misfolded mutant SOD1 has been shown to have toxic effects on both autophagy and the proteasome-dependent degradation[430,431].

In further support of the prion paradigm, self-templating properties have also been observed for TDP-43. Similar to some mutant SOD1 species, TDP-43 and its derived fragments have a high propensity to aggregate in vitro and mutations expressed within the protein can enhance this property[432]. Aggregated TDP-43 isolated from the brains of ALS and frontotemporal lobar degeneration patients exogenously applied to cultured human neuroblastoma cells can serve as seed for the self-propagation of additional ubiquitinated and phosphorylated TDP-43 aggregates. Most importantly, the induced intracellular aggregates of TDP-43 were toxic to cultured neuroblastoma cells, possibly via a mechanism involving proteasome dysfunction, establishing a solid link between propagated TDP-43 misfolding and disease pathology. It should be noted that possible cell-to-cell spread has also been observed for propagated TDP-43 aggregation as phosphorylated aggregates of TDP-43 expressed in cultured neuroblastomas have been shown to induce TDP-43 aggregation in cells that did not originally contain them[426.]

So the study of cellular mechanisms of prion-like protein misfolding, and neuroanatomical pathology propagation are essential for a comprehensive understanding of the etiology of disease and for effective therapeutic development. It is certainly interesting that both vesicles and free aggregates of pathogenic proteins may be involved in releasing SOD1 from affected cells consistent with contiguous propagation; however, it remains to be determined which of these mechanisms result in the effective seeding of template-directed misfolding or the acquisition of toxic properties in the receipt cell. It is tempting to speculate that both mechanisms play significant roles during the course of disease, perhaps at different times, or simultaneously but in dynamic ratios. Future work with vesicles and SOD1 aggregates derived from biofluids and tissues of ALS patients and mouse models are going to provide answers to these important questions.

AIM OF THE WORK

Extracellular vesicles (EVs) are released by many cell types and they are highly conserved in both prokaryotes and eukaryotes. They are secreted in biofluids like urine, blood and cerebrospinal fluid (CSF) and they are regulators of important physiological processes such as immune response, pregnancy, tissue repair and blood coagulation, among others[433]. The transport of different cargo molecules such as mRNA, miRNA and proteins makes EVs really relevant for the modulation of different processes such as gene expression or protein regulation. Pressure has emerged to define and centralize which are the most suitable biofluids from normative biological samples[434]. In the

majority of published studies on circulating EVs, plasma is the physiological medium of EVs most used in the blood.Thanks to the growing interest in EVs, technical standardization procedure for EVs isolation is an argument of central importance. Many methodologies have been used to isolate and analyse EVs but among them (ExoQuick from System Bioscience, ultrafiltration procedures, mass spectrometry-HPLC), differential ultracentrifugation procedure is the first-line technique for routine preparations of MVs and EXOs[433]. In the first work this research project a major task was the establishment of a protocol that discriminate between EXOs and MVs removing contaminating non-vesicular particles and the analysis of EVs role in plasma of ALS patients. This work results really innovative because there are not recent studies that focus on the importance of EVs role in propagation of the disease in ALS patients except for Fenenberg at al. who showed TDP43 presence in exosomes isolated from CSF in ALS patients[436] and Zacau et al. who proved higher presence of leukocyte derived MVs in CSF of one ALS patient compared to four healthy controls[435].

At the beginningwe decided to isolate MVs and EXOs from plasma of ALS patients by ultracentrifugation and we confirmed their purity by Nanotracking Analysis and by Western Blotting. Then we investigated markers of different cellular derivation such as leukocyte CD45, endothelial CD31, platelet CD61, erythrocyte CD235a and the apoptotic marker Annexin V on plasma derived MVs of ALS patients compared to healthy controls, in order to understand if any of those mentioned category was overexpressed and it could be a disease signature.

EVs can mediate both protective and pathogenic effects depending on the precise state of the system in which they are released. For example, in the central nervous system (CNS),EVs support and protect neurons especially during ageing, as well as control inflammation, remove debris and infectious agents. In neurodegenerative diseases, secreted vesicles not only remove misfolded proteins, but also transfer aggregated proteins and prions and are thus thought to perpetuate diseases by ‘infecting’ neighbouring cells with these pathogenic proteins[419].ALS, as a classical proteinopathy, is typified by the formation of inclusions consisting of aggregated protein within motor neurons that contribute to neurotoxicity. It is well established that misfolded/aggregated proteins such as SOD1, TDP-43 and FUS contribute to the toxicity of motor neurons and they play a prominent role in the pathology of ALS. Recent work has identified propagated protein misfolding properties in both mutant and wild-type SOD1 and to a lesser extent TDP-43 in human neuronal cells, which may provide the molecular basis for the clinically observed contiguous spread of the disease through the neuroaxis[437]. It is still unknown if there is a difference in SOD1, TDP-43 and FUS protein level in plasma derived EVs from ALS patients compared to healthy controls. Another aim of this project was the characterization of SOD1, TDP43 and FUS proteins level in plasma derived MVs and exosomes from ALS patients compared to healthy controls by Western Blotting using specific MVs (Annexin V) and EXOs (Alix) markers.

So once investigated a relevant category of plasma derived MVs among leukocyte, endothelial, platelet, erythrocyte derivation, we discovered that the main cells involved in MVs secretion were lymphocytes and we analysed if they were carriers of aggregated proteins involved in ALS pathogenesis. The susceptibility of these ALS patients to inflammatory processes could be an interesting field of study for a better comprehension of the immune cells’response to these circulating CD45+ MVs. For this reason the second part of the work allowed us to investigate phenotyping of Mv with another instrument imaging flow cytometry (IFC) continuing our work on the influence of the immune response mediated by microvesicles in Als; infact the broadly useful

technology, flow cytometry has been evolving slowly until (IFC) became a resurgence of interest in the past decade. Due to its high-throughput and multiparametric analysis, by supporting detection of single cell properties at rates from hundreds to 100000 cells per second,conventional flow cytometry is an irreplaceable cytologic instrumentation when a study of high-volume cell populations and subpopulations needs to be performed[438,439,440] .Meanwhile, due to the lack of spatial resolution in exchange for higher throughput, users have to make gating decisions blind to some of the most informative and relevant sample attributes contained in cell images. The same problem can occur in the microvesicular field, thereforethe possibility of investigate the qualitative content of microvesicles from a body fluid by combining the image directly, it was significant to study the Mvs functional role in this disease elimining the background;in this second part we used other immune antibodies to deepen this understanding having in our minds the work prior by Appel[83]; Monitoring rare events such as Treg Mvs may take some time and a more precise resolution effectively contributes for a better discussion on the biological significance of the data.Overall this work of thesis has the final aim to better understand EVs cellular nature in ALS pathological conditions,in fact we divided patients also for the state of progress of the pathologyand their involvement in prion like propagation of misfolded proteins, cause of neuronal cell death in ALS and their relation with the impairment of immune system found in ALS patients. This kind of study may allow the use of extracellular vesicles as ALS biomarkers and the development of a more precise and personalised therapy for the treatment of this kind of neurodegenerative disease.

MATERIALS AND METHODS

Patients' enrolment

Patients affected by ALS (N=32) and AD (N=28) were enrolled at the "C. Mondino"National Neurological Institute in the first work; ALS diagnosis was made according to the revised El Escorial Criteria Brooks et al. 2000] . Mutations in the SOD1, FUS/TLS, TARDBP, C9ORF72 and ANG genes were excluded in ALS patients (SALS). Thirtytwo sex and age-matched healthy controls (N=32) were recruited at the Transfusion Centre of the IRCCS Policlinico S. Matteo Foundation, Pavia(Italy). The study design was examined by the IRBs of the enrolling Institutions.

Patients affected by ALS (20)were enrolled at the "C. Mondino" National Neurological Institute in the second work comparedwith the same number of healthy controls to investigarefurther immunological markers;a validated rating instrument for monitoring the progression of disability in patientswith amyotrophic lateral sclerosis (ALS) it was used. We utilized the ALS Functional Rating Scale (ALSFRS) measuring physical function in in the implementation of activities of function without altering the overall properties, utility, ordaily living (ADL) of patients with ALSas it reported in the guidelines[441].

EVs isolationfrom plasma The processing of the specimen was carried out in the same way for both works:venous blood in 3.5 ml sodium citrate tubes was centrifuged at 1000 g for 15 minutes. Then the supernatant was transferred to fresh tubes and centrifuged at 1600 g for 20 minutes to remove debris and platelets, which have same sizes. The supernatant was stored in aliquotes at -80°C. **(Figure 13)**

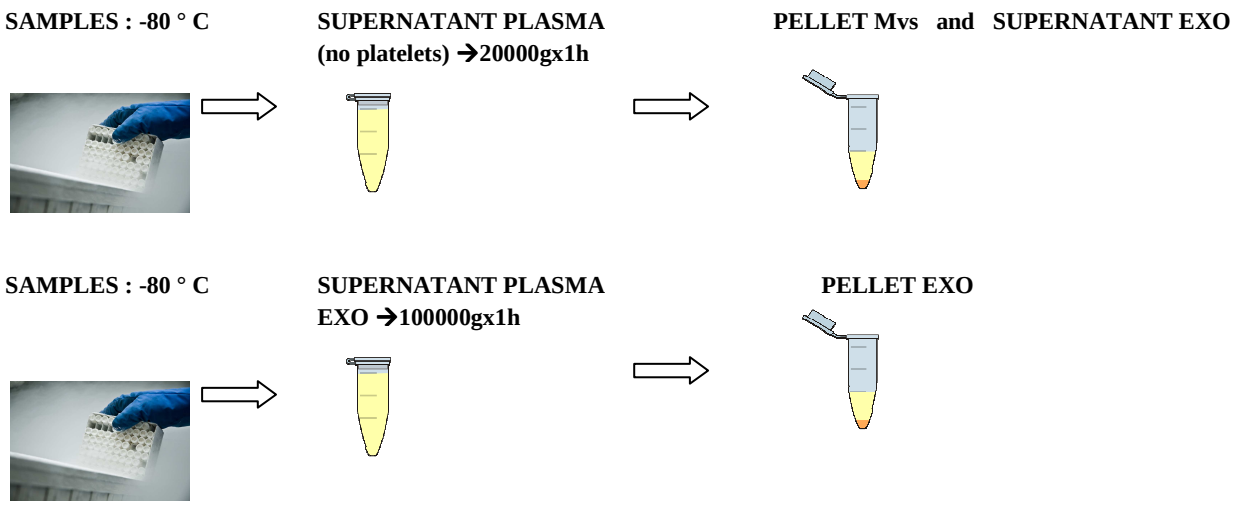

Figure 13. Steps required for isolation of both MVs and EXOs through the use of differential centrifugation phases. Here we report the methods used in this research project for EVs characterization based on Nano Tracking Analysis, qNano Analysis, conventional flow cytometry and IFC and western.We used the following centrifuges to separate Mvs and Exos : F453011 R Beckman Coulter max 30x3,75 g, max RCF (xg) at r=14,000 and 5417 R Beckman Coulter TLA-55, max RPM/k factor= 55,000; max RCF (xg) at r= 186,000respectively.

In the midst of growing interest in EVs, technical standardization is of central importance because many methodologies have been used to isolate and analyze EVs. Following isolation, a variety of techniques have been employed to purify and to study them and unfortunately the influence of these disparate techniques on the results remainssometimes unclear. The current approach use different tools and thecniques with differentproperties and limits keep in mind for each of them **(Figure14).**

The optics of the BD FACSCanto II system consist of an excitation source with up to three lasers, a blue (488-nm, air-cooled, 20-mW solid state), a red (633-nm, 17-mW HeNe) and a violet (405-nm, 30-mW solid state). It has a high degree of automation and quality control helping to save time, reduce cost, and improve reproducibility of results.

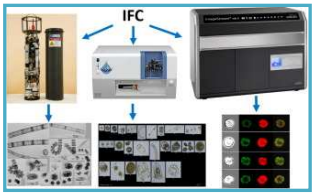

Amnis® imaging flow cytometers combine the speed and sample size of flow cytometry with the resolution and sensitivity of microscopy in a single instrument. Microscopic images provide qualitative and quantitative image data of every event acquired in flow.

qNano Gold directly measures the properties of individual nanoparticles in solution:
Particle diameter or volume
Effective surface charge and Zeta Potential
The measurement precision for each individual particle enables concentration to be defined across a size range allowing meaningful comparison of results from research groups around the world.

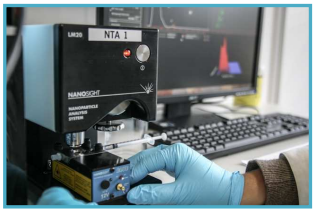

Nano Tracking Analysis provides high resolution particle size, concentration and aggregation measurements while a fluorescence mode provides specific results for labelled particles. The range provides real time monitoring of the subtle changes in the characteristics of particle populations with all of these analyses confirmed by visual validation.

Figure14.itemizedtool list to determine Evs. Here we summarized 4 different way to study Evs each of which mandates a different level of quality control and operating procedure.

MVs and EXOs isolation by ultracentrifugation

The most commonly used methodology for EVs isolation is differential centrifugation which employs a number of different centrifugation steps. The stored plasma was centrifuged at 20,000 g for 1 hour at 4 °C to obtain MVs pellet. Once the supernatant was removed, MVs pellet was resuspended in 1 ml of filtered PBS (Sigma Aldrich) and centrifuged at 20,000 g for 1 hour at 4 °C. MVs pellet was subsequently subjected to analysis. The supernatant of MVs pellet was collected, filtered through a 0.2 μm filter and spun in an ultracentrifuge at 100,000g for 1 hours at 4 °C. After ultracentrifugation, the supernatant was removed, and EXOs pellet was washed with 1 ml of filtered PBS at 100,000g for 1 hour at 4°C. The obtained EXOs pellet was processed for analysis **(Figure 13).**

Nanoparticle tracking Analysis (NTA)

The size and concentration of MVs and EXOs were detected by NTA using a LM10HSBF instrument (NanoSight, Amesbury, UK). The NTA technique can measure the size distribution of vesicles ranging from 50 nm – 1 μm in diameter. The threshold of particle concentration detection was between 107-109 particles/ml. For more accurate detection, MV and EXO samples were diluted with PBS to a particle concentration of about 108 particles/ml. After dilution, 700 μl of diluted sample was loaded to the machine for recording particle movement videos in a rate of about 30 frames/s. Particle movement videos were recorded 3 times per test at different positions and particle movements were analyzed by the NTA software (version 2.2, NanoSight). The results of NTA were presented as the mean of the 3 tests. The final particle concentration was calculated after considering the dilution factor of the NTA results **(Figure 15).**

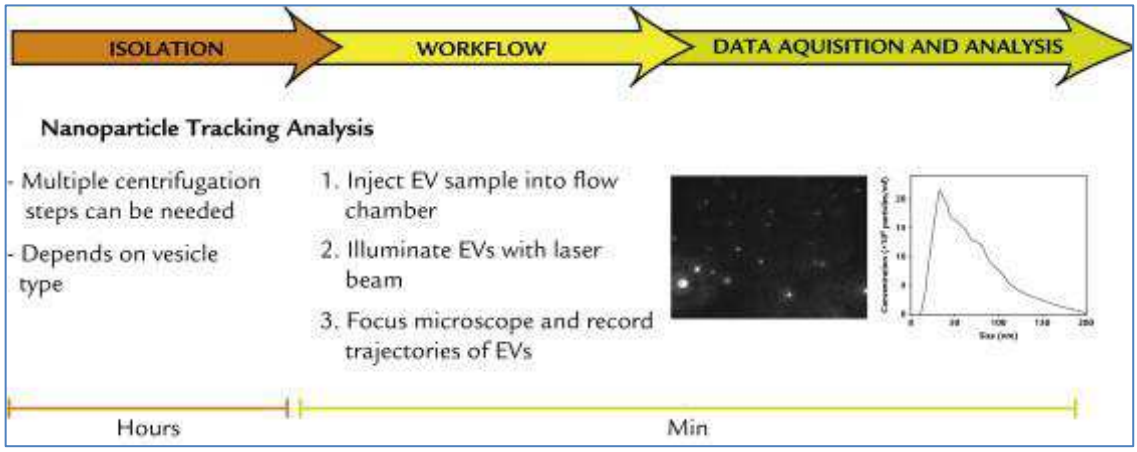

Figure 15. General procedure applied for Nanoparticle Tracking Analysis fundamental for determination of MVs' and EXOs' dimensions[425].

Tunable Resistive Pulse Sensing (TRPS)

In this work we used qNano Gold with NP400 and we measured with the concentration of particles in the fluid as a number of particles per unit volume of fluid, across a specified detectable particle size range and a size distribution of these particles ideally plotted as a histogram of concentration v particle diameter (or volume). We can tune optimising particle measurementthe following parameters: (**Figure 16)**

1) Nanopore Stretch (S) – changing the nanopore size
2) Bias Voltage (V)– changing electrical forces on the particles
3) Applied Pressure(P) – changing the fluid flow rate

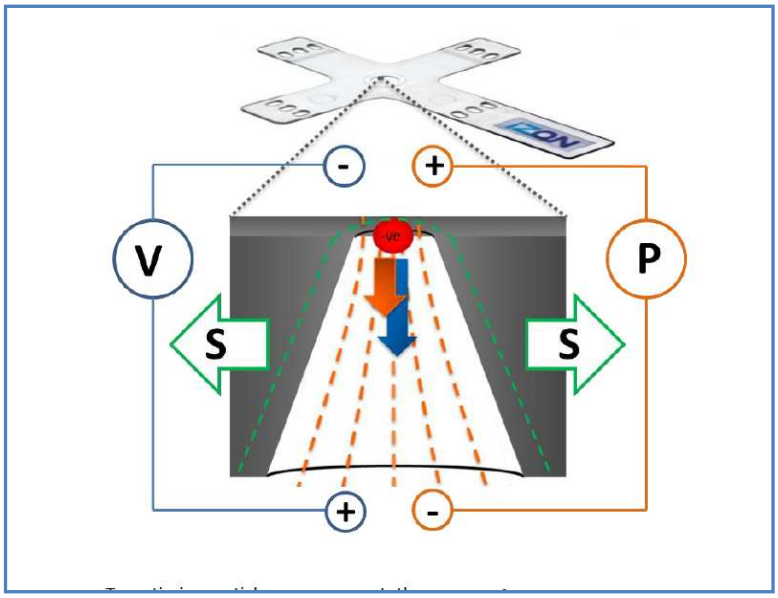

Figure16. Setting Nanoparticle suspensions. A scientific measurement must be quantifiable and reproducible soonce chosen the nanopore and adjusted the stretch, it is possible by varying the pressure to get a more accurate measure resembling reality.

The calibration beads measure is essential to do before to analyze samples beacuse calibration particles are used to convert blockade magnitude (nA) into a diameter (nm).

Blockade magnitude is thedetermined current amplitude and it is proportional to the volume of the particle passing through the nanopore, giving very high resolution of particle diameter**(Figure 17).** For each sample particle passing through the nanopore:

$$\text{Particle Vol} = \frac{\text{Particle Blockade Mag}}{\text{Cal Blockade Mag (Mean)}} \times \text{Cal Vol (Mean)}$$

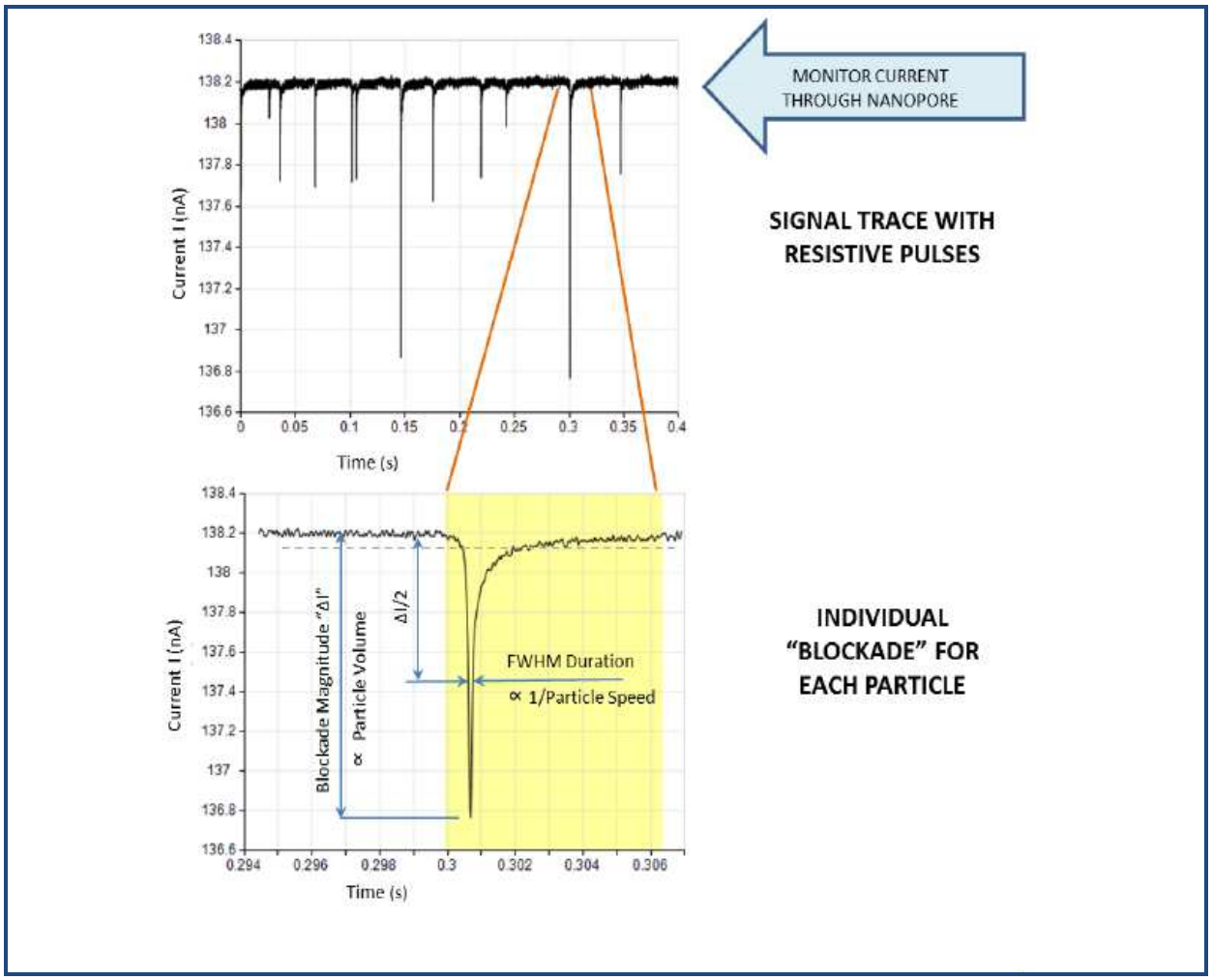

Figure17. Signal Trace with resistive pulses. For each particle that passes through the pore, it is measures the relative current which will have its amplitude. This amplitude defined "blokade" is proportional to the size of the particles

Identification of the MVs by BD FACS Canto II Flow Cytometry

Due to their small size, EVs analysis requires working conditions close to the size-related sensitivity limit of the cytometers. Standardization of particles count requires to set up this limit for an optimal compromise between EV analysis and background exclusion. This limit has significantly progressed with the advent of the latest generations of instruments and nowadays flow cytometry is a preferred method in the studies of MVs because of its ability to quantitate the number of particles and multicolor analysis attributes, allowing detection of several markers simultaneously.

We used Megamix-Plus SSC (Megamix-Plus SSC-7803 0.16-0.20 µm and 0.24-0.5 µm), a reagent mix of fluorescent beads of varied diameters, selected to cover a major part of the theoretical MVs size range, using SSC as a size-related parameter. Beads acquisition allows setting the cytometer to study MVs within a constant size region and getting reproducible MVs counts.

At the end of this analysis we can identify different populations of beads according to their size obtained with a specific parameters setting that we have to maintain for a correct MVs identification and accurate exclusion of debris or other particles similar in dimensions.

Once obtained MVs pellet, it was resuspended in previously diluted Annexin Buffer 10X (0.1 M HEPES, pH 7.4; 1.4 M NaCl; 25 mM CaCl2) to 1X concentration with filtered distilled water and incubated for 20’ at room temperature with specific antibodies. After a resuspension in filtered PBS, we identified MVs cellular provenience using different antigenic fluorochormes as markers specifically expressed on cellular surface such as mouse monoclonal leukocyte Anti-human CD45 (ab 641417APC-H7- BD); mouse monoclonal endothelial Anti-human CD31 (ab 560983PE- BD); mouse monoclonal platelet Anti-human CD61 (ab 347408 Per-cy- BD); mouse monoclonal endothelial erythrocyte Anti-human CD235a (ab 563666 Pe-cy7- BD) derivation and the apoptotic marker Annexin V (ab 550407 APC-BD).

5.3 Imaging Flow Cytometry to determine different subpopulations of vesicles

Our interest was focused especially in refine a method with the Imaging Flow Cytometry (IFC) initially only observing the morphology and different markings. For this reason we have compared the action that two different types of dyes can show during the staining and keeping in mind the maximum limit of the machine to discern the morphology with SSC. In particular we used carboxyfluorescein succinimidyl ester CFSE (ab113853 Abcam) as a cell permeant, non-fluorescent pro-dye. Intracellular esterases in live cells or entire vesicles cleave the acetate groups which results in the green fluorescent molecule carboxyfluorescein that is showed membrane impermeant and FM 1-43 (F-35355 Termo Fisher Scientific)membrane probe is resulted an excellent reagent both for identifying actively firing neurons and for investigating the mechanisms of activity-dependent vesicle cycling. This water-soluble dye, which is nontoxic to cells/vesicles and virtually nonfluorescent in aqueous medium, is believed to insert into the outer leaflet of the cell membrane where it becomes intensely fluorescent.

The system combines a precise method of electronically tracking moving cells/vesicles with a high resolution multispectral imaging system to acquire multiple images of each cell/vesicle in different imaging modes. Objects passing through the ImageStream cell analysis system are illuminated in different directions by lasers and/or brightfield LEDs. Light emitted from the object is focused through an objective lens and relayed to a spectral decomposition element, which divides the light into six spectral bands located side-by-side across a charge-coupled detector (CCD), as shown in the following diagram. **(Figure 18).**Therefore, each object has six images that can be individually analyzed or, because they are in spatial register with respect to one another, reconstructed. Each of the separate bands is called a channel. Below is an example of collecting 6 images. The ImageStreamx system has a second camera option which enables collection of up to 12 images per object.

This instrument has allowed usthe enumeration andphenotyping with IFC (AmnisImageStreamX Mark II) the followingmarkers:CD4 (ab IV T114 FITCBD),CD8 (ab 560273 APC-H7 BD), CD25 (ab 101919 APC BioLegend) ,CD45RO (ab 304248 PE/dazzle BioLegend) and CD45RA (ab 304122 PerCp-cy5.5 BioLegend); Annexin V (ab 642903 BV421 Biolegend) and Calcein-AM (ab 56496 FITC Sigma) were used as generalMV membrane markers.

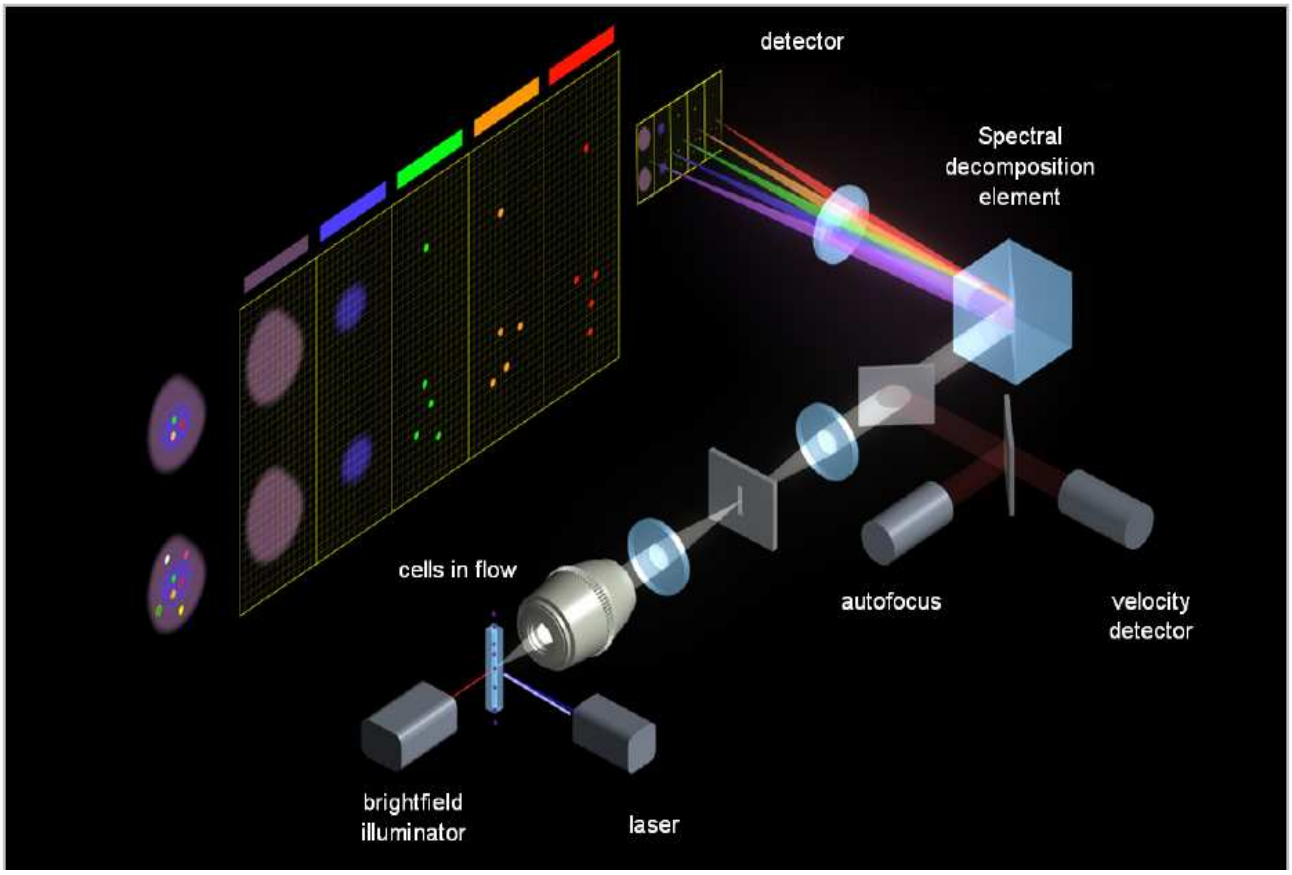

Figure 18: Modular design of the ImageStream®X Mark II Imaging Flow Cytometer; in this representation is reported CCD camera. It operates in TDI (time delay integration) mode that electronically tracks moving objects by moving pixel content from row to row down the rows of pixels in synchrony with the velocity of the object (cell) in flow as measured by the velocity detection system.

Preparation of Total Proteins Extracts

MVs and EXOs pellet were lysed in 70 µl of cold Radio-Immunoprecipitation Assay (RIPA) buffer (150 mM sodium chloride, 1.0% NP-40 or Triton X-100, 0.5% sodium deoxycholate, 0.1% SDS, 50 mM Tris, pH 8.0), containing a mixture of phosphatase and protease inhibitors (Sigma-Aldrich), incubated for 20 minutes in ice and centrifuged at 16,000 g for 5 min at 4°C. The supernatant was transferred to a fresh tube and stored in aliquots at -80°C representing the total protein extract together with the remaining pellet of insoluble proteins.

BCA Protein Assay

Protein concentration of previously extracted samples in RIPA buffer was determined using bicinchoninic acid (BCA) method (Sigma-Aldrich) and BSA (bovine serum albumin) as standard. A solution of copper (Cu+2) and BCA was prepared depending on the total number of samples and 20 µl of this solution are mixed with 2,5 µl of an intermediate dilution 1:10 of each sample. The principle of this method is that proteins can reduce Cu^{+2} to Cu^{+1} in an alkaline solution (the biuret reaction) resulting in a purple color formation which is directly proportional to the proteic component present. The sample was incubated at 37°C, temperature requested for the formation of

peptide bonds involved in reaction complex development. Proteic quantification was determined using NanoDrop (Celbio).

Western blotting analysis

WB main steps are summarized in figure 14. It was performed by SDS–polyacrylamide gel electrophoresis (SDS-PAGE). Sample containing 30 µg were boiled at 80°C in Laemmli sample buffer (0.6 g/100 ml Tris, 2 g/100 ml SDS, 10% glycerol, 1% β-mercaptoethanol,pH 6.8) for 10 min and then loaded on 12.5% SDS-PAGE gel (Bio-Rad Laboratories, Italy)**(Figure 19).**

After electrophoresis, samples were transferred to a nitrocellulose membrane (Trans-blot, Bio-Rad Laboratories, Italy) using a liquid transfer apparatus (Bio-Rad). Nitrocellulose membranes were treated with a blocking solution containing 5% of non-fat dry milk in TBS-T buffer (10 mM Tris-HCl, 100 mM NaCl, 0.1% Tween, pH 7.5) for 1h to block unspecific protein binding sites and then were incubated overnight with the primary antibodies prepared in blocking solution at 4°C in continuous shaking such as rabbit polyclonal Anti-TDP43 (Proteintech, 1:1000), mouse Anti-Fus (GeneTex, 1:1000); mouse Anti-SOD1 (Santa Cruz Biotechnology, 1:1000); rabbit polyclonal Anti-Annexin V (Santa Cruz Biotechnology 1:500); rabbit polyclonal Anti-Alix (Abcam,1:1000). Anti-misfolded SOD1-3H1 clone was kindly given by Prof. Neil Cashman. Immunoreactivity was detected using the donkey anti-rabbit or anti-mouse (GE Healthcare) secondary peroxidase-conjugated antibodies **(Table 3) .** The immunoreactive bands were then visualized using the enhanced chemiluminescence detection kit (ECL Select, GE Healthcare).

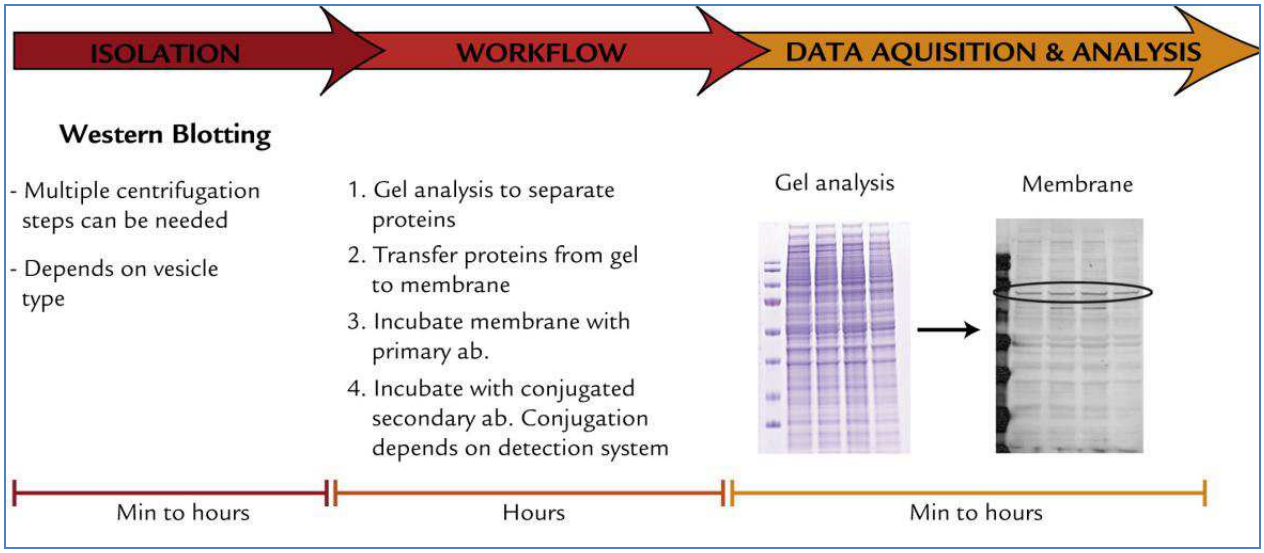

Figure 19. Western Blot main steps explained for the detection of protein expressed in the sample of interest[433].

For subsequent staining, primary and secondary antibodies were removed from the membrane by incubation for 20 min in Stripping Solution (100 mM Mercaptoethanol, 2% SDS, and 62.5 mM Tris/HCl, pH 6.7), washed with TBS-T (3 times ×10 min at room temperature); the membranes were then processed as described above. Densitometric analysis of the bands was performed using

Quantity One software (BioRad, Italy) and normalized with the correspondent value of the loading control i.e. Alix for exosomes and Annexin V for microvesicles.

Antibody	Species	Concentration	Type	Supplier
Anti-TDP43	Rabbit	1:1000	I Ab	Proteintech
Anti-FUS	Rabbit	1:1000	I Ab	Gene Tex
Anti-3H1	Mouse	1:1000	I Ab	Santa Cruz Biotechnology
Ani-Annexin V	Rabbit	1:500	I Ab	Santa Cruz Biotechnology
Anti-Alix	Rabbit	1:1000	I Ab	Abcam
HRP conjugated	Donkey Anti-Rabbit	1:10000	II Ab	GE healthcare
HRP conjugated	Donkey Anti-Mouse	1:10000	II Ab	GE healthcare

Table 3. Antibodies used in Western Blotting Analysis

MVs immunoprecipitation

Anti-CD45 antibody (Santa Cruz Biotechnology, 2 ug) was coupled to 25 ul Dynabeads (Invitrogen) for 2 h at 4oC. Microvesicles were separated as described above and resuspended in PBS+BSA 1%. The mixture was then applied to CD45 coupled Dynabeads overnight at 4oC. Fluid not retained on the column was collected and termed the flow- through fraction. Beads were washed three times with cold PBS buffer. Protein and microvesicles retained on the beads were recovered by adding 15 ul of RIPA buffer containing a mixture of phosphatase and protease inhibitors (Sigma-Aldrich), incubated for 15 minutes on ice. Laemmli buffer 2x (15ul was added to the beads) and then boiled at 95 oC for 5 minutes to generate the eluate/CD45-captured fraction. The tube was placed in a magnet for 1 min and the supernatant transferred to a new tube.

Each fraction: Flow-through (FT) and input (starting material of microvesicles) were centrifuged at 20,000xg at 4°C for 30 minutes in a TLA 120.2 rotor using a TLA ultracentrifuge (Beckman Instruments) and subjected to Western Blotting for Anti-CD45, rabbit polyclonal Anti-TDP43, mouse Anti-Fus, rabbit monoclonal Anti-SOD1, mouse Anti-SOD1 3H1 and rabbit polyclonal Anti-Annexin V.

Statistical analysis

Statistical analysis was performed by Student t-test and by One-Way Analysis of Variance (ANOVA test) followed by post hoc comparison as a post-test (GraphPad Prism version 5, San

Diego, CA, USA and Program R version 3). Values were considered statistically significant when p values were < 0.05.

RESULTS AND DISCUSSION

1. EXTRACELLULAR VESICLES ISOLATION AND CHARACTERIZATION

1.1 Nanoparticle Tracking Analysis (NTA) confirmed extracellular vesicles dimensions

MVs and EXOs isolation was performed from plasma of 32 ALS patients, 28 AD patients and 32 age- and gender- matched healthy controls with a procedure of subsequent centrifugation steps as described in Material and Methods. To confirm the purity of MVs and EXOs preparations we analysed MVs and EXOs dimension by Nanoparticle Tracking Analysis (NTA). NTA allows size determination and quantification of EVs in a suspension. The technique is based on relating the Brownian motions of a particle to its size as described in Materials and Methods. In this project MVs and EXOs dimensions were determined through the use of the NTA instrument LM10HSBF (NanoSight Itd) at Dipartimento di Biotecnologie e Bioscienze, Università degli Studi di Milano, Bicocca (thanks to Prof. Prosperi Davide). For this kind of analysis, the "average particle size" describes a size distribution, based on a calculated average (or mean) of three measurements. Rather than use a single point in the distribution as a specification, we included three size parameters in order to describe the width of the distribution. A three-point specification featuring the D10, D50, and D90 has been considered complete and appropriate. For D90 it is meant that the diameter of 90% of the distribution has a smaller particle size and 10% has a larger particle size, The D10 diameter has 10% smaller and 90% larger and D50 has 50% smaller and 50% larger **(Figure 20).**

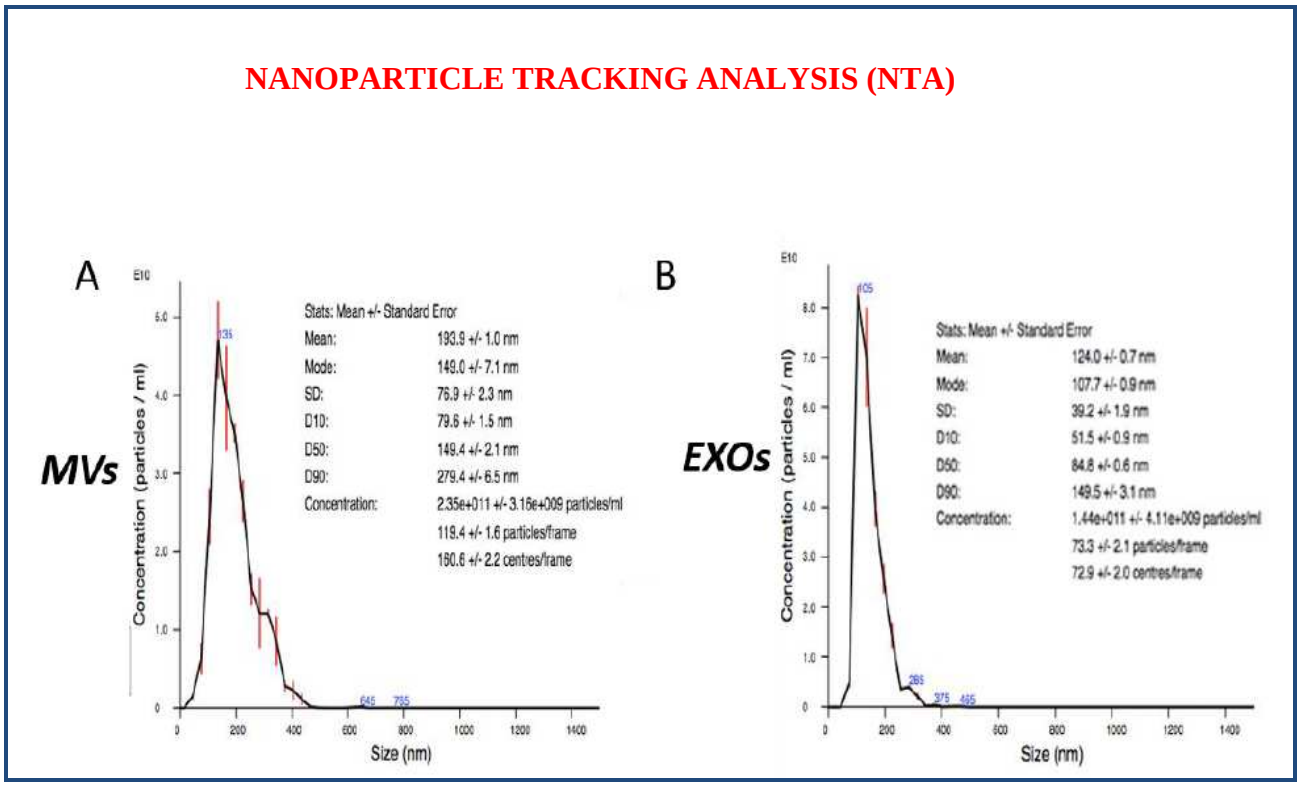

Figure 20. A e B) NTA analysis confirmed the purity of MVs included in the range 80- 279.4 nm and of EXOs in the range 51.5-149.5 nm.

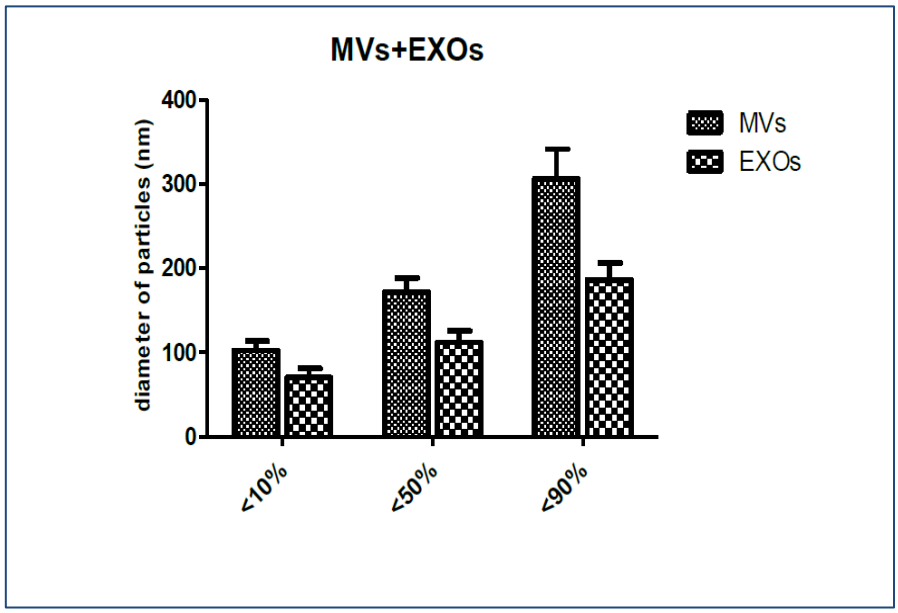

Figure 21. Histograms representing the mean ± SEM of dimension distribution, D10, D50, D90 of MVs and EXOs analysed into 4 controls by NTA.

Figure 20 and Figure 21 report the analysis that we carried out for the determination of MVs and EXOs dimensions through NTA. Figure 16 shows histograms of the mean of three-point size parameters D10, D50, D90 in plasma samples from 4 healthy controls. 90% of EXOs are smaller than 200 nm, while 90% of MVs are smaller than 400 nm. MVs are large membranous vesicles of 100–1,000 nm diameter while EXOs are vesicles in the range of 40–150 nm diameter[414]. Even if

20% of MVs were smaller than 100 nm, and 20% of EXOs were bigger than 150 nm, **figure 20** shows the difference in the distribution of the two population and highlighting that we were able to perform a complete purification of EXOs and MVs. As better discussed later, this even explain why we decided to use specific beads with dimensions between 200-500 nm (and not 500-1000 nm) for MVs flow cytometry analysis. Extending this analysis even to ALS patients and Alzheimer's Disease patients, we observed that 20% of MVs pellet included smaller particles than 100 nm in plasma and we even noticed that in D90 group some differences are present between ALS, AD patients and healthy controls group but without a significant relevance, probably due to the small cohort considered for the NTA analysis (only 4 ALS patients and 3 AD patients-data not shown). The standardisation of a common protocol for EVs isolation is fundamental for the development of a method that allows direct comparison of results between studies and leading to a greater understanding of MVs role in disease[3]. So the most important result is that through NTA we were able to distinguish and purify MVs and EXOs populations depending on their dimensions. Further characterization of these particles were confirmed in the following paragraph by WB analysis of surface markers (Annexin V for MVs and Alix for EXOs)

1.2. MVs and EXOs markers confirmation by Western Blotting analysis

Once confirmed MVs and EXOs purity through NTA analysis, we investigated scientifically accepted MVs and EXOs surface markers by Western Blotting. MVs secretion from cells is associated with a dynamic interplay between phospholipid redistribution and cytoskeletal protein contraction that in the end leads to a translocation of phosphatidylserine to the outer-membrane leaflet and to exposure of membrane receptors like integrins[442]. Annexin V (that binds phosphatidylserine) is used as common marker for MVs. Baietti et al. demonstrated that Alix was involved in exosome biogenesis and in exosomal sorting of syndecans through an interaction with syntenin[443]. We can see from the Western Blotting analysis represented in **figure 22** that MVs are recognized by Annexin V and Integrin α2β. EXOs are recognized by Alix but not exclusively since a lower presence of the same marker was visible in MVs lysate. This confirm the slight carry-over of exosome pellet in MVs purification steps (as previously reported in NTA analysis discussion and as described in literature)[444]. Flotillin-1 is used as common marker expressed on surface of both kinds of particles proved with visualisation of similar bands.

Further characterization of these particles have been performed through the use of flow cytometry and of Western Blotting for proteins cargo analysis.

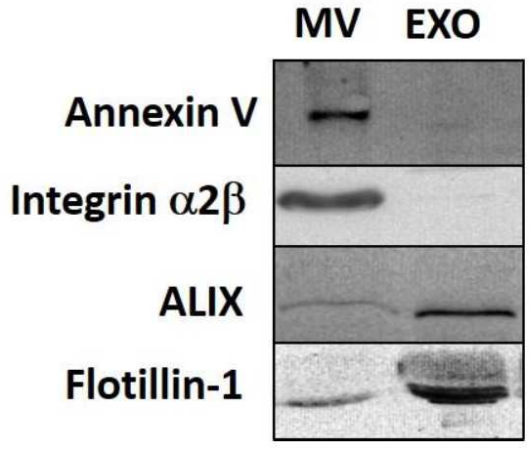

Figure 22.Western Blotting of microvesicle and exosomal fractions shows the presence of the endosomal marker Alix, Flotillin-1, in both exosomal and microvesicles fractions, whereas Annexin V and Integrin α2β is only present in microvesicles fraction.

1.3. qNano Analysis

The impedance of a nanopore in an electrolyte fluid cell is sampled 50,000 times per second. Sample particles are driven through the nanopore by applying a combination of pressure and voltage, and each particle causes a resistive pulse or "blockade" signal that is detected and measured by the application software. The first step when using the qNano Analysis is to perform beads calibration that matches with used nanopore(in this work we have employ NP400). Magnitude, duration and frequency values are converted into particle measurements by calibration with particles of known size, concentration and surface charge; it confers three types of information:

1) Blockade magnitude is directly proportional to the volume of each particle.

2)Blockade duration changes with the velocity of the particle and can be used to calculate the surface charge of each particle.

3)Blockade frequency is used to determine particle concentration.

We can obtain Blockade Full Trace Analysis both Sample and Calibrazion **Figure 23 A,B and C,D** respectively.

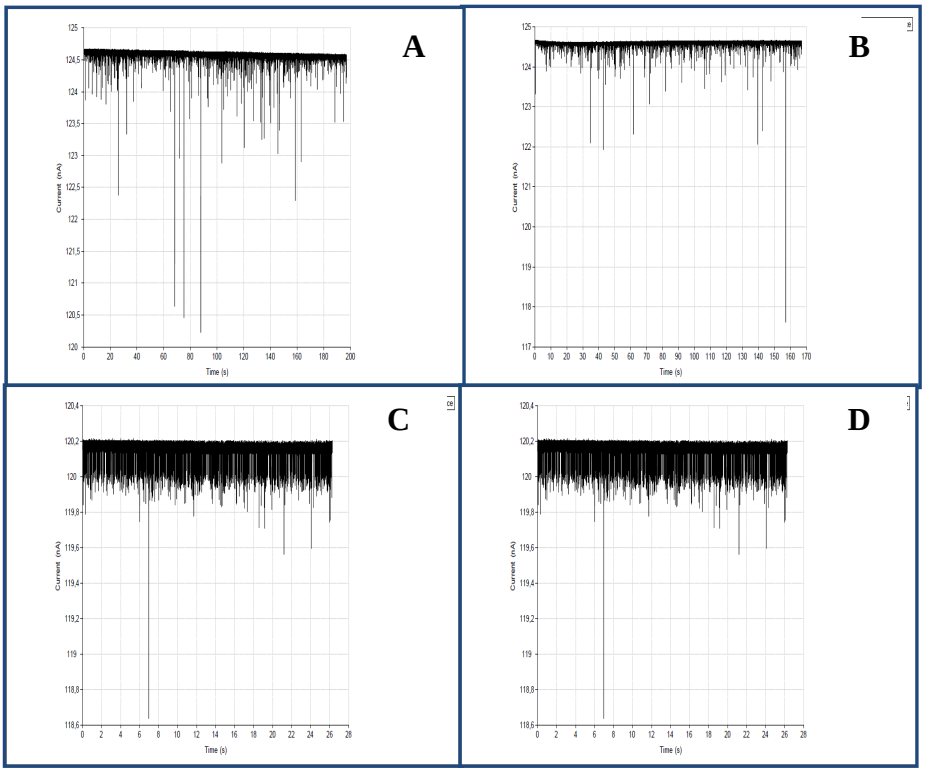

Figure 23 A,B,C,D. Full Trace Analysis. **A-B)** Blockade is measured for sample Analysis and **C-D)**Blockade is measured for calibration Analysis. If during the acquisition the suspension liquid is not continuous, renew ing the measurement it is necessary and the Full Trace will show the current jumps.

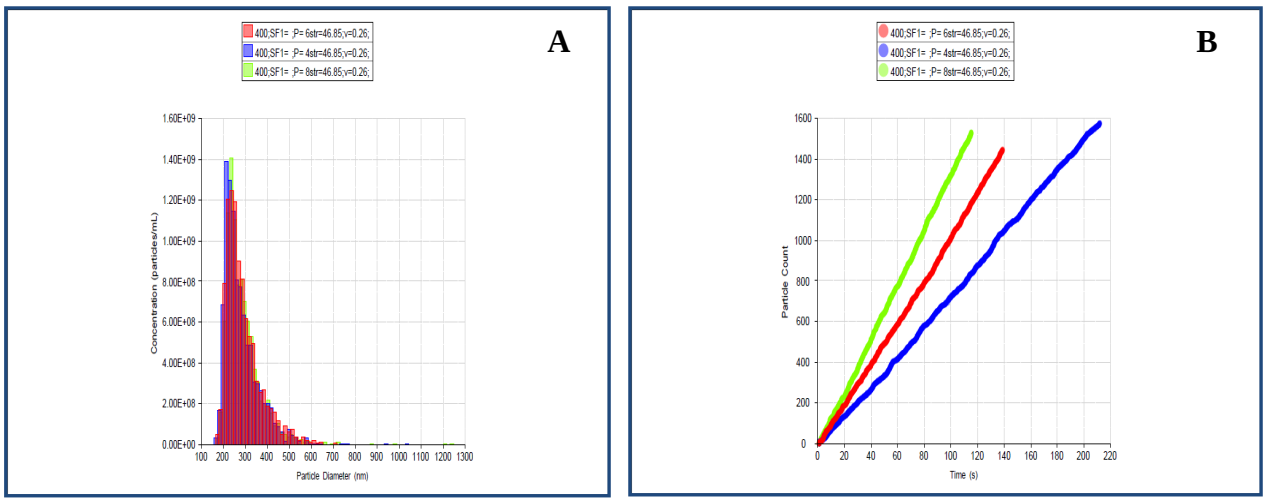

Figure 24A and B.Particle Concentrazion Plot **(A)** and Particle Rate Plot **(B).** Each sample is measured with 3 different pressures so we can notice **(B)** 3 different acquisition speed reducing error intrinsic measurement . In this way we have obtained 3 overlapping size distribution plot **(A).**

In **Figure 24A,B**are displayed Raw Concentration(/ml)and Partcle(/min) which they are compared Particle Diameter and Time, respectively. Concentration values are typically derived at 2 or more pressures using calibration particles of a known concentration. If concentration is calculated at a single pressure the software will calculate a gradient based on the fitted line passing through the origin. This can introduce significant errors, especially with smaller nanopores (NP200 and below) where a large proportion of particles are driven through the nanopore due to applied voltage V.

We can retain the of the nanopore's characteristics and relative concentrations and size distribution plot as it is showed in (**Table4)**

Nanopore Caracteristic	Mean	Mode Dia	Raw Cont(/ml)	Particle Kount	Parttle Rate(/min)
400;SF1= ;P= 6str=46.85;v=0.26;	288	236	9.9E+009	1443	624,10
400;SF1= ;P= 4str=46.85;v=0.26;	281	213	9.9E+009	1574	446,30
400;SF1= ;P= 8str=46.85;v=0.26;	290	236	9.9E+009	1529	795,90

Table4. qNano framework Analysis. The table summarizes nanopore characteristics upon Mvs measure.During the time, an accurate microvesicular concentration if we use three different pressures it is so obtained.

2. CHARACTERIZATION OF MVS BY FLOW CYTOMETRY ANALYSIS

Different approaches are applied for characterization of either MVs or EXOs by flow cytometry. Flow cytometry is widely used to identify expression of particular antigens that may reveal the cell of origin of extracellular vesicles[445], but it has the limit that it cannot detect EVs < 200 nm in size[447]. Use of flow cytometry to characterize EXOs normally depends on adsorption of these vesicles onto antibody-coated beads. The beads are large enough to facilitate the detection of these small vesicles, which would otherwise fall below the lower limit of detection[425].

While the previous generation of flow cytometers is challenged by the small size and signals from most EVs, and several laboratories have reported that a size of 500 nm is the cut off value for accurate identification, the enhanced sensitivity of modern digital flow cytometers allows the detection of EVs in the range of approximately 200 nm to 1.0 mm192.

Figure 25 illustrates how MVs can be distinguished using a blend of size-calibrated fluorescent beads. Size-calibrated fluorescent beads are of known size and count allowing quantitation and delineation of heterogeneous EVs since scatter detection alone is an inefficient method for analysing smaller vesicles[446]. When examining a plasma sample, better specificity of MVs detection is obtained by identifying those MVs that expose phosphatidylserine and cell-specific markers.

In this work of thesis, we analysed MVs (but not EXOs) by flow cytometry with a new generation flow cytometer FACS Canto II. We used specific beads (Megamix-Plus SSC-7803 0.16-0.20 and 0.24-0.5 μm) to determine the size of the MVs. The range 0.16-0.20 μm was used to discriminate between the background and MVs.

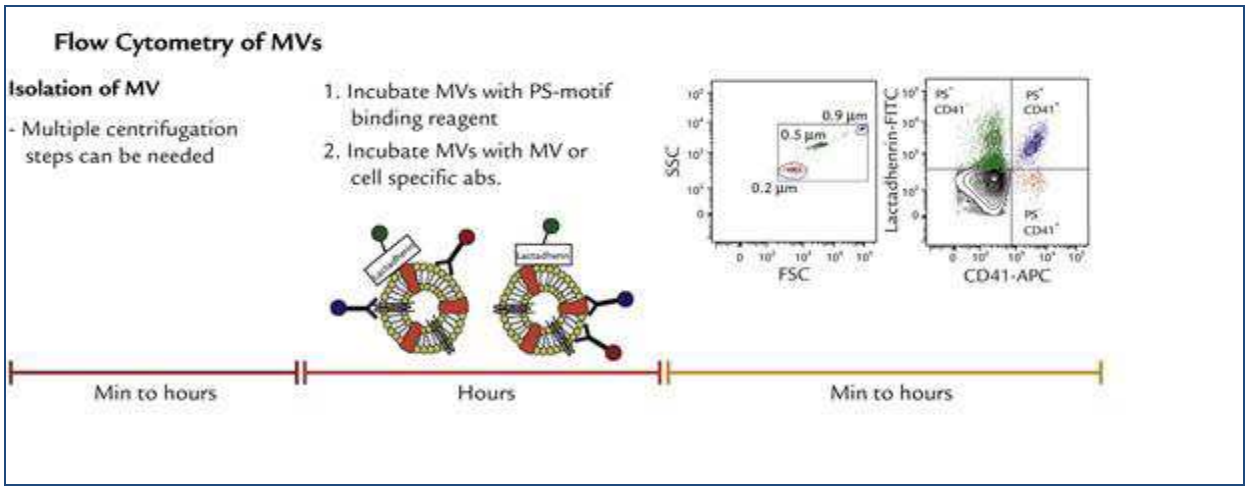

Figure 25. Flow cytometry analysis for MVs characterization[425].

2.1 Polystyrene/latex beads setting up and determination of positivity

Since the analysis by NTA showed that 90% of MVs were smaller than 400 nm, we concentrated our attention on specific polystyrene/latex beads in the range of 0.24-0.5 μm (Megamix-Plus SSC-7803, 0.16-0.20 μm and 0.24-0.5 μm). The polystyrene/latex beads used (Megamix-Plus SSC) were a mix of fluorescent beads of varied diameters, selected to cover a theoretical MVs size range (0.16-0.20 and 0.24-0.5 μm), using SSC as a size-related parameter. Polystyrene/latex beads acquisition setting allows the cytometer to study MVs within a constant size region and getting reproducible MV counts. The range 0.16-0.20 μm was used to define the threshold background and the real MVs range is between 0.24-0.5 μm **(Figure 26).**

The plasma membrane of living cells is a highly organized asymmetric three-dimensional system. The electrically neutral phosphatidylcholine (PC), sphingomyelin (SM) and glycosphingolipids are mainly located on the outer leaflet of the plasma membrane, whereas aminophospholipids such as phosphatidylethanolamine (PE) and anionic phosphatidylserine (PS) and phosphatidic acid (PA) are exclusively present in the cytoplasmic or inner leaflet[448,449]. So plasma membrane, as well-structured entity besides lipids and proteins between the two leaflets, presents also a lateral organization in domains termed "rafts." Following stimulation (like increase of Ca^{2+}), a general redistribution occurs, leading to local or global changes in lipid asymmetry and raft structuration and this yields to a strong distribution of electrostatic charge between the two membrane surfaces. PS is externalized and MVs are released after an increase in intracellular calcium levels. Different methods have been developed to detect the early PS expression on the extracellular face of the plasma membrane of stimulated cells. This phospholipid can be detected by dye-labelled PS-binding proteins (annexins). Humans express twelve different annexins, some of them with splicing variants, which exert differential functions, but all of them contain a conserved homologous calcium-membrane binding core that allows the peripheral docking of these proteins to membranes. One of the most popular non-invasive tool for the detection of apoptosis is the use of Annexin A5 (commercially known as Annexin V) labelled with a fluorescent dye[450,451]. Annexins have been reported to be present in MVs from different cellular origins[452]. So a lot of studies are based on the use of Annexin A5 as markers for MVs.

Therefore, in this thesis project we used Annexin V as marker for MVs characterization as reported in **Figure 26.**

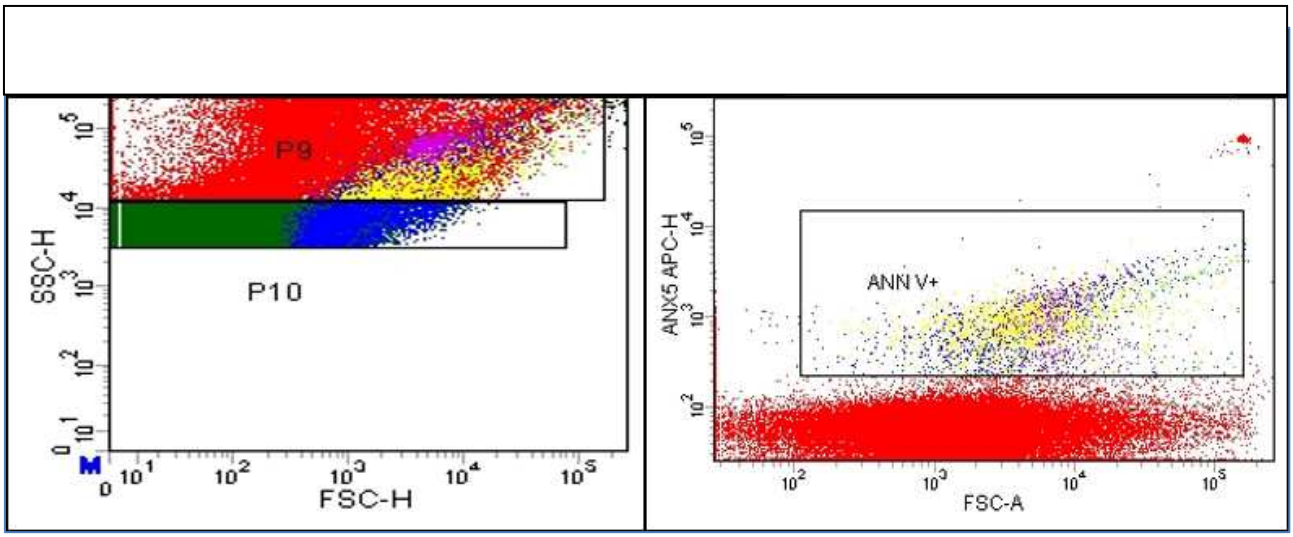

Figure 26.MVs are separated in two different populations P9 (200-500 nm) and P10 (160-200 nm) on the base of their dimensions and are selected through labelling with surface marker Annexin V.

The different beads sub-populations were discriminated first according to light scatter (SSC-H) and beads fluorescence (FITC) and secondary on SSC-H and forward scatter (FSC-H) **(Figure 27 A and 27 B)** while **Figure 27 C** reports the own fluorescence peaks. In**Figure 27 D** the number of events are highlighted, which are important to calculate background's thresholds setting. Multicolour flow cytometry analysis of EVs, using monoclonal antibodies, opened a new way of extensive investigation and characterization. Multicolour analysis is used to detect the cellular origin of MVs based on their phenotype. Simultaneous analysis of many parameters/factors in one sample is possible since each population can be recognized by a unique fluorescence intensity.

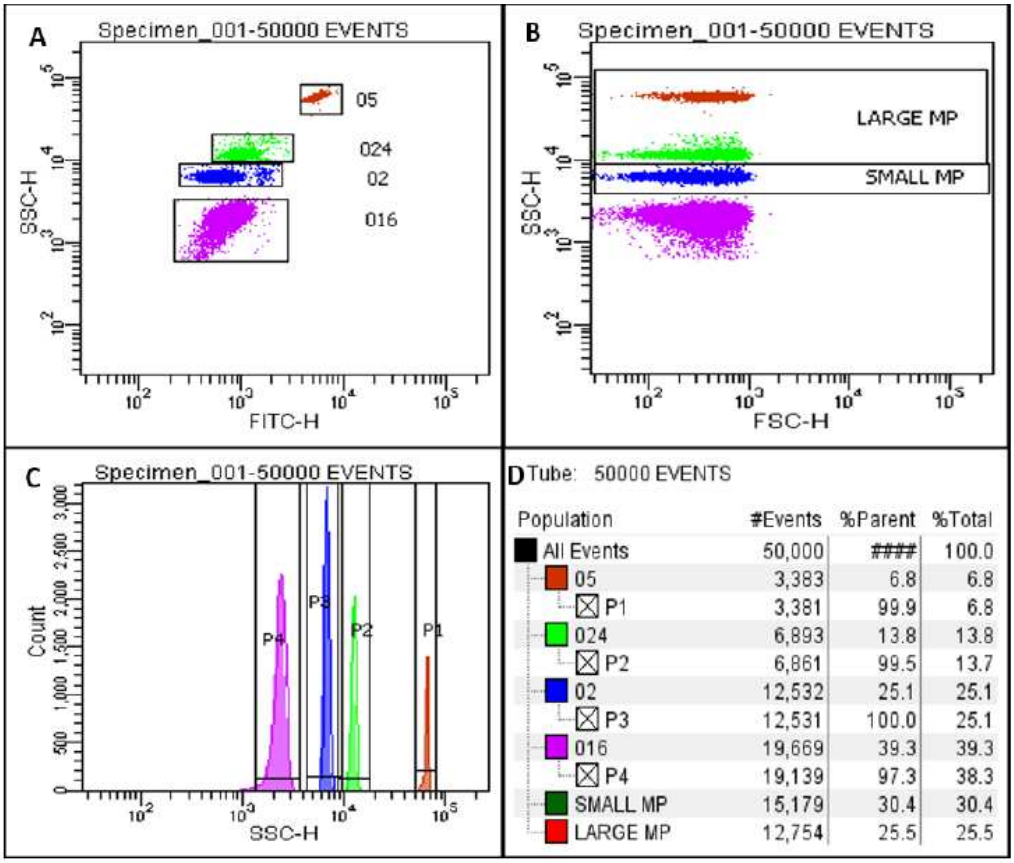

Figure 27. Flow cytometry bead analysis of four different factors**. Aand B)** Identification of the different bead's sub-populations discrimination according to light scatter (SSC-H). **C)** Own fluorescence peaks are reported. **D)** The events important to calculate background's thresholds setting are highlighted.

Owing to the plasticity of the lateral organization of plasma membrane into raft domains, known to segregate particular proteins and lipid species, a given stimulus can be expected to elicit a "private" response resulting in an inclusive or exclusive sorting. We investigated Annexin V+ MVs of leukocyte (CD45), erythrocyte (CD235), endothelial (CD31) and platelets (CD61) origin in plasma from 32 ALS patients, 28 Alzheimer's Disease patients,32 healthy controls matched in age and gender. Logarithmic amplification was used for all channels and isotype controls on plasma samples were used as negative controls as shown in **Figure 28.**

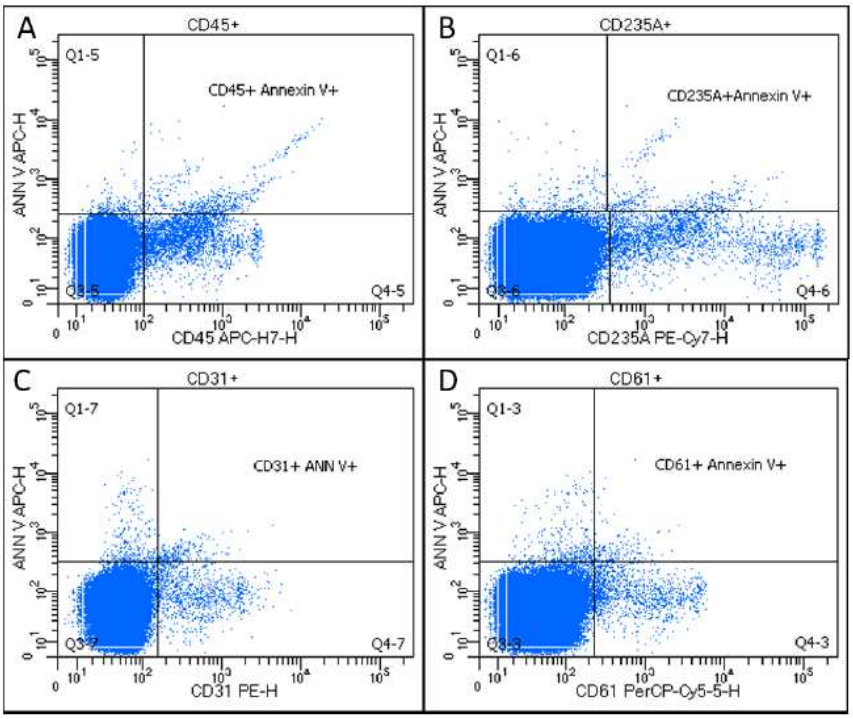

Figure 28.Representative flow cytometry dot plots of MVs, isolated from plasma of an ALS patient. **A)** MVs were labelled with Annexin V and leukocyte-derivative CD45 marker. **B)** MVs were labelled with Annexin V and erythrocyte-derivative CD235A marker. **C)** MVs were labelled with Annexin V and endothelial-derivative CD31 marker. **D)** MVs were labelled with Annexin V and platelet-derivative CD61marker.

2.2 Higher levels of CD45 MVs in plasma of amyotrophic lateral sclerosis patients

A number of reports showed that EVs can be taken under consideration as predictors of various pathological conditions. ALS is known to have multiple influences and regarded as a multi-cellular/multi-systemic disease[453]. In fact, motorneurons' death seems to be driven by a convergence of damaging mechanisms, including glial cell pathology and inflammatory conditions, microglial activation or the invasion of lymphocytes, and calcium dysregulation. Other processes include neurovascular changes and compromised barriers of the central nervous system (CNS), so that over time can be reached a dysfunctional communication between neurons, which leads to abnormal neuron–glia interactions and microglia-astroglia loss of function. For the optimal functioning of the CNS, for example, brain and spinal cord (SC), accounts the constant immune surveillance promoted by cells such as microglia, and the blood–brain barrier (BBB), the blood–SC barrier (BSCB), and the blood–cerebrospinal fluid (BCSF) barrier that uniquely shield CNS from potential mediators of infection and damage. For this reason, MVs of leukocyte (CD45), erythrocyte (CD235), endothelial (CD31) and platelets (CD61) origin in plasma of ALS patients were investigated in comparison with a group of controls and patients with another neurodegenerative disease, such as Alzheimer's Disease **(Figure 29).** Our patients' samples displayed the same number of phosphatidylserine (PS)-positive (Annexin V+) MVs in plasma, measured as absolute total number of events compared to healthy controls and Alzheimer's Disease patients.

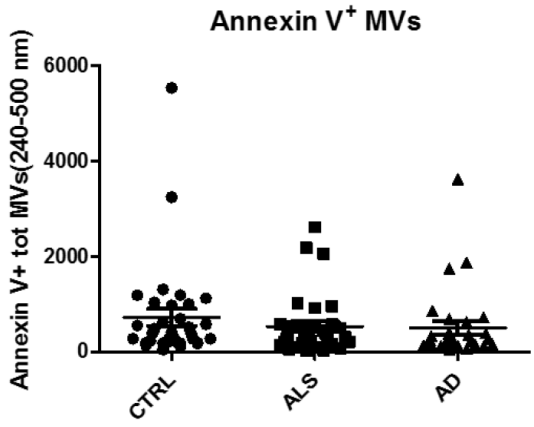

Figure 29. Detection of Annexin V + plasma derived MVs in control (CTRL), ALS and AD group. There is no a statistically significant difference between the three groups.

As we can see from **Figure 30**, not even percentage of Annexin V+ CD31+, Annexin V+ CD61+ or Annexin V+ CD235+ MVs of ALS patients were statistically different compared to controls or AD patients. The results that we obtained in the Annexin V+ CD45+ group of ALS patients was really interesting. In this case 70% of ALS patients considered in our cohort (24 out of 32 patients) presented a higher content of Annexin V+ CD45+ MVs in their plasma in comparison with the mean of the percentage of Annexin V+ CD45+ in controls and AD group.

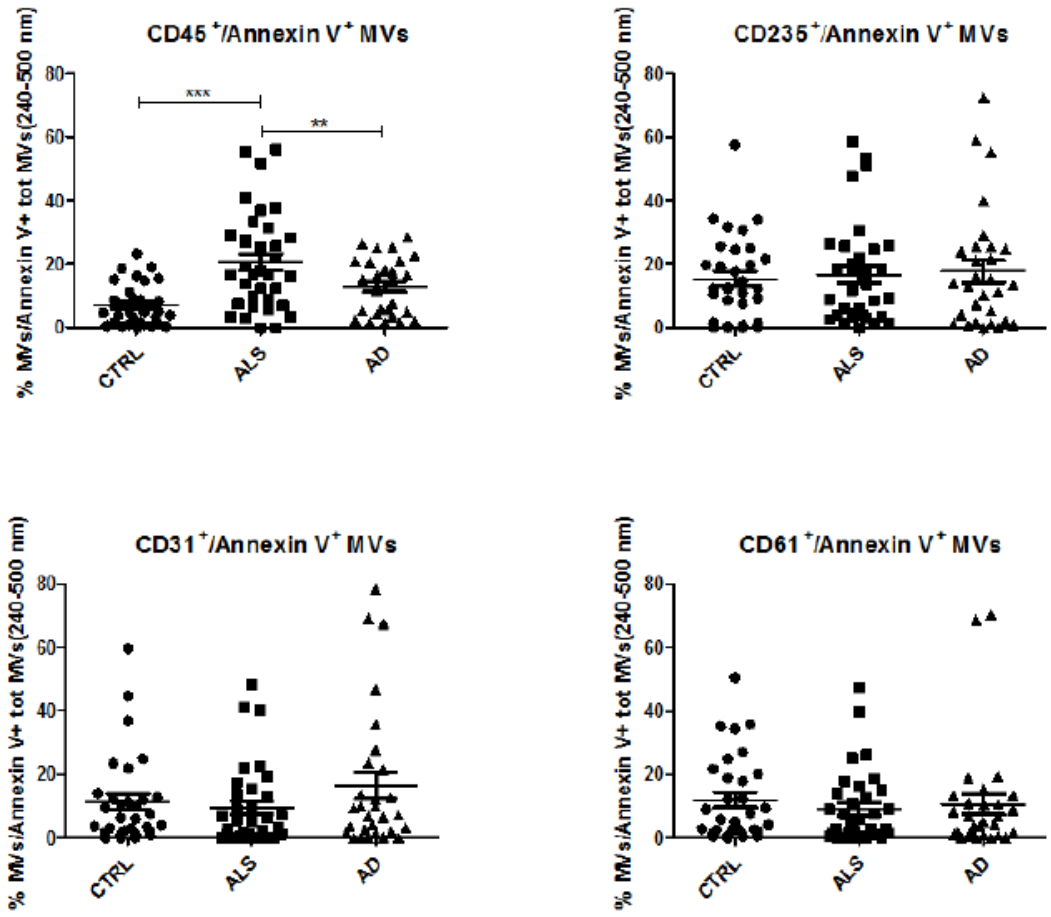

Figure 30. Detection of MVs subpopulations in human plasma: leukocyte-derived MVs (CD45), erythrocyte-derived MVs (CD235a), endothelial-derived MVs (CD31) and platelet-derived MVs (CD61).

The level of CD45+ AnnexinV+ MVs in ALS patients was even investigated by the use of flow cytometry analysis. **Figure 31** shows the expression of CD45+ AnnexinV+ MVs in control, low CD45+ AnnexinV+ and high CD45+ AnnexinV+ in ALS patients. The marked MVs were compared with the respective isotype for a correct elimination of autoflorescence. As we can see from figure 24 we can discriminate in a very clear way how the CD45+ AnnexinV+ MVs are distributed in the patients allowing their reported classification.

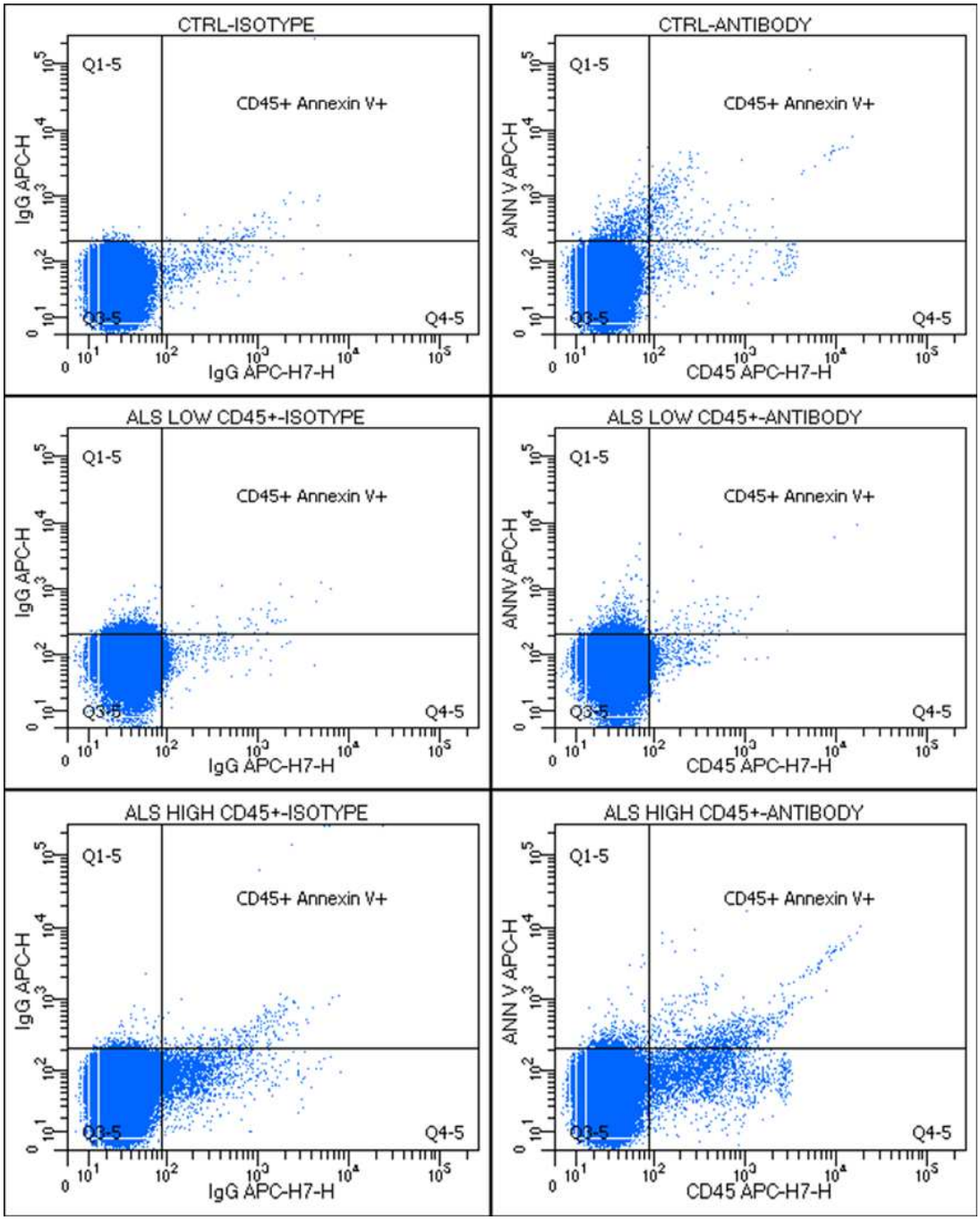

Figure 31. Representative flow cytometry dot plots of MVs isolated from plasma of an healthy donor, an ALS patient with low and one with high expression of CD45+ AnnexinV+ MVs compared to the respectively isotype.

We had clinical data of 24 ALS patients of our cohort and we defined their progression rate at baseline (PRB). Progression rate was calculated at baseline (PRB) as 48 minus the ALS.

Functional Rating Scale–Revised score (ALSFRS), divided by the disease duration from onset of symptoms (48-ALSFRS/Δt from beginning of symptoms). ALS Functional Rating Scale–Revised score is a physician-generated indicator of patient's degree of functional impairment and disease duration from onset of symptoms as reported in the study of Lu et al.[455]. In another study, Henkel et

al. demonstrated that when ALS patients were separated based on the rate of disease progression into rapidly versus slowly progressing ALS patients, the percent of CD4+ CD25high TREGs were reduced in rapidly progressing patients compared with slowly progressing patients and reduced compared with control volunteers[454]. The increased number of MVs may contribute to the ALS inflammatory process by formation of immune complexes enabling prion-like propagation of misfolded proteins in neural cells[456]. So, we divided CD45+ AnnexinV+ MVs data of ALS patients into three different groups considering their PRB: slow, intermediate and fast disease progression rate. As we can see in **Figure 32** B these three groups are not statistically different, but this may be related to the unequal distribution of ALS patients into the analysed groups (Slow PRB: 14 ALS patients, Intermediated PRB: 3 patients, Fast PRB: -7 ALS patients).

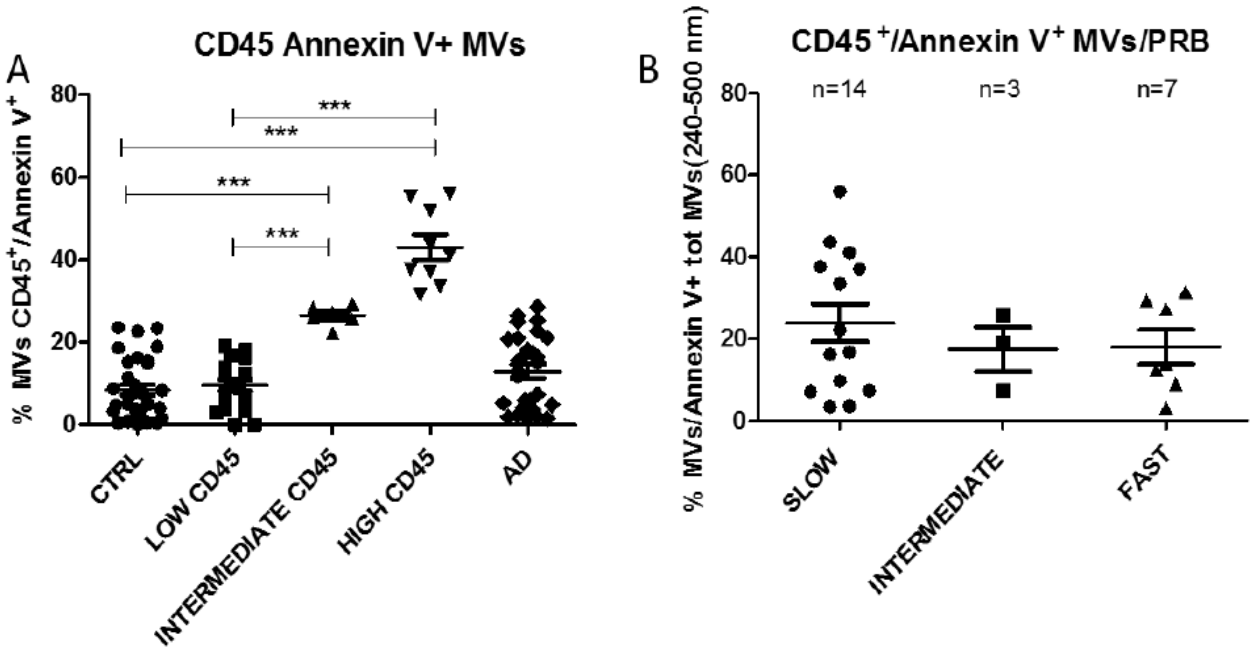

Figure 32.A) Annexin V+ CD45+ MVs percentage values for ALS patients were classified in three groups and the difference was statistically significant (ANOVA test ***p<0,0001). **B)** Annexin V+ CD45+ MVs percentage classification based on progression rate baseline (PRB). The three groups were not statistically different.

Considering the 14 ALS patients that were characterized by a slow PRB, we were able to divide them in two groups, one with high percentage of CD45+ MVs and the other with low amount of CD45+ MVs. As we can see in **Figure 33** the data we obtained were statistically significant (t test, p<0,001). The analyzed patients are very homogeneous without important mismatches in age or gender (7 male patients and 1 female patient in slow PRB/CD45+ low; 3 male patients and 3 female patients in slow PRB/CD45+high).

Once identified and classified, we decided to analyze if CD45+ Annexin+ MVs in these patients were possible carriers of misfolded or aggregated proteins correlated with the pathological prion-like spread of ALS disease.

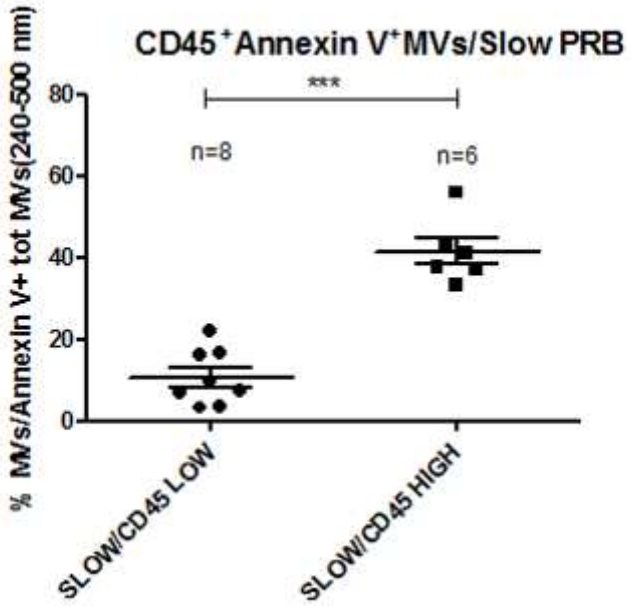

Figure 33. Slow PRB ALS patients could be classified in low CD45+ MVs (n=8) and high CD45+ MVs (n=6). These data were statistically significant (t test ***p <0,0001)

2.3 Imaging flow cytometry to compare two different dyes in Extracellular Vesicles

Both direct and indirect evidence exists to suggest that EVs are internalized into recipient cells. EVs have been shown to transfer functional mRNA and miRNA from mouse to human mast cells where mouse proteins were identified in the recipient human cells. EV-mediated siRNA delivery has beenshown to knockdown target gene expression, and administration of EVs laden with luciferin substrate to luciferase expressing cells resulted in production of bioluminescence.These results imply that merging of the EV cytosol and the cytoplasmic compartment had occurred through membrane fusion at the plasma membrane or by uptake through other pathways followed by fusion with the endosomal membrane[457]. EV uptake can also be visualized directly. The most common method for detecting EV uptake involves the use of fluorescent lipid membrane dyes to stain EV membranes. Examples of lipophilic dyes arePKH67, PKH26,FM 1-43 and long-chain dialkylcarbocyanines in particular DiIand DiD. Membrane permeable chemical compounds are also used to stain EVs. These include carboxyfluorescein succinimidyl ester (CFSE) and 5(6)-carboxyfluorescein diacetate (CFDA). These compounds become confined to the cytosolic lumen and fluoresce as a consequence of esterification. Subsequent entry of EVs into recipient cells can be measured using methods such as flow cytometry and confocal microscopy.

In our case we tested two dyes respectively 10 uM,1uM,100uM of CFSE and 10 ug/ml,1ug/ml and 100 ng/ml of FM1-43 observed within plot flow cytometry and imaging to obtain a higher resolution between the observed data and the artifact that can arise during capture **(Figure 34 A e B)**

A)

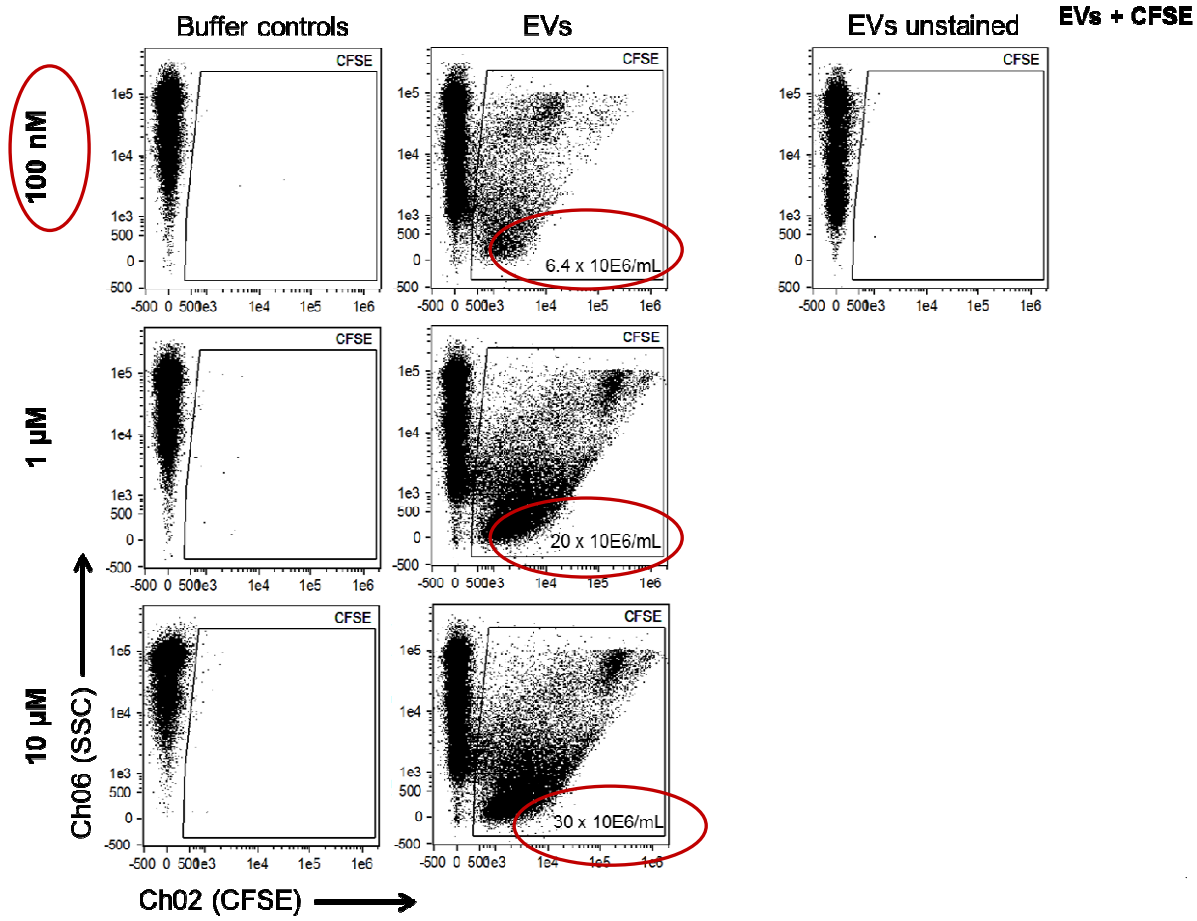
Buffer controls
EVs
EVs unstained
EVs + CFSE
100 nM
1 µM
10 µM
CFSE
6.4 x 10E6/mL
20 x 10E6/mL
30 x 10E6/mL
Ch06 (SSC)
Ch02 (CFSE)

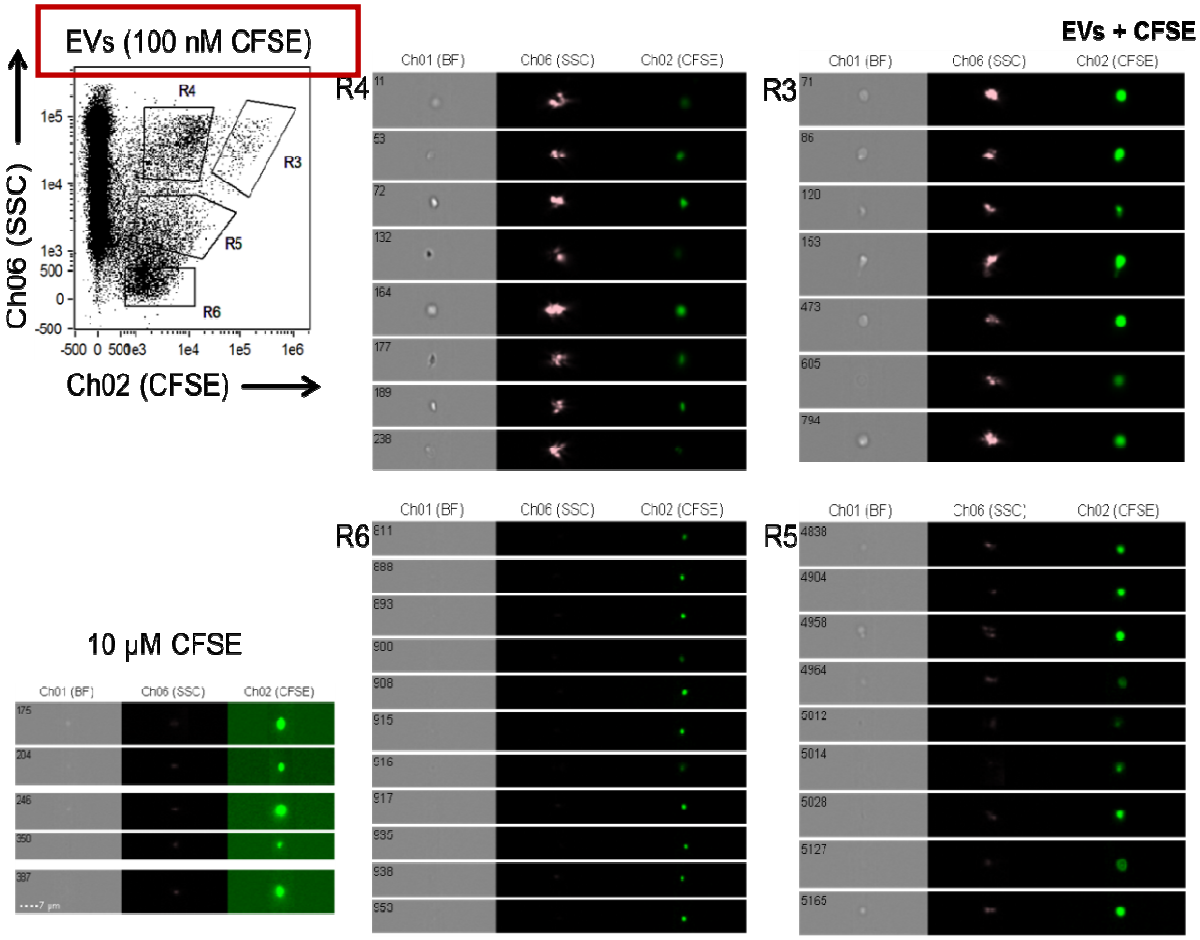

Figure 34A : Flow cytometric analysis:It is reported main differences in the standing concentration of CSFE and and it is tested its skills to detectare vesicular membranes (R5 and R6) than to cell populations (R3 and R4). Note how the SSC in R5 and R6 decreases sharply stressing the importance to test different colors for different groups of Evs.

B)

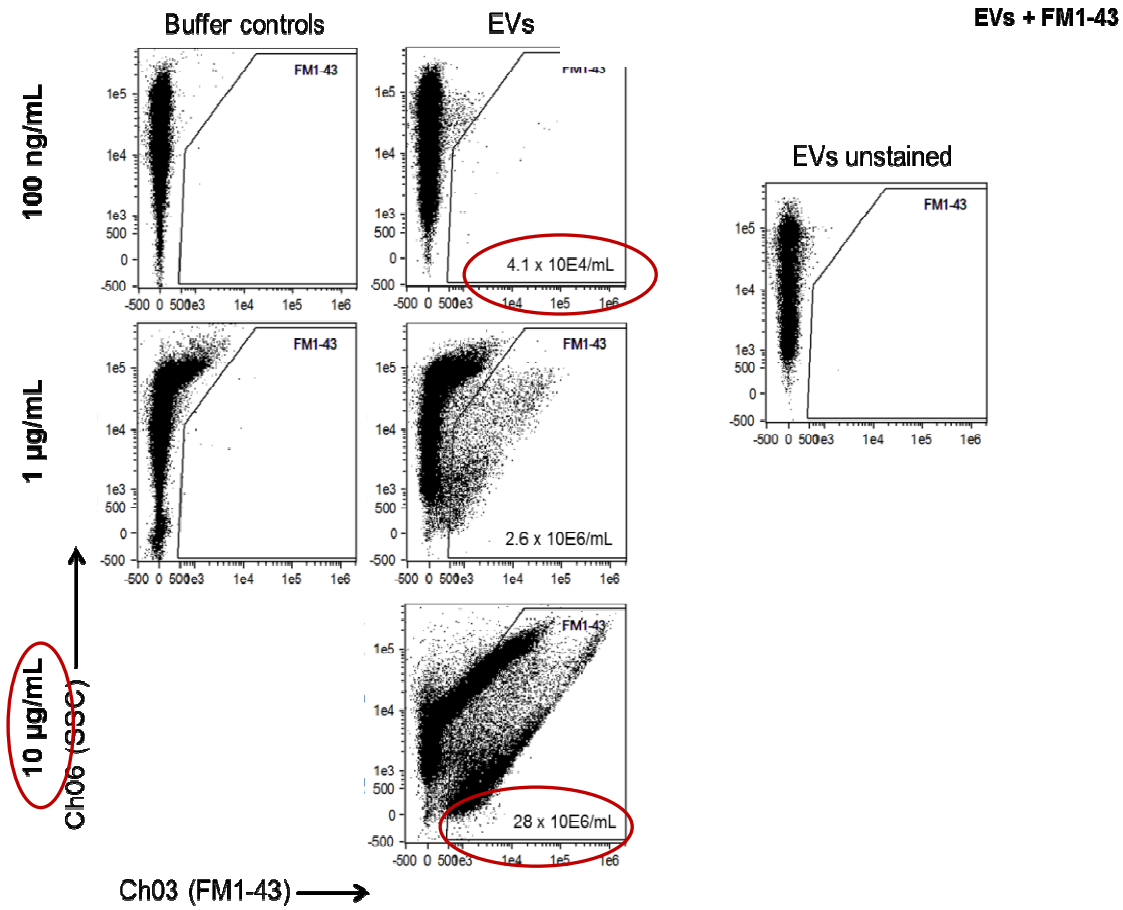
Buffer controls
EVs
EVs + FM1-43
EVs unstained
100 ng/mL
1 µg/mL
10 µg/mL
Ch06 (SSC)
Ch03 (FM1-43)
FM1-43
4.1 x 10E4/mL
2.6 x 10E6/mL
28 x 10E6/mL

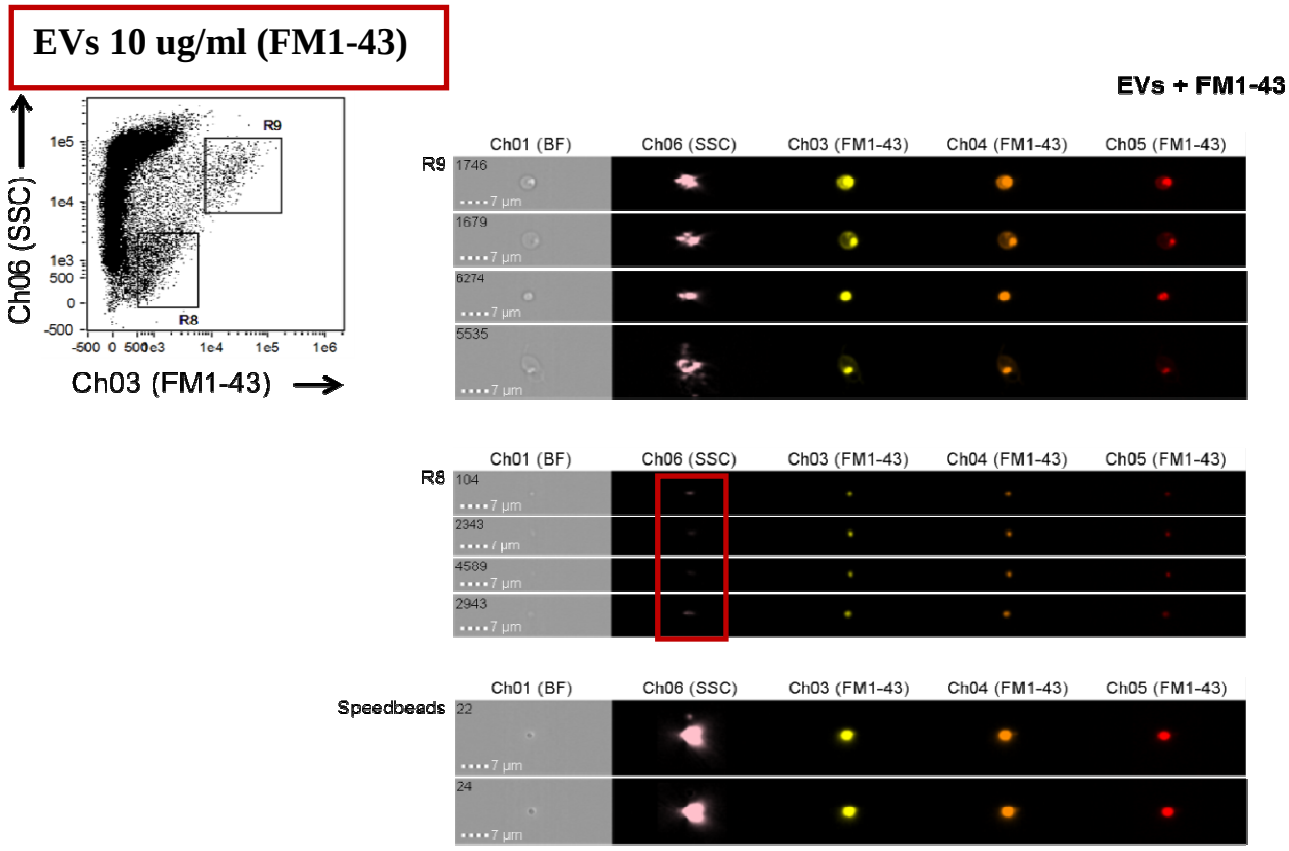

Figure 34 B : Flow cytometric analysis:It is reported main differences in the standing concentration of FM1-43 and and it is tested its skills to detectare vesicular membranes R8 than to cell populations R9. Note how the SSC decreases sharply stressing the importance to test different colors for different groups of Evs.

2.4Phenotyping immune Microvesicles by Imaging flow cytometry

Amyotrophic lateral sclerosis (ALS) is a fatal neurodegenerative disease of the motor neuron. Immune responses from active T cells play likely an important pathogenetic role;MVs arereleased by almost all cell types via membrane budding and are thought to be important bio-activators andcommunicators. They carry surface markers of the parent cell which can be used to identify their origin.The aim of this part was to characterize MVs as novel biomarkers in plasma of ALS patients by Imaging Flow Cytometry(IFC) focusing on MVs deriving from immune cells. MVs from 20 ALS patients and 20 healthy volunteers were isolated from platelet poor plasma and it were used the following markers:CD4,CD8,CD25,CD45RO and CD45RA; Annexin V (AnnV) and Calcein were used as general MV membrane markers.

Figure 35 shows how the instrument distinguishes vesicles than cells's size (red box) using scatter parameter. Moreover it became evident as the green population is Ann V + and is present as a population Ann V-, in our case yellow plot. Furthermore, for each individual event of every interest gate it is possible to discriminate with certainty vesicles than the debris through different multiplefluorescences.As can be seen from **Figure 35**, each vesicle can have a single or double marking for own identification. An improved understanding of MVs biological processes in ALS will help to define markers related to the progression of the disease and contribute to future vesicular potential therapies.

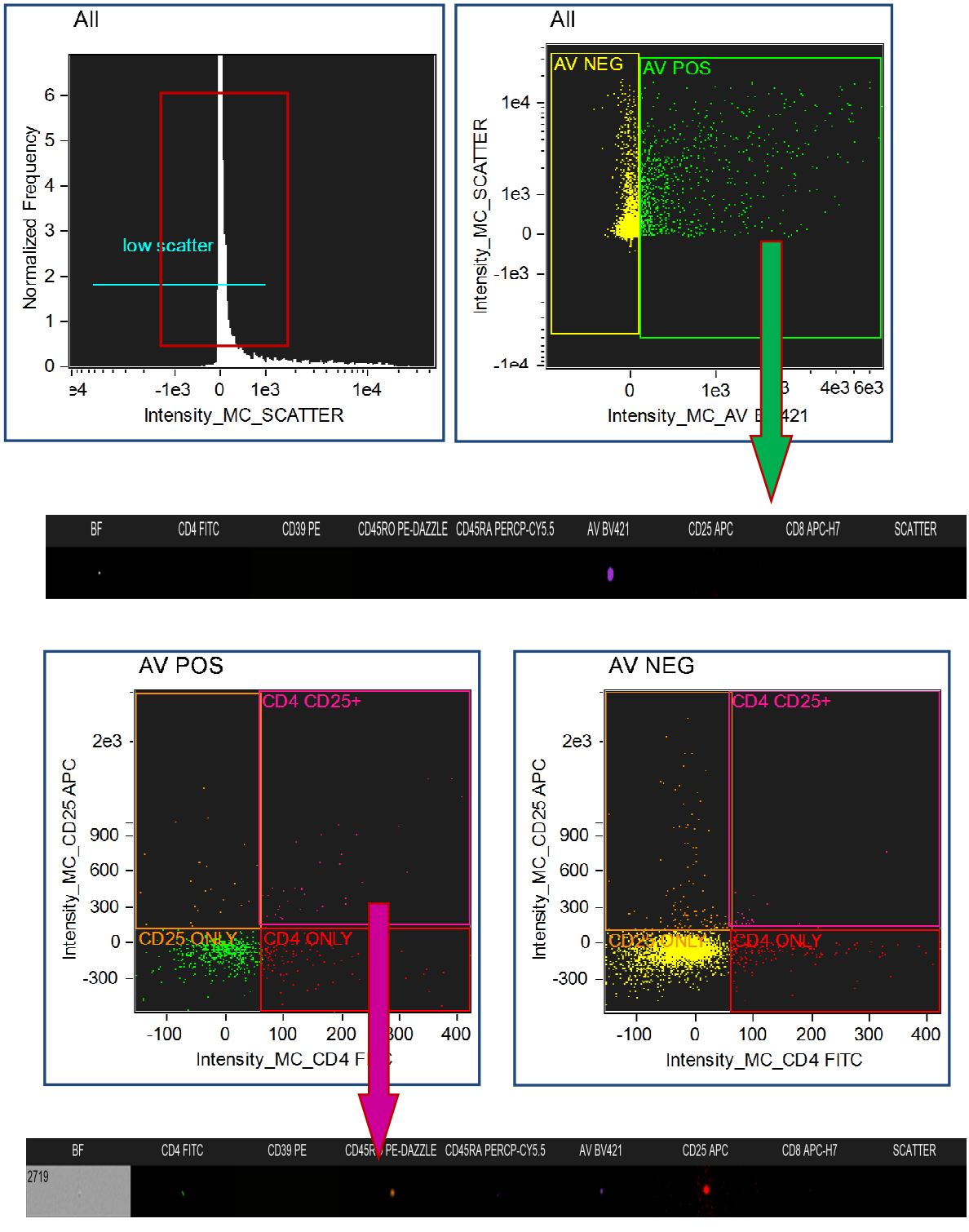

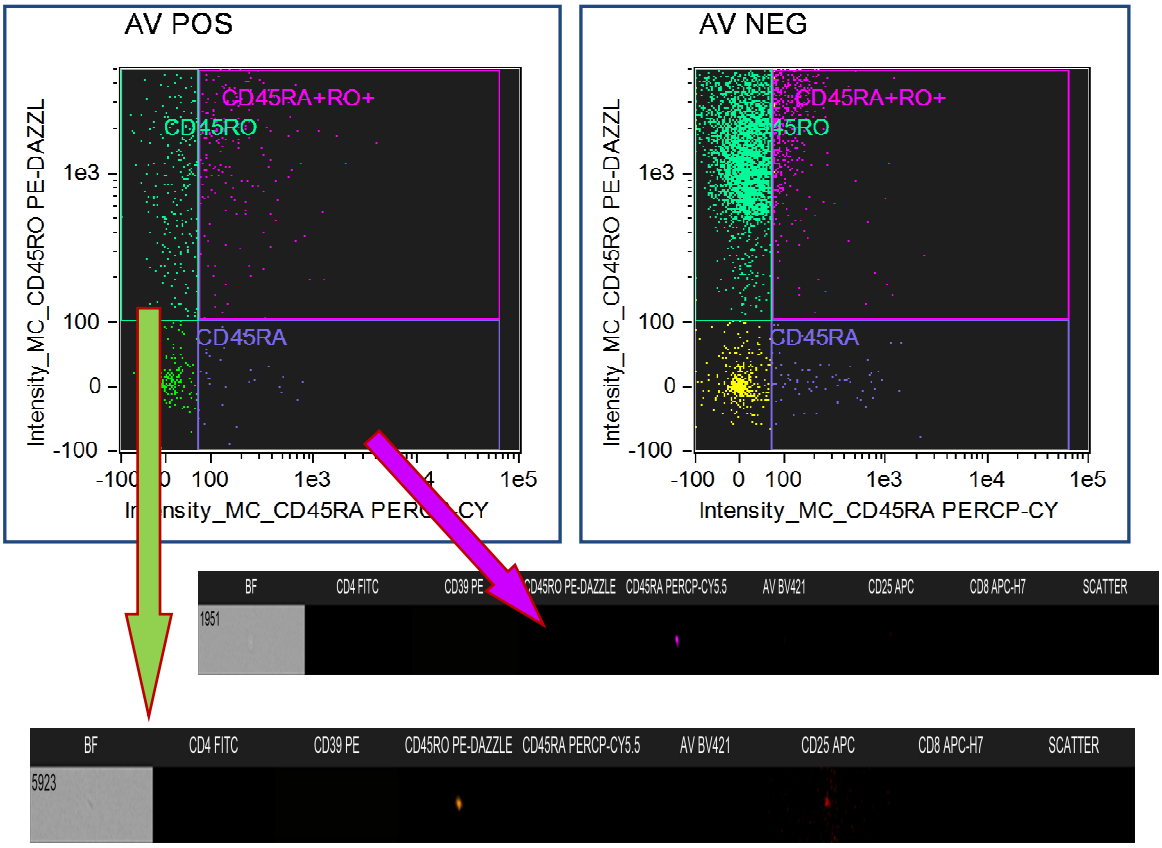

Figure 35. Gating strategy for determining different microvesicular phenotypes. Positivity of the following vesicle populations have therefore been reported:(Cd4+/Cd25+/AnnV+)(Cd4+/Cd25+/AnnV-)(Cd45RO+/AnnV+) (Cd45RO+/AnnV-) (Cd45RA+/AnnV+)(Cd45RA+/AnnV-).

As initially reported in the work by Appel[83]a rise CD4 + / CD25 + / PoxP3+ Treg cells it was more expressed in slow Als patients than patients with a already progression advanced disease. MVs arereleased by almost all cell types via membrane budding and are thought to be important bio-activators and communicators. In **Figure 36**we observed high levels of CD4+/CD25+/AnnV+ MVs in plasma samples from ALS patients (MVs 2,5 particles/ul (p=0.04)) compared to controls (Mvs 0,9 particles/ul) supporting previous finding that regulatory T-lymphocytes (Tregs) are neuroprotective in ALS[83] .

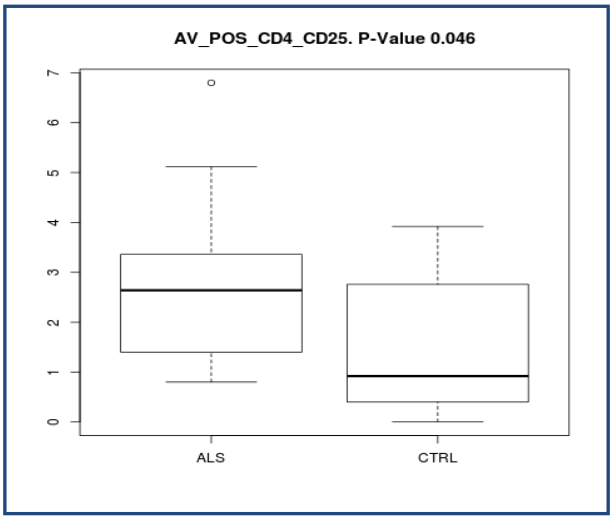

Figure 36. Monitored CD4+/CD25+/AnnV+ Analysis in MVs from 20 Als patients marched controls (t test** p <0.04) No significant differences were found observingCD4+/CD25+/AnnV- MVs.

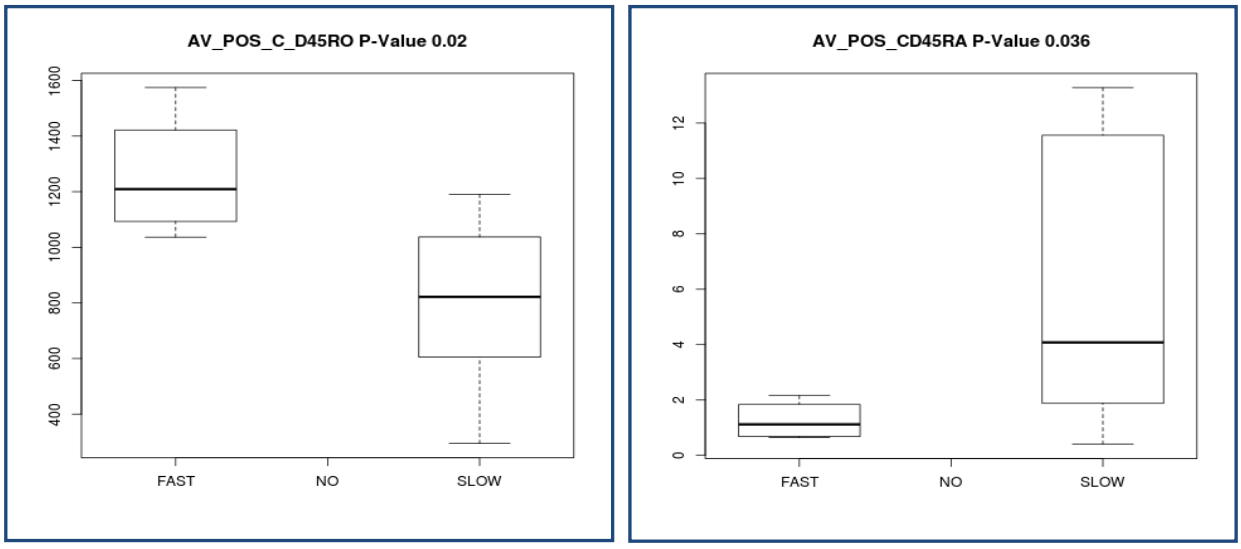

Figure 37. Detecting CD45RO/AnnV+ and CD45RA/AnnV+ Mvs from 20 Als patients compared controls (t test** p <0.02 and (t test**p<0.036) respectively.No significant differences were found in CD45RO/AnnV- and CD45RA/AnnV- Mvs.

Our data indicates that MVs of ALS patients carry markers of naive T lymphocytes (CD45RA) and activated and memory T lymphocytes(CD45RO). There is also a difference between fast and slow ALS patients using CD45RA/AnnV+(1,0 particles/ul in fast vs slow 5,4 particles/ul(p=0.02)) and CD45RO/AnnV+ (25,2 particles/ul fast vs slow 9,1 particles/ul(p=0.036)) **(Figure 37)**
Further studies are needed to understand this new role of CD45RA/AnnV+ and CD45RO/AnnV+ Mvs inthe slow and fast progression group of ALS patients and and this time point may be useful to understand the mediation Treg Mvs in the neuroimmune response .

3. RECOGNITION OF SOD1, TDP43 AND FUS PROTEIN LEVEL IN PLASMA DERIVED MVS AND EXOS FROM ALS PATIENTS

Grad et al. reported that both mutant and misfolded wild-type SOD1 can propagate from cell-to-cell, either as protein aggregates that are released from dying cells and taken up by neighbouring cells via macropinocytosis, or in association with vesicles which are released into the extracellular environment[458]. So we performed WB analysis for the investigation of protein cargo present in MVs and EXOs released in the plasma of 20 ALS patients' groups compared to healthy controls.

3.1 Misfolded SOD1 protein level is higher in plasma derived MVs of ALS patients compared to healthy controls

We analyzed MVs and EXOs obtained from plasma of 20 ALS patients (16 patients were in common with the flow cytometry analysis) compared to 22 age-matched healthy controls by WB for SOD1, TDP43 and FUS protein level. In literature loading controls used for whole cell lysate are not recognized for MVs or in EXOs. So SOD1, TDP43 and FUS protein levels in MVs and in EXOs were normalized respectively against a MVs marker (Annexin V) and an EXOs marker (Alix).

FUS antibody typically recognized a band at 72 kDa in whole lysate and in the nuclear extract of peripheral blood mononuclear cell (PBMC) from 2 controls and 2 ALS patients as shown in **(Figure38).**

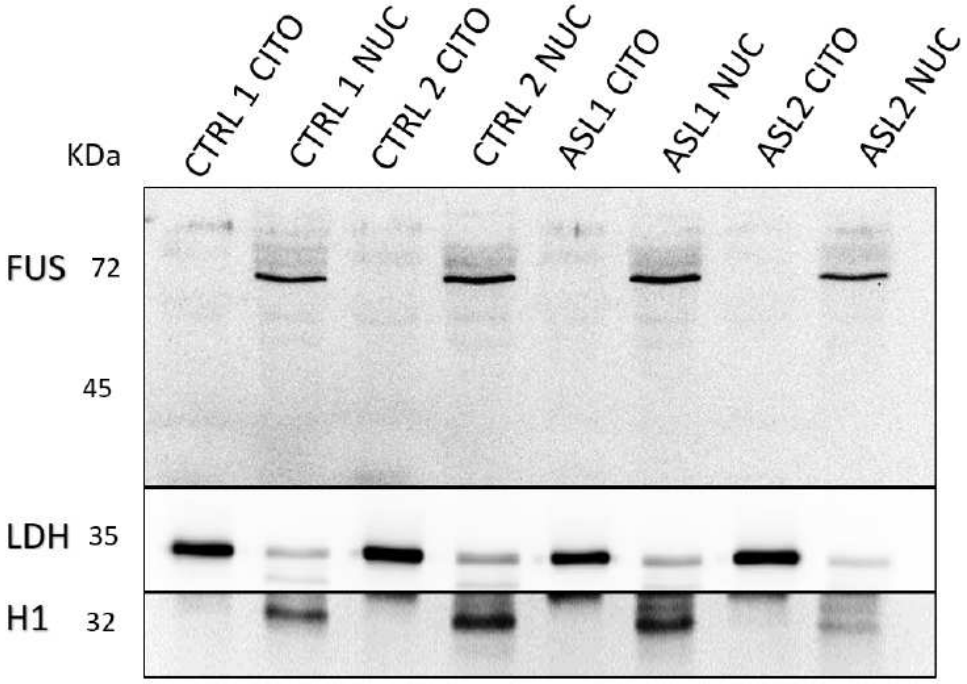

Figure 38. Western Blotting analysis of FUS protein on Nuclear and Cytoplasmic extracts of PBMC from 2 controls and 2 ALS patients. A band at 72 kDa was detected in the nuclear protein both in controls and in ALS samples. No band at 45 kDa was detected. LDH (Lactate Dehydrogenase) and H1 (Anti-Histone H1) were used as cytoplasmic and as nuclear loading control, respectively

The normal FUS band at 72 kDa was not present in any EVs samples, where instead we can distinguish an aspecific band at 45 kDa. Different from what we expected was the presence of SOD1 in MVs and EXOs from plasma of ALS and healthy controls. As we can see in **Figure 39** SOD1 band was not present in all samples. We used a mouse monoclonal misfolded SOD1-specific antibody 3H1 (Kindly given by Prof. Neil Cashman), able to recognize an extended electrostatic loop in misfolded SOD1 that is not antibody-accessible in its wild-type native conformation. As even reported by Liu et al.[459], the monomeric/misfolded SOD1 presence is characterised by a band at 19 kDa and we saw its presence in MVs and EXOs of controls and ALS patients. We could even detect a higher band at 38 kDa that could be associated with the dimeric form of SOD1. On the contrary of SOD1 wild-type, misfolded SOD1 was highly present in MVs of ALS patients compared to healthy controls, and even more in EXOs of the two groups. TDP43 bands (43 kDa and 20 kDa) were recognized in MVs and in EXOs as presented in **Figure 39**. The band at 25 kDa fragment was more present in exosomes that in MVs. According to Zhang et al.[460] the band at 25 kDa fragment is identified as pathological because it is able to induce cell death through a toxic gain-of-function.

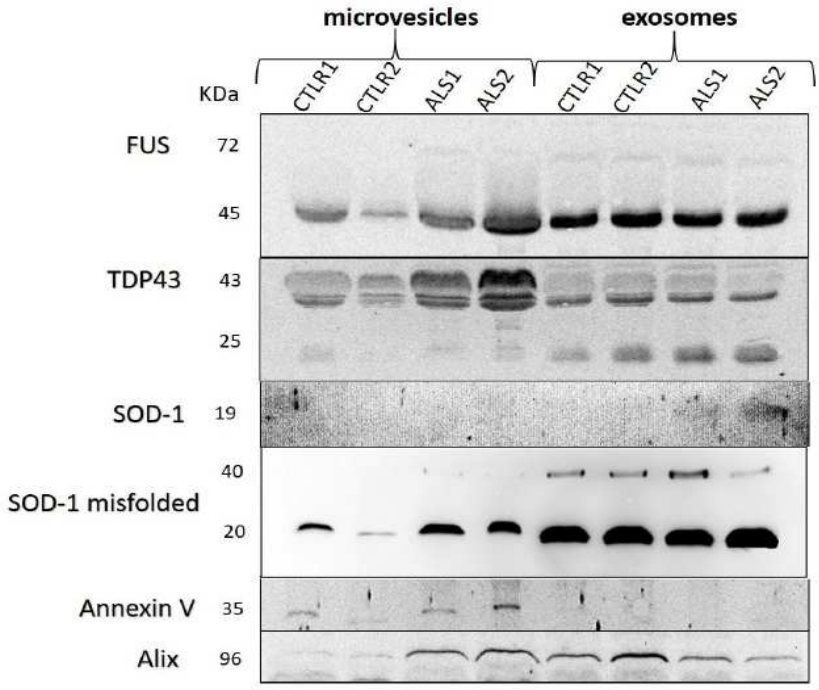

Figure 39. WB analysis of MVs and EXOs lysate of 2 ALS patients and 2 healthy controls. Annexin V and Alix were used as MVs and EXOs loading control. SOD1 and FUS bands were not present in all samples. Misfolded SOD1 (recognized with specific antibody 3H1), was present in MVs and EXOs of ALS patients compared to healthy controls. TDP43 bands (43 kDa and 25 kDa) were recognized in MVs and in EXOs. The band at 25 kDa fragment is more present in EXOs that in MVs.

As it can be seen in **Figure 40,** densitometric analysis, carried out by ImageJ software, showed no significant difference in TDP43 protein level between MVs of healthy controls and ALS patients and between EXOs of healthy controls and ALS patients. On the contrary, misfolded SOD1 protein level was upregulated in plasma MVs from ALS patients compared to healthy controls. Misfolded SOD1 protein level was also slightly upregulated in plasma EXOs from ALS patients compared to healthy controls. Data obtained were statistically significant (ANOVA test, *** $p<0,001$). As we can see in **Figure 40**, misfolded SOD1 protein level was considered both in its dimeric and monomeric form. It is reported that SOD1, normally present in its dimeric isoform, dissociates to monomers prior to aggregation for both wild-type and mutant proteins and this dissociation is accompanied by minimal changes in the secondary structure. This indicates a common aggregation prone monomeric intermediate for wild-type and fALS associated mutant SODs and provides a link between sporadic and familial ALS [461].

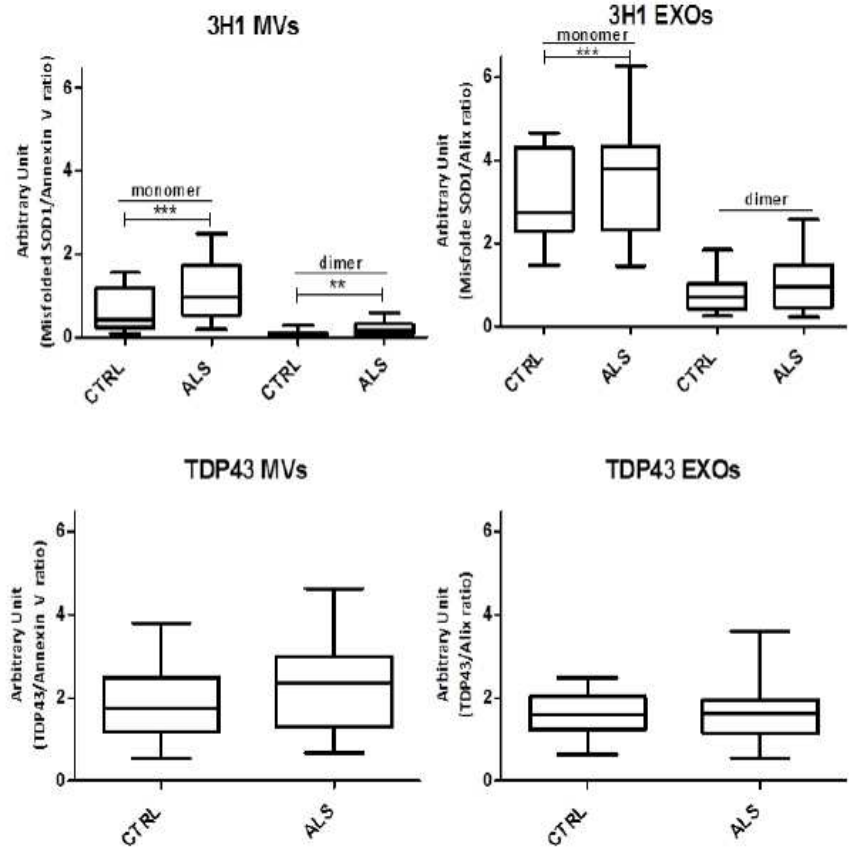

Figure 40. Misfolded SOD1 and TDP43 densitometric analysis in MVs and EXOs lysate from 20 ALS patients and 22 matched controls (ANOVA test **p<0.05; *** p<0.001). No significant differences were found in protein levels of TDP43. Monomer SOD1 protein level was increased in MVs of ALS patients in comparison with controls. Less difference could be detected in plasma derived EXOs from ALS patients compared to controls.

Following the model proposed by Grad et al., i.e. the intercellular propagation from cell to cell of misfolded SOD1 in ALS patients through the spreading of EVs in biofluids[18], we demonstrated that this pathological protein is highly present in ALS patients MVs in comparison with MVs in control samples. So we can hypothesise that the accumulation of toxic SOD1 protein inside the cells in the development of ALS disease, may be related with a compensatory mechanism by which the elimination of these protein aggregates are enriched with their inclusion in EVs secreted in plasma of patients.From our data this model cannot be true for FUS and TDP43 which dispersion should be further investigated.

3.2 Misfolded SOD1 in CD45 + MVs distinguishes slow progression patients with high levels of plasma derived CD45 MVs

The detection of the same proteins was carried out in plasma derived CD45+ MVs from two slow progression ALS patients of the two groups, one with high percentage of CD45+ MVs and the other with low amount of CD45+ MVs. CD45+ MVs were isolated by immunoprecipitation technique as described in Material and Methods. As we can see in Figure 30, TDP43 and FUS are not detected in CD45+ MVs, on the contrary the result obtained for SOD1 was really interesting. Wild-type SOD1 was not present in CD45+ MVs from healthy control and the two ALS patients **(Figure 41).** The expression of misfolded SOD1 in CD45+ MVs instead was mainly detected in the ALS patient that belonged to the slow PRB/high plasma CD45+ MVs compared to the slow PRB/low plasma CD45+ MVs that did not show misfolded SOD1 protein level. These data were confirmed in 6 patients of the slow PRB/high plasma CD45+ MVs and 6 patients slow PRB/low plasma CD45+ MVs ALS patients compared to 6 healthy controls.

This result can be used to further classify ALS patients considering their high or low expression of misfolded SOD1 in secreted MVs. Further analyses are needed in a larger cohort to understand the exact mechanism of supposed prion-like propagation of misfolded proteins. Henkel et al. demonstrated that when the ALS patients were separated based on the rate of disease progression into rapidly versus slowly progressing ALS patients, the percent of CD4+ CD25high TREGs were reduced in rapidly progressing patients compared with slowly progressing patients and reduced compared with control volunteers[83]. This was even confirmed by Beers et al. who, studying double transgenic mice carrying mSOD1 and lacking CD4, showed development of a more aggressive ALS phenotype[84]. So CD45+ might function as scavenger of misfolded SOD1 to help or to worsen disease progression. Indeed, it would be interesting to investigate the follow-up of these patients in order to understand if SLOW/high plasma CD45+ can become fast progressing ALS patients or stayed stable in their disease prognosis. This may allow the development of personalised therapy for the removal of targeted MVs with high content of misfolded SOD1 that are responsible of disease spreading. So, it is needed a deep investigation of EVs as vehicles of toxic protein cargo in other

ALS patients. This may provide the explanation of mechanisms through which ALS disease is able to spread and induce pathogenicity in patients, making EVs suitable and accessible biomarkers.

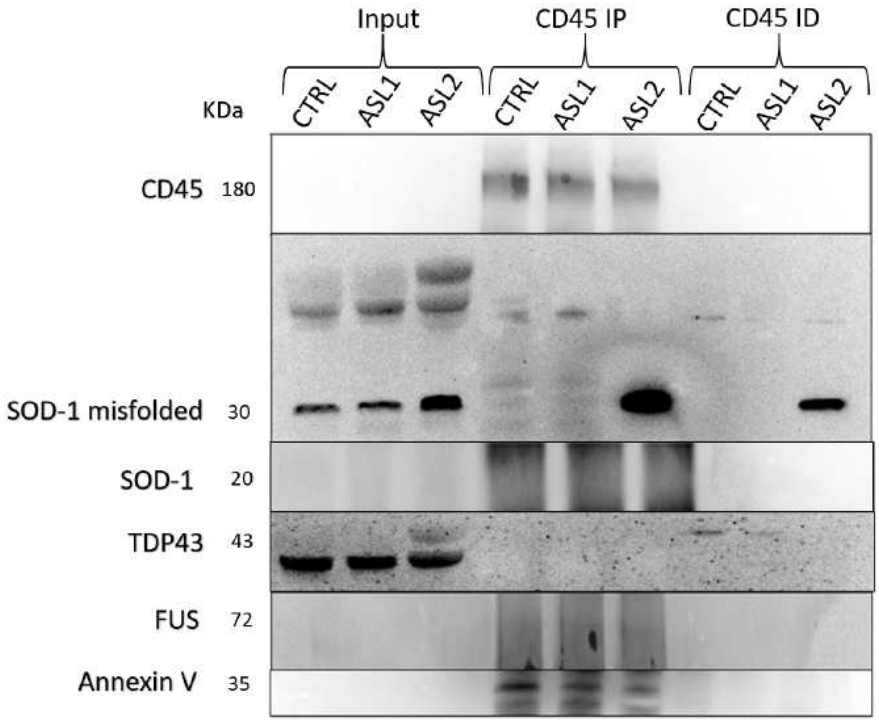

Figure 41. Immunoprecipitation of CD45+ MVs in healthy controls and 2 ALS patients, one with high percentage of CD45+ MVs and the other with low amount of CD45+ MVs (input = starting material, CD45 IP MVs = eluate, CD45 ID MVs = flow through). High expression of misfolded SOD1 was seen in CD45+ MVs in slow PRB/high CD45 ALS patient in comparison with slow PRB/low CD45 that does not express misfolded SOD1. TDP43 and FUS were not detected in CD45+ MVs of healthy control and ALS patients. These data were seen in 12 ALS patients and 6 healthy control.

CONCLUSIONS:

Patients suffering from sporadic ALS have been reported to have increased levels of circulating inflammatory (CD16+) monocytes in peripheral blood[462]which correlated well with increased levels of plasma LPS[463], a potent inducer of M1 activation in macrophages indicating that in Als inflammatory response is not limited to the CNS but it concerns an systemic immune activation. Cerebrospinal fluid is not always easy to find and not being a diagnostic marker its frequent unavailability is well known and this is why the search of biomarkers as microvesicles and the possibility to investigate them systemically, it has increasingly affected the scientific field. EVs are spherical vesicles classified mainly for size and biological function in EXOs and MVs. In the first part of this work we have dealt the set up a protocol to isolate MVs and EXOs from plasma of ALS patients and controls for a better understanding of their role in this neurodegenerative disease and for a deep investigation about of their involvement in ALS pathogenesis by conventional flow cytometry. Instead the second part is focused on the first of phenotyping Mvs Treg approach in Als by image flow cytometry. It is known that MVs from prion-infected neuronal cells can initiate prion propagation in uninfected cells, underlying a new mechanism of the disease propagation[464]. First of all, Nanotracking Analysis (NTA) and Western Blotting were used to confirm the purity of the two populations of vesicles respectively based on their dimension and based on their membrane markers (Annexin V for MVs and Alix for EXOs). We determined Annexin V+ MVs of a particular cellular signature (CD235a for erythrocyte derived MVs, CD45 for leukocyte derived MVs, CD61 for platelet derived MVs and CD31 for endothelial derived MVs) by flow cytometry analysis in plasma from 32 ALS, 28 AD patients and 32 healthy controls. We found a significant presence of CD45+ Annexin V+ leukocyte derived-MVs in a group of ALS patients. Considering 14 ALS patients that were characterized by a slow PRB we were able to divide them in two groups, one with high percentage of CD45+ MVs and the other with low amount of CD45+ MVs (t test, $p<0,001$). Once identified and classified MVs, we decided to further investigate ALS patients and to analyse if CD45+ MVs in these patients could be indicated as possible carriers of misfolded or aggregated proteins correlated with the pathological prion-like spread of ALS disease through the WB technique. We investigated the protein level of TDP43, FUS and SOD1. In plasma MVs and in EXOs from 20 ALS patients no significant differences were found in protein levels of TDP43 compared to healthy controls. Misfolded SOD1 protein level was increased in MVs of ALS patients in comparison with healthy controls. Less differences were detected for misfolded SOD1 in plasma derived exosomes from ALS patients compared to controls. Interestingly, we found a significant presence of misfolded SOD1 in high CD45+ Annexin V+ MVs/slow PRB ALS patients compared to a group of patients with low CD45+ Annexin V+ MVs/slow PRB ALS patients. No SOD1, TDP43 and FUS were detected in CD45 MVs. These results allow us to hypothesise a mechanism through which MVs and EXOs are released by cells as a way for discharging misfolded/aggregated toxic SOD1 during the arise of ALS disease. The regulation of this process results fundamental

because the production of these EVs enriched in toxic proteins has been demonstrated to be mainly involved in a prion-like distribution enabling and facilitating the spread of ALS disease[465].

Neurodegenerative diseases including ALS are characterized by the death of specific populations of neurons accompanied by a neuroinflammatory response that isaddressed to microglial activation and T-cell infiltrates in spread regions. In the literature previous articles established that mRNA levels of TDP-43 and the p65 subunit of nuclear factor kB (NF-kB), a transcription factor involved in the expression of proinflammatory mediators, are upregulated in the spinal cords of ALS patients[466]and microglial cultures treated with LPS and modified to obtain a overexpression TDP-43 confirming the presence of high levels of pro-inflammatory cytokines and neurotoxic factors compared to wild-type microglia[466]; after these observations, the therapeutic research has been carried out in order to modulate the inflammatory response infact once considered a consequence of neuron death in chronic neurodegenerative disease, neuroinflammation is now recognized to influence disease progression in ALS and the mSOD mouse model. As it will be reported subsequently experimental evidence has demonstrated that microglial activation together with the infiltration of T cells has different effects on surrounding neurons until late stages of disease[467,468]. Increased numbers of activated microglia are observed at early presymptomatic stages of disease in mSOD mice culminating in the end-stages at which point levels of proinflammatory cytokine IL-1 and TNF-α increase, as do levels of NADPH oxidase[467,468].This suggests that during initial stages of disease in mSOD mice, microglia exhibit an M2 phenotype with the majority neuronal survival and subsequently the phenotype remains M1 phenotype and the physiological mechanism that leads to the switchbetween these two forms of activated microglia has not yet been exhausted. On the other side phenotypical analysis indicated that T cells populating in the mSOD spinal cord were limited to the CD4+ subsets until disease end-phase at which point 40% of T cells were CD8+ T cells.[469]For these reasons microvesicles are a new communication to investigate the role of T cells in neuroinflammation especially understanding how these cells influence the phenotypic profile of activated microglia. In two independent studies, ablation of T cells in mSOD mice was achieved by crossing mice with a $TCR^{-/-}$ strain or with an $RAG2^{-/-}$ strain, andit follows that disease progression was accelerated in the mSOD mice[470,471]. In both studies a change in the microglial morphological activation accompanied by reduced functional T cells it was present.To understand what kind of T cells were involved, mSOD mice crossed onto a strain lacking only functional CD4+ T cells. The observed result was similar to that demonstrated by the studies in which all T cells were ablated, indicating that CD4+ T cells in the mSOD spinal cord function to modulate microglial activation and they unbalance it towards an M2 neuroprotective phenotype[469]During the second work with IFC ,high levels of CD4+/CD25+/AnnV+ (T regulatory cells) MVs are found in our cohort of ALS patients supporting previous finding that regulatory T-lymphocytes (Tregs) are neuroprotective in ALS[83].Recently it was demonstrated that the passive transfer of CD4+ Tregs into mSOD mice extended the stable phase of disease progression and survival times, suggesting that manipulation of the microglial response through the adoptive transfer of Treg cells or pharmaceutical agents that potentiate M2 activation in microglia may have therapeutic value[472]. In fact, Neuraltus Pharmaceuticals is currently conducting phase II clinical trials in patients suffering from ALS, PD, and AD using NP100, a pharmaceutical drug designed to skew macrophage activation towards an M2 phenotype to determine its efficacy in prolonging disease duration. In addition, our data indicates that MVs of ALS patients carry markers of naive T lymphocytes (CD45RA) and activated and memory T lymphocytes(CD45RO) showing a distinction between of CD45RA/AnnV+ and

CD45RO/AnnV+ Mvs in the slow and fast progression group of ALS patients. This finding might indicate different steps of T cell activation in subsequent times regarded as instead tumor-derived EVs (TEVs) are already widely studied in adaptive immune response. Cancer EVs can stimulate the immune response by transferring tumor antigens to DCs[473]leading to Ag-specific T cell activation, in particular of CD8 cytotoxic T lymphocytes (CTL) clones[474,475]or they can also behave as immunosuppressive favoring cancer escape from immune surveillance; infact TEVs can induce T cell apoptosis via FasL and galectin-9, inhibit IL-2-induced T cell proliferation, promote Tregs, reduce CD8+ T cells proliferation.[477,478,479].

A deeper understanding of the role that microvesicles play in the microenvironment and how they affect other cells in the immune system, it could help to identify new adaptive immune steps in Als and still unknown way of therapeutic approaches.

References

1. Robberecht W and Philips T. The changing scene of amyotrophic lateral sclerosis. *Nat Rev Neurosci*., 14, 248–264,(2013).

2. Joffroy J. and M. C. A. Deux cas d'atrophie musculaire progressive avec lesions de la substance grise et des faisceaux antero-lateraux de la moelle epiniere. *Arch Physiol Neurol Path*., 2, 406-744,(1869).

3. Ingre C. et al. Risk factors for amyotrophic lateral sclerosis. *Clin Epidemiol.,* 7, 181–93,(2015).

4. Pasinelli P.and Brown R. H. Molecular biology of amyotrophic lateral sclerosis: insights from genetics. *Nat Rev Neurosci*., 7, 710–23,(2006).

5. Roland Brandt. Cytoskeletal mechanisms of neuronal degeneration.*Cell and Tissue Research.,* 305, 255–265, (2001).

6. Worms P. M. The epidemiology of motor neuron diseases: a review of recent studies. *J Neurol Sci*., 191, 3–9,(2001).

7. Chiò A. et al. Epidemiology of ALS in Italy: a 10-year prospective population-based study. *Neurology.,*72, 725–31, (2009).

8. Logroscino G. et al. Descriptive epidemiology of amyotrophic lateral sclerosis: new evidence and unsolved issues. *J Neurol Neurosurg Psychiatry.,* 79, 6–11, (2008).

9. Hong S.T. X-linked dominant locus for late-onset familial amyotrophic lateral sclerosis (Abstract). *Soc Neurosci,*. 24, 478–478, (1998).

10. Millecamps S. et al. SOD1, ANG, VAPB, TARDBP, and FUS mutations in familial amyotrophic lateral sclerosis: genotype-phenotype correlations. *J Med Genet*., 47, 554–60,(2010).

11. Mandrioli J. et al. The epidemiology of ALS in Modena, Italy. *Neurology*., 60, 683–9,(2003).

12. Gordon P. H. Amyotrophic Lateral Sclerosis: An update for 2013 Clinical Features, *Pathophysiology, Management and Therapeutic Trials.*,4, 295–310,(2013).

12. Al-Chalabi A. et al. An estimate of amyotrophic lateral sclerosis heritability using twin data. *J Neurol Neurosurg Psychiatry*., 81, 1324–6,(2010).

13. Hanby M.F. et al. The risk to relatives of patients with sporadic amyotrophic lateral sclerosis. *Brain.,* 134, 3454–7,(2011).

14. Ajroud-Driss S. and Siddique T. Sporadic and hereditary amyotrophic lateral sclerosis (ALS). *Biochim Biophys Acta.,* 1852, 679–684,(2015).

15. Andersen P. M. and Al-Chalabi A. Clinical genetics of amyotrophic lateral sclerosis: what do we really know? *Nat Rev Neurol*., 7, 603–615,(2011).

16. Bosco D. A. et al. Wild-type and mutant SOD1 share an aberrant conformation and a common pathogenic pathway in ALS. *Nat Neurosci.*, 13, 1396–1403,(2010).

17. Forsberg K. et al. Novel antibodies reveal inclusions containing non-native SOD1 in sporadic ALS patients. *PLoS One.*, 5, 11-552, (2010).

18. Brites D and Vaz A. Microglia centered pathogenesis in ALS: insights in cell interconnectivity. *Front. in cellular Neuroscience.*, 8, 117, (2014).

19. Mc Combe P.A. and Henderson R.D. The Role of Immune and Inflammatory Mechanisms in ALS.*Molecular Medicine.*, 11, 1566-5240, (2011).

20. Zhao W. et al. Activated microglia initiate motor neuron injury by a nitric oxide and glutamate-mediated mechanism. *Journal of Neuropathology and Experimental Neurology.*, 63, 964–977, (2004).

21. Melzer N. et al. CD8+ T cells and neuronal damage: direct and collateral mechanisms of cytotoxicity and impaired electrical excitability. *The FASEB Journal*., 23, 3659–3673, (2009).

22. Huang X. et al. CD4+ T cells in the pathobiology of neurodegenerative disorders. *Journal of Neuroimmunology.*, 211, 3–15, (2009).

23. Mokarizadeh A. et al. Microvesicles derived from mesenchymal stem cells: potent organelles for induction of tolerogenic signaling. *Immunol*., 147, 47–54, (2012).

24. Admyre C. et al. Exosomes with major histocompatibility complex class II and co-stimulatory molecules are present in human BAL fluid. *Eur. Respir. J.*, 22, 578–583, (2003).

25. Shaw P.J. Molecular and cellular pathways of neurodegeneration in motor neurone disease. *J Neurol Neurosurg Psychiatry.*, 76,1046-1057, (2005).

26. Tadic V. et al. The ER mitochondria calcium cycle and ER stress response as therapeutic targets in amyotrophic lateral sclerosis. *Front Cell Neurosci.,* 8, 135-147, (2014).

27. Weiduschat N. et al. Motor cortex glutathione deficit in ALS measured in vivo with the J-editing technique. *Neurosci Lett.*, 570, 102–7, (2014).

28. Vargas M. R. et al Decreased glutathione accelerates neurological deficit and mitochondrial pathology in familial ALS-linked hSOD1(G93A) mice model. *Neurobiol Dis.,* 43, 543–51, (2011).

29. Iguchi Y. et al. Oxidative stress induced by glutathione depletion reproduces pathological modifications of TDP-43 linked to TDP-43 proteinopathies. *Neurobiol Dis.*, 45, 862–70, (2012).

30. Kiskinis E. et al. Pathways disrupted in human ALS motor neurons identified through genetic correction of mutant SOD1. *Cell Stem Cell.,* 14, 781–95, (2014).

31. Carrì M. T. et al. M. Oxidative stress and mitochondrial damage: importance in non-SOD1 ALS. *Front Cell Neurosci.*,9, 23-41, (2015).

32. Guareschi S. et al. An over-oxidized form of superoxide dismutase found in sporadic amyotrophic lateral sclerosis with bulbar onset shares a toxic mechanism with mutant SOD1. *Proc Natl Acad Sci U S A.*,109, 5074–5079, (2012).

33. Shodai A. et al. Aberrant assembly of RNA recognition motif 1 links to pathogenic conversion of TAR DNA-binding protein of 43 kDa (TDP-43). *J Biol Chem.,* 288, 1486–905, (2013).

34. Parker S. J. et al. Endogenous TDP-43 localized to stress granules can subsequently form protein aggregates. *Neurochem Int.*,60, 415–24, (2012).

35. Vance C. et al. ALS mutant FUS disrupts nuclear localization and sequesters wild-type FUS within cytoplasmic stress granules. *Hum Mol Genet.,* 22, 2676– 88, (2013).

36. Baron D. M. et al. Amyotrophic lateral sclerosis-linked FUS/TLS alters stress granule assembly and dynamics. *Mol Neurodegener.,* 8, 23- 30, (2013).

37. Colombrita C. et al. TDP-43 is recruited to stress granules in conditions of oxidative insult. *J Neurochem.,* 111, 1051–61, (2009).

38. Peters O. M. et al. Emerging mechanisms of molecular pathology in ALS. *J Clin Invest.,*125, 1767–1779, (2015).

39. Caughey B. and Lansbury P. T. Protofibrils, pores, fibrils, and neurodegeneration: separating the responsible protein aggregates from the innocent bystanders. *Annu Rev Neurosci.,* 26, 267–98, (2003).

40. Reaume A. G. et al. Motor neurons in Cu/Zn superoxide dismutase-deficient mice develop normally but exhibit enhanced cell death after axonal injury. *Nat. Genet.,* 13, 43–7, (1996).

41. Xu Y. F. et al. Wild-type human TDP-43 expression causes TDP-43 phosphorylation, mitochondrial aggregation, motor deficits, and early mortality in transgenic mice. *J Neurosci.,* 30, 10851–9, (2010).

42. Lee Y. B. et al. Hexanucleotide repeats in ALS/FTD form length-dependent RNA foci, sequester RNA binding proteins, and are neurotoxic. *Cell Rep.,* 5, 1178–86, (2013).

43. Donnelly C. J. et al. RNA toxicity from the ALS/FTD C9ORF72 expansion is mitigated by antisense intervention. *Neuron.,* 80, 415–28, (2013).

44. Sareen D. et al. Targeting RNA foci in iPSC-derived motor neurons from ALS patients with a C9ORF72 repeat expansion. *Sci Transl Med.,* 5, 208-149, (2013).

45. Ash P. E. A. et al. Unconventional translation of C9ORF72 GGGGCC expansion generates insoluble polypeptides specific to c9FTD/ALS.*Neuron.,* 77, 639–46, (2013).

46. Gendron T. F. et al. Antisense transcripts of the expanded C9ORF72 hexanucleotide repeat form nuclear RNA foci and undergo repeat-associated non-ATG translation in c9FTD/ALS. *Neuron.,* 126, 829–44, (2013).

47. Wen X. et al. Antisense proline-arginine RAN dipeptides linked to C9ORF72ALS/FTD form toxic nuclear aggregates that initiate in vitro and in vivo neuronal death. *Neuron.,* 84, 1213–25, (2014).

48. Ciechanover A. and Kwon, Y. T. Degradation of misfolded proteins in neurodegenerative diseases: therapeutic targets and strategies. *Exp Mol Med.,* 47, 120-147, (2015).

49. Hara T. et al. Suppression of basal autophagy in neural cells causes neurodegenerative disease in mice. *Exp Mol Med.,* 441, 885–9, (2006).

50. Munch C. and Bertolotti A. Self-propagation and transmission of misfolded mutant SOD1: prion or prion-like phenomenon? *Cell Cycle.,* 10, 17-11, (2011).

51. Grad L. I. et al. Intercellular propagated misfolding of wild-type Cu/Zn superoxide dismutase occurs via exosome-dependent and -independent mechanisms. *Proc Natl Acad Sci U S A.,* 111, 3620–5, (2014).

52. Gitler A. D. and Shorter J. RNA-binding proteins with prion-like domains in ALS and FTLD-U. *Prion.,* 5, 179–87, (2011).

53. Kim H. J. et al. Mutations in prion-like domains in hnRNPA2B1 and hnRNPA1 cause multisystem proteinopathy and ALS. *Nature.,* 95, 467–73,(2013).

54. Mori K. et al. hnRNP A3 binds to GGGGCC repeats and is a constituent of p62positive/TDP43-negative inclusions in the hippocampus of patients with C9orf72 mutations. *Acta Neuropathol.,* 125, 413–23, (2013).

55. Li Y. R. et al. Stress granules as crucibles of ALS pathogenesis. *J Cell Biol.,* 01, 361–72, (2013).

56. Bosco D. A. et al. Mutant FUS proteins that cause amyotrophic lateral sclerosis incorporate into stress granules. *Hum Mol Genet.,* 19, 4160–75, (2010).

56. Bosco D. A. et al. Mutant FUS proteins that cause amyotrophic lateral sclerosis incorporate into stress granules. *Hum Mol Genet.,* 19, 4160–75, (2010).

57. Rothstein, J.D. et al. Decreased glutamate transport by the brain and spinal cord in amyotrophic lateral sclerosis. *N Engl J Med.,* 326, 1464-1468, (1992).

58. Howland, D.S. et al. Focal loss of the glutamate transporter EAAT2 in a transgenic rat model of SOD1 mutant-mediated amyotrophic lateral sclerosis (ALS). *Proc Natl Acad Sci U S A.,* 99, 1604-1609, (2002).

59. Morel L. et al. Neuronal exosomal miRNA-dependent translational regulation of astroglial glutamate transporter GLT1. *J Biol Chem.,* 288, 7105-7116, (2013).

60. Li K. et al. GLT1 overexpression in SOD1(G93A) mouse cervical spinal cord does not preserve diaphragm function or extend disease. *Neurobiol Dis.,* 78, 12-23, (2015).

61. Milanese M. et al. Abnormal exocytotic release of glutamate in a mouse model of amyotrophic lateral sclerosis. *J Neurochem.,* 116, 1028-1042, (2011).

62. Mesci P. et al. System xC- is a mediator of microglial function and its deletion slows symptoms in amyotrophic lateral sclerosis mice. *Brain.,* 138, 53-68, (2015).

63. Van Damme P. et al. Astrocytes regulate GluR2 expression in motor neurons and their vulnerability to excitotoxicity. *Proc Natl Acad Sci U S A.,* 104, 1482-5148, (2007).

64. Mikoshiba K. Role of IP3 receptor signalling in cell functions and diseases. *Adv Biol Regul.,* 57, 217-227, (2015).

65. Staats K. A. et al. Neuronal overexpression of IP3 receptor 2 is detrimental in mutant SOD1 mice. Biochem Biophys Res.*Commun.,* 429, 210-213, (2012).

66. Popoli M. et al. The stressed synapse: the impact of stress and glucocorticoids on glutamate transmission. *Nat Rev Neurosci.*,13, 22–37, (2012).

67. Damiano M. et al. Neural mitochondrial Ca2+ capacity impairment precedes the onset of motor symptoms in G93A Cu/Zn-superoxide dismutase mutant mice. *Nat Rev Neurosci.,* 96, 1349-1361, (2006).

68. Liu J. et al. Toxicity of familial ALS-linked SOD1 mutants from selective recruitment to spinal mitochondria. *Neuron.,*43, 5-17, (2004).

69. Tan W. et al. Small peptides against the mutant SOD1/Bcl-2 toxic mitochondrial complex restore mitochondrial function and cell viability in mutant SOD1mediated ALS. *J Neurosci.,*33, 11588-11598,(2013).

70. Israelson A. et al. Misfolded mutant SOD1 directly inhibits VDAC1 conductance in a mouse model of inherited ALS. *Neuron.,* 67, 575-587, (2010).

71. Reyes N.A. et al. Blocking the mitochondrial apoptotic pathway preserves motor neuron viability and function in a mouse model of amyotrophic lateral sclerosis. *J Clin Invest.,* 120, 3673-3679, (2010).

72. Rodolfo C. et al. Proteomic analysis of mitochondrial dysfunction in neurodegenerative diseases. *Expert Rev Proteomics.,*7, 519–42, (2010).

73. Atkin J.D. et al. Endoplasmic reticulum stress and induction of the unfolded protein response in human sporadic amyotrophic lateral sclerosis. *Neurobiol Dis.,* 30, 400-407 (2008).

74. Saxena S. et al. A role for motoneuron subtype-selective ER stress in disease manifestations of FALS mice. Nat. Neurosci. *Nat Neurosci.,* 12, 627-636, (2009).

75. Kikuchi H. et al. Spinal cord endoplasmic reticulum stress associated with a microsomal accumulation of mutant superoxide dismutase-1 in an ALS model. *Proc Natl Acad Sci U S A.,* 103, 6025-6030, (2006).

76. Zoghbi H.Y. Silencing misbehaving proteins. *Nat Genet.,* 37, 1302-1303, (2005).

77. Etang F. et al. Marinesco-Sjogren syndrome protein SIL1 regulates motor neuron subtype-selective ER stress in ALS. *Nat Genet.,* 18, 227-238, (2005).

78. Homma K. et al. SOD1 as a molecular switch for initiating the homeostatic ER stress response under zinc deficiency. *Mol Cell.,* 52, 75-86, (2013).

79. Atkin J.D. et al. Mutant SOD1 inhibits ER-Golgi transport in amyotrophic lateral sclerosis. *J Neurochem.,* 129, 190-204, (2014).

80. Nagai M. et al. Astrocytes expressing ALS-linked mutated SOD1 release factors selectively toxic to motor neurons. *Nat Neurosci.,* 10, 615–22, (2007).

81. Mantovani S.et al. Immune system alterations in sporadic amyotrophic lateral sclerosis patients suggest an ongoing neuroinflammatory process. *J Neuroimmunol.,* 210, 73–9, (2009).

82. Kipnis J.et al. Dual effect of CD4+CD25+ regulatory T cells in neurodegeneration: A dialogue with microglia. *Proc Natl Acad Sci U S A.,* 101, 14663–14669, (2004).

83. Henkel J. S.et al. Regulatory T-lymphocytes mediate amyotrophic lateral sclerosis progression and survival. *EMBO Mol Med.,* 5, 64–79, (2013).

84. Beers D. R.et al. CD4+ T cells support glial neuroprotection, slow disease progression, and modify glial morphology in an animal model of inherited ALS. *Proc Natl Acad Sci U S A.,* 105, 58–63, (2008).

85. Munch C.et al. Prion-like propagation of mutant superoxide dismutase-1 misfolding in neuronal cells. *Proc Natl Acad Sci U S A.,* 108, 3548–3553, (2011).

86. Zachau A. C. et al. Leukocyte-derived microparticles and scanning electron microscopic structures in two fractions of fresh cerebrospinal fluid in amyotrophic lateral sclerosis: a case report. *Journalof Medical Case Reports.,* 6, 274-360, (2012).

87. Zelko I.N. et al. Superoxide dismutase multi gene family: a comparison of the Cu Zn-SOD(SOD1), Mn-SOD(SOD2), and EC- SOD (SOD3) gene structures, evolution, and expression. *Free Radic Biol Med.,* 33, 337–349, (2002).

88. Pardo C.A. et al. Superoxide dismutase is an abundant component in cell bodies, dendrites, and axons of motor neurons and in a subset of other neurons. *Proc Natl Acad Sci U S A.,* 92, 954–958, (1995).

89. Fukai T. and Ushio-Fukai M. Superoxide dismutases: role in redox signalling, vascular function, and diseases. *Antioxid Redox Signal.,* 15, 1583–1606, (2011).

90. Kayatekin C.et al. Zinc binding modulates the entire folding free energy surface of human Cu, Zn superoxide dismutase. *J Mol Biol.,* 384, 540–555, (2008).

91. Rhee S.G. et al. Cell signalling H2O2, a necessary evil for cell signalling. *Science.,* 312, 1882–1883, (2006).

92. Brown D.I. and Griendling K.K. Nox proteins in signal transduction. *Free Radic Biol Med.,* 47, 1239–1253, (2009).

93. Mondola P. et al. Secretion and increase of intracellular Cu, Zn superoxide dismutase content in human neuroblastoma SK-N-BE cells subjected to oxidative stress. *Brain Res Bull.,* 45, 517–520, (1998).

94. Mondola P. et al. The Cu, Zn superoxide dismutase in neuroblastoma SK-N-BE cells is exported by a microvesicles dependent pathway. *Brain Res Mol Brain Res.,* 10, 45–5, (2003).

95. Cimini V. et al. CuZn-superoxide dismutase in human thymus: immunocytochemical localisation and secretion in thymus-derived epithelial and fibroblast cell lines. *Histochem Cell Biol.,* 118, 163–169, (2002).

96. Owland L.P. and Shneider N.A. Amyotrophic Lateral Sclerosis. *N Engl J Med.,* 344, 1688–1700, (2001).

97. Abel O. et al. ALSoD: a user friendly online bioinformatics tool for amyotrophic lateral sclerosis genetics. *Hum Mutat.,* 33, 1345–1351, (2012).

98. Fujisawa, T. et al. A novel monoclonal antibody reveals a conformational alteration shared by amyotrophic lateral sclerosis-linked SOD1 mutants. *Ann Neurol.,*72, 739-749, (2012).

99. Munch C and Bertolotti A. Exposure of hydrophobic surfaces initiates aggregation of diverse ALS-causing superoxide dismutase-1 mutants. *J Mol Biol,.* 399, 512-525, (2010).

100. Gurney M.E. et al. Motor neuron degeneration in mice that express a human Cu,Zn superoxide dismutase mutation. *Science.,* 264, 1772-1775, (1994).

101. Watanabe M. et al. Histological evidence of protein aggregation in mutant SOD1 transgenic mice and in amyotrophic lateral sclerosis neural tissues. *Neurobiol Dis.,* 8, 933-941, (2001).

102. Parone P.A. et al. Enhancing mitochondrial calcium buffering capacity reduces aggregation of misfolded SOD1 and motor neuron cell death without extending survival in mouse models of inherited amyotrophic lateral sclerosis. *J Neurosci.,* 33, 4657-4671, (2013).

103. Wang Q. et al. Protein aggregation and protein instability govern familial amyotrophic lateral sclerosis patient survival. *PLoS One.,* 6, 120-170, (2008).

104. Prudencio M. et al. Variation in aggregation propensities among ALSassociated variants of SOD1: correlation to human disease. *Hum Mol Genet.,* 18, 3217-3226, (2009).

105. Urushitani M. et al. Chromogranin-mediated secretion of mutant superoxide dismutase proteins linked to amyotrophic lateral sclerosis. *Nat Neurosci.,* 9, 108-118, (2006).

106. Zhao W. et al. Extracellular mutant SOD1 induces microglial-mediated moto neuron injury. *Glia.*, 58, 231–243, (2010).

107. Prell T. et al. The unfolded protein response in models of human mutant G93A amyotrophic lateral sclerosis. *Eur J Neurosci.*, 35, 652–660, (2012).

108. Tiwari A. et al. Aberrantly increased hydrophobicity shared by mutants of Cu,Zn-superoxide dismutase in familial amyotrophic lateral sclerosis. *Journal of Biological Chemistry.*, 280, 29771–2977, (2005).

109. Galaleldeen A. et al. Structural and biophysical properties of metal-free pathogenic SOD1 mutants A4V and G93A. *Arch Biochem Biophys.*, 492, 40–47, (2009).

110. Rotunno M. S. and Bosco D. A. An emerging role for misfolded wild-type SOD1 in sporadic ALS pathogenesis. *Front Cell Neurosci.*, 7, 1–16, (2013).

111. Cereda, C. et al. Altered Intracellular Localization of SOD1 in Leukocytes from Patients with Sporadic Amyotrophic Lateral Sclerosis. *PLoS One.*, 8, 350-234,(2013).

112. Grad L.I. et al. Intermolecular transmission of superoxide dismutase 1 misfolding in living cells. *Proc Natl Acad Sci U S A.*,108, 16398–16403, (2011).

113. Munch C. et al. Prion-like propagation of mutant superoxide dismutase-1 misfolding in neuronal cells. *Proc Natl Acad Sci U S A.*, 108, 3548–3553, (2011).

114. Sundaramoorthy V. et al. Extracellular wild type and mutant SOD1 induces ERGolgi pathology characteristic of amyotrophic lateral sclerosis in neuronal cells. *Cell Mol Life Sci.*, 70, 4181–4195, (2013).

115. Ayers J. I. et al. Experimental transmissibility of mutant SOD1 motor neuron disease. *Acta Neuropathol.*, 128,791–803, (2014).

116. Mackenzie I. R. A. et al. Pathological TDP-43 Distinguishes Sporadic Amyotrophic Lateral Sclerosis from Amyotrophic Lateral Sclerosis with SOD1 Mutations. *Ann Neurol.*, 4, 427–434, (2007).

117. Pokrishevsky, E. et al. Aberrant Localization of FUS and TDP43 Is Associated with Misfolding of SOD1 in Amyotrophic Lateral Sclerosis. *PLoS One.*, 7, 1–9, (2012).

118. Pokrishevsky, E. et al. N. R. TDP-43 or FUS-induced misfolded human wildtype SOD1 can propagate intercellularly in a prion- like fashion. *Sci Rep.*, 6, 22155, (2016).

119. Pokrishevsky, E. et al. Aberrant Localization of FUS and TDP43 Is Associated with Misfolding of SOD1 in Amyotrophic Lateral Sclerosis. *PLoS One.*, 7, 1–9, (2012).

120. Smith R. et al. D. Nervous translation, do you get the message? A review of mRNPs, mRNA–protein interactions and translational control within cells of the nervous system. *Cell Mol Life Sci.*, 71, 3917–3937, (2014).

121. Dubyak G.R. et al. P2X7 receptor regulation of non-classical secretion from immune effector cells. *Cell Microbiol.*, 14, 1697–1706, (2012).

122. Barmada S. J. et al. Linking RNA Dysfunction and Neurodegeneration in Amyotrophic Lateral Sclerosis. *Neurotherapeutics.*, 12, 340–51, (2015).

123. Couthouis, J. et al. Evaluating the role of the FUS/TLS-related gene EWSR1 in amyotrophic lateral sclerosis. *Hum Mol Genet.*, 21, 2899–2911, (2012).

124. Couthouis, J. et al. A yeast functional screen predicts new candidate ALS disease genes. *Proc Natl Acad Sci U S A.,* 108, 20881–20890, (2011).

125. Donnelly C. J.et al. Aberrant RNA homeostasis in amyotrophic lateral sclerosis: potential for new therapeutic targets? *Neurodegener Dis Manag.,* 4, 417–437, (2014).

126. Rojas F. et al. Astrocytes expressing mutant SOD1 and TDP43 trigger motoneuron death that is mediated via sodium channels and nitroxidative stress. *Front Cell Neurosci.,* 8, 24-69, (2014).

127.Höög J and Lötvall J. Diversity of extracellular vesicles in human ejaculates revealed by cryo-electron microscopi. *Journal Extracellular vesicles.,* http://dx.doi.org/10.3402/jev.v4.28680, (2015)

128. Bruce A. et al. Molecular Biology of the Cell, 4th edition. *Garland Science*; ISBN-10: 0-8153-3218-1ISBN-10: 0-8153-4072-9, (2002)

129. Meer G.V. et al. Membrane lipids: where they are and how they behave. *Nature Reviews Molecular Cell Biology* 9, 112-124, (2008)

130. Kastelowitz N. et al. Exosomes and Microvesicles: Identification and Targeting By Particle Size and Lipid Chemical Probes.*Chembiochem.,* 15, 923–928, (2014).

131. Demchenko A.P The change of cellular membranes on apoptosis: fluorescence detection. *Exp Oncol.,* 34,263-268, (2012).

132. Osteikoetxea X. et al. Improved Characterization of EV Preparations Based on Protein to Lipid Ratio and Lipid Properties. *Plos* ; 10.1371/journal.pone.0121184, (2015).

133. Bence György B.et al Detection and isolation of cell-derived microparticles are compromised by protein complexes resulting from shared biophysical parameters *Blood.*,117, 39-48 ,(2011).

134. Osteikoetxea X. et al.Differential detergent sensitivity of extracellular vesicle subpopulations. Organic e *Biomolecular Chemistry,*. 13, 97-75, (2015).

135. Mulcahy L. A. et al. Routes and mechanisms of extracellular vesicle uptake.*Journal of Extracellular vesicles*. 3, 24-41, (2014).

136. Subra C. et al. Exosomes account for vesicle-mediated transcellular transport of activatable phospholipases and prostaglandins. *J Li pìid Res*., 51, 2105-20, (2010).

137. Mikolay L. et al. Extracellular Vesicles: Composition,Biological Relevance, and Methods of Study.*Bioscience.,* 34-9775, (2015).

138. Beloribi S. et al. Exosomal Lipids Impact Notch Signaling and Induce Death of Human Pancreatic Tumoral SOJ-6 Cells. *PLoS One*., 7, 10-47480, (2012).

139. Subra C. et al. Exosome lipidomics unravels lipid sorting at the level of multivesicular bodies. *Biochimie*., 89, 2-205, (2007).

140. Palmerini C. et al. Role of Cholesterol, DOTAP, and DPPC in Prostasome/Spermatozoa Interaction and Fusion.*The Journal of Membrane Biology.,* 211, 185–190, (2006).

141. Kim S. Tissue repair and the dynamics of the extracellular matrix The International.*Journal of Biochemistry and Cell Biology.*,36, 1031–1037, (2004).

142. Holthuis M. Lipid landscapes and pipelines in membrane homeostasis. *Nature*., 510, 48–57,(2014).

143. Kiessling V. Et al. Domain coupling in asymmetric lipid bilayers. *Biochim Biophys Acta*; 88, 64–71,(2009).

144. Yamaji-Hasegawa A and Tsujimoto M. Asymmetric distribution of phospholipid. *EMBO J.*, 24, 3159–65, (2007).

145. Van Meer G. et al. Cellular lipidomics. *EMBO J.*, 24, 3159–65, (2005).

146. Zwaal R. F. et al. Surface exposure of phosphatidylserine in pathological cells. *Cell Mol Life Sci.*, 62, 971–88, (2005).

147. Mourdjeva M. et al. Dynamics of membrane translocation of phosphatidylserine during apoptosis detected by a monoclonal antibody. *Apoptosis*., 10, 209–17, (2005).

148. Balasubramanian K. et al. Binding of annexin v to membrane products of lipid peroxidation. *Biochemistry*., 40, 8672–6, (2001).

149. Kuijpers T. W. et al. Neutrophils in Barth syndrome (BTHS) avidly bind annexin-V in the absence of apoptosis. *Blood.*,103, 3915-3923, (2004).

150. Dong H. P. et al. Measurement of apoptosis in cytological specimens by flow cytometry: Comparison of annexin V, caspase cleavage and dutp incorporation assays. *Cytopathology.*, 22, 365–72, (2011).

151. Van Engeland M et al. Annexin v-affinity assay: A review on an apoptosis detection system based on phosphatidylserine exposure. *Cytometry.*, 31, 1–9, (1998).

152. Meers P et al. Calcium-dependent annexin v binding to phospholipids: Stoichiometry, specificity, and the role of negative charge. *Biochemistry*., 32, 11711–21, (1993).

153. Lemmon M. A. et al. Membrane recognition by phospholipid-binding domains. *Nat Rev Mol Cell Biol*., 9, 99–111, (2008).

154. Vance J. E. et al. Steenbergen R. Metabolism and functions of phosphatidylserine. *Prog Lipid Res.*, 44, 207–234, (2005).

155. Fairn G. D. et al. Schieber NL, Ariotti N, Murphy S, Kuerschner L, Webb RI, Grinstein S, Parton RG. High-resolution mapping reveals topologically distinct cellular pools of phosphatidylserine. *J Cell Biol.*, 194, 257–275, (2011).

156. Kay J. G. et al. Phosphatidylserine dynamics in cellular membranes. *Mol Biol Cell.*, 23, 2198–2212, (2012).

157.Bohdanowicz M and Grinstein S. Role of phospholipids in endocytosis, phagocytosis, and macropinocytosis. *Physiol Rev.*, 93, 69–106, (2013).

158. Di Paolo G and De Camilli P. Phosphoinositides in cell regulation and membrane dynamics.*Nature.*,443, 651–657, (2006).

159. Peter A. et al. Leventis and Sergio Grinstein The Distribution and Function of Phosphatidylserine in Cellular Membranes. *Annu. Rev Biophys.*, 39,407–27, (2010).

160. Di Paolo G and De Camilli P. Phosphoinositides in cell regulation and membrane dynamics. *Nature.*, 443, 651–657, (2006).

161. Janmey P. A. et al. Biophysical properties of lipids and dynamic membranes. *Trends Cell Biol.*, 16, 538–546, (2006).

162. Bigay J. et al. Curvature, lipid packing, and electrostatics of membrane organelles: defining cellular territories in determining specificity. *Dev Cell.*, 23, 886–895, (2012).

163. Rusinova R. et al. Phosphoinositides alter lipid bilayer properties. *J Gen Physiol.*, 141, 673–690, (2013).

164. Levental I. et al. PA combined electrostatics and hydrogen bonding determine intermolecular interactions between polyphosphoinositides. *J Am Chem Soc.*, 130, 9025–9030, (2008).

165. Redfern D. A. et al. Domain formation in phosphatidylinositol monophosphate/ phosphatidylcholine mixed vesicles. *Biophys J*., 86, 2980–2992, (2004).

166. Sechi A.S. and Wehland J. The actin cytoskeleton and plasma membrane connection: PtdIns(4,5)P(2) influences cytoskeletal protein activity at the plasma membrane. *J Cell Sci.*,113, 3685–3695, (2000).

167 .Fukami K. T. e al. Alpha-Actinin and vinculin are PIP2- binding proteins involved in signaling by tyrosine kinase. *J Biol Chem.*, 269, 1518–1522, (1994).

168. Gilmore A. Pand Burridge K. Regulation of vinculin binding to talin and actin by phosphatidyl-inositol-4 –5-bisphosphate. *Nature.*, 381, 531–535, (1996).

169. Fukami K. etal. Requirement of phosphatidylinositol 4,5-bisphosphate for alpha-actinin function. *Nature*., 359, 150– 152, (1992).

170 . Yonezawa N. et al. Inhibition of the interactions of cofilin, destrin, and deoxyribonuclease I with actin by phosphoinositides. *J Biol Chem.*, 265, 8382–8386, (1990).

171. Janmey P. A. et al.Polyphosphoinositide micelles and polyphosphoinositide- containing vesicles dissociate endogenous gelsolin-actin complexes and promote actin assembly from the fast-growing end of actin filaments blocked by gelsolin. *J Biol Chem.*, 262, 12228–12236, (1987).

172. Takenawa T and Suetsugu S. The WASP-WAVE protein network: connecting the membrane to the cytoskeleton. *Nat Rev Mol Cell Biol.*, 8, 37–48, (2007).

173. Shibasaki Y. et al. Massive actin polymerization induced by phosphatidylinositol-4-phosphate 5-kinase in vivo. *J Biol Chem.*, 272, 7578–7581, (1997).

174 252. Sakisaka T. et al. Phosphatidylinositol 4,5-bisphosphate phosphatase regulates the rearrangement of actin filaments. *Mol Cell Biol.*, 17, 3841–3849, (1997).

175. Itoh T. et al. Role of the ENTH domain in phosphatidylinositol-4,5-bisphosphate binding and endocytosis. *Science*., 291, 1047–1051, (2001).

176. Pike LJ et al. Cholesterol depletion delocalizes phosphatidylinositol bisphosphate and inhibits hormone-stimulated phosphatidylinositol turnover. *J Biol Chem.*, 273, 22298–22304, (1998).

177. Golub T et al. PI(4,5)P2-dependent microdomain assemblies capture microtubules to promote and control leading edge motility. *J Cell Biol.*, 169, 151–165, (2005).

178. Harlan J. E. et al.Pleckstrin homology domains bind to phosphatidylinositol-4,5-bisphosphate. *Nature*., 371, 168–170, (1994).

179. Cheever M. L. et al. Phox domain interaction with PtdIns(3)P targets the Vam7 t-SNARE to vacuole membranes. *Nat Cell Biol.,* 3, 613–618, (2001).

180. Iero M. et al. Tumour-released exosomes and their implications in cancer immunity. *Cell Death Differ*., 15, 80-88,(2008).

181. Peinado H. et al. Melanoma exosomes educate bone marrow progenitor cells toward a pro-metastatic phenotype through MET. *Nat. Med.,* 18, 883-891, (2012).

182. Zimmermann P. et al. PIP2 PDZ domain binding controls the association of syntenin with the plasma membrane. *Mol Cell.,* 9, 1215–1225, (2002).

183. Santagata S. et al. G-protein signaling through tubby proteins. *Science.,* 292, 2041–2050, (2001).

184. Côté J. F.et al. A novel and evolutionarily conserved PtdIns (3,4,5) P3-binding domain is necessary for DOCK180 signalling. *Nat Cell Biol.,* 7, 797– 807, (2005).

185. Dippold H. C. et al. GOLPH3 bridges phosphatidylinositol-4- phosphate and actomyosin to stretch and shape the Golgi to promote budding. *Cell.,* 139, 337–351, (2009).

186. Davletov B. A. et al. A single C2 domain from synaptotagmin I is sufficient for high affinity Ca2/phospholipid binding. *J Biol Chem.,* 268, 26386–26390, (1993).

187. Hirao M. et al. Regulation mechanism of ERM (ezrin/radixin/moesin) protein/plasma membrane association: possible involvement of phosphatidylinositol turnover and Rhodependent signaling pathway. *J Cell Biol*., 135, 37–51, (1996).

188. Tsujita K.et al. Myotubularin regulates the function of the late endosome through the gram domain-phosphatidylinositol 3,5-bisphosphate interaction. *J Biol Chem.,* 279, 13817–13824, (2004).

189. Wishart M. J.et al.Phoxy lipids: revealing PX domains as phosphoinositide binding modules. *Cell,* 105, 817–820, (2001).

190. McMahon H. T.et al. Membrane curvature and mechanisms of dynamic cell membrane remodelling. *Nature,*438, 590–596, (2005).

191. Bacia K.et al. Sterol structure determines the separation of phases and the curvature of the liquid-ordered phase in model membranes. *Proc Natl Acad Sci USA.,* 102, 3272–3277, (2005).

192. Bacon C. et al. Dynamic expression of the Slit-Robo GTPase activating protein genes during development of the murine nervous system. *J Comp Neurol.,* 513, 224–236, (2009).

193. Gallop J. L.et al. Endophilin and CtBP/BARS are not acyl transferasesn in endocytosis or Golgi fission. *Nature.,* 438, 675–678, (2005).

194. Emoto K. et al. Isolation of a Chinese hamster ovary cell mutant defective in intramitochondrial transport of phosphatidylserine. *Proc Natl Acad Sci USA.,* 96, 12400–12405, (1999).

195. Kato U. et al. Role for phospholipid flippase complex of ATP8A1 and CDC50A proteins in cell migration. *J Biol Chem.,* 288, 4922–4934, (2013).

196. Suzuki J.et al. Calcium-dependent phospholipid scrambling by TMEM16F. *Nature.*, 468, 834–838, (2010).

197. Di Paolo G and De Camilli P. Phosphoinositides in cell regulation and membrane dynamics. *Nature*., 443, 651–657, (2006).

198 . Antonny B.et al. Mechanisms of membrane curvature sensing. *Annu Rev Biochem.*, 80, 101–123, (2011).

199. Stachowiak J. C.et al. A cost-benefit analysis of the physical mechanisms of membrane curvature. *Nat Cell Biol.*, 15, 1019–1027, (2013).

200. McMahon H. T. et al. Membrane curvature and mechanisms of dynamic cell membrane remodelling. *Nature*.,438, 590–596, (2005).

201. Muziol T. et al.Structural basis for budding by the ESCRT-III factor CHMP3. *Dev Cell.*,10, 821–830, (2006).

202. Raiborg C and Stenmark H. The ESCRT machinery in endosomal sorting of ubiquitylated membrane proteins. *Nature.*, 458, 445–452, (2009).

203. Antonny B. Mechanisms of membrane curvature sensing. *Annu Rev Biochem*., 80, 101– 123, (2011).

204. Yoon Y. et al.Molecular basis of the potent membrane-remodeling activity of the epsin 1 N-terminal homology domain. *J Biol Chem.*, 285, 531–540, (2010).

205. Bigay J. et al.Lipid packing sensed by ArfGAP1 couples COPI coat disassembly to membrane bilayer curvature. *Nature.*, 426, 563–566, (2003).

206. Antonny B.et al. Mechanisms of membrane curvature sensing. *Annu Rev Biochem.*, 80, 101– 123, (2011).

207. Yoon Y.et al.Molecular basis of the potent membrane-remodeling activity of the epsin 1 N-terminal homology domain. *J Biol Chem.*, 285, 531–540, (2010).

208. Bigay J.et al. Lipid packing sensed by ArfGAP1 couples COPI coat disassembly to membrane bilayer curvature. *Nature.*, 426, 563–566, (2003).

209. Antonny B. et al.Mechanisms of membrane curvature sensing. *Annu Rev Biochem*., 80, 101– 123, (2011).

210. Drin G.et al.A general amphipathic alpha-helical motif for sensing membrane curvature. *Nat Struct Mol Bio.,l* 14, 138–146, (2007).

211. Stachowiak J. C. A cost-benefit analysis of the physical mechanisms of membrane curvature. *Nat Cell Biol.*, 15, 1019–1027, (2013).

212. Shen H. et al. SnapShot: membrane curvature sensors and generators. *Cell.*,150, 1301–1302, (2012).

213. Daumke O.et al.Architectural and mechanistic insights into an EHD ATPase involved in membrane remodelling. *Nature.*, 449, 923–927, (2007).

214. Yu H.et al.Doc2b promotes GLUT4 exocytosis by activating the SNARE-mediated fusion reaction in a calcium-and membrane bending- dependent manner. *Mol Biol Cell*., 24, 1176–1184, (2013).

215. McMahon H. T. et al. Membrane curvature in synaptic vesicle fusion and beyond. *Cell.*,140, 601–605, (2010).

216. Suetsugu S. Synergistic BAR-NPF interactions in actin-driven membrane remodeling. *Trends Cell Biol*., 22, 141–150, (2012).

217. Boucrot E. et al. Membrane fission is promoted by insertion of amphipathic helices and is restricted by BAR domains. *Cell.,* 149, 124–136, (2012).

218. Goh S. L. Versatile membrane deformation potential of activated pacsin. *PLoS One.*, 7, 51-28, (2012).

219. Saengsawang W. et al. CIP4 coordinates with phospholipids and actin-associated proteins to localize to the protruding edge and produce actin ribs and veils. *J Cell Sci.*, 126, 2411– 2423, (2013).

220. Li P.et al. Phase transitions in the assembly of multivalent signalling proteins. *Nature.,* 483, 336–340, (2012).

221. Lundmark R. et al. Driving membrane curvature in clathrin-dependent and clathrin-independent endocytosis. *Semin Cell Dev Biol.,* 21, 363–370, (2010).

222. Taylor M. J.et al. A high precision survey of the molecular dynamics of mammalian clathrin-mediated endocytosis. *PLoS Biol*., 9, 10-04, (2011).

223. Umasankar P. K.et al. Distinct and separable activities of the endocytic clathrin-coat components Fcho1/2 and AP-2 in developmental patterning. *Nat Cell Biol.,* 14, 488–501, (2012).

224. Henne W. M. et al. FCHo proteins are nucleators of clathrin-mediated endocytosis. *Science.,* 328, 12-81, (2010).

225. Uezu A.et al. Characterization of the EFC/F-BAR domain protein, FCHO2. *Genes Cells.,* 16, 868–878, (2011).

226. Neumann S and Schmid S. L. Dual role of BAR domain-containing proteins in regulating vesicle release catalyzed by the GTPase, Dynamin-2. *J Biol Chem.,* 288, 25119–25128, (2013).

227. Kaksonen M.et al. A modular design for the clathrin- and actinmediated endocytosis machinery. *Cell.,* 123, 305–320, (2005).

228. Soulard A.et al. The WASP -Las17p-interacting protein Bzz1p functions with Myo5p in an early stage of endocytosis. *Protoplasma.,* 226, 89–101, (2005).

229. Yoon Y.et al. Phosphatidylinositol 4,5-bisphosphate [PtdIns(4,5)P2] specifically induces membrane penetration and deformation by Bin/amphiphysin/Rvs (BAR) domains. *J Biol Chem.,* 287, 34078–34090, (2012).

230. Schuske K. R..et al. Endophilin is required for synaptic vesicle endocytosis by localizing synaptojanin. *Neuron*,40, 749–762, (2003).

231. Takeda T. et al. Drosophila F-BAR protein Syndapin contributes *Open Biol.,* 3, 13-81, (2013).

232. Gallop J. L. Phosphoinositides and membrane curvature switch the mode of actin polymerization via selective recruitment of toca-1 and Snx9. *Proc Natl Acad Sci USA.,* 110, 7193–7198, (2013).

233. Suetsugu S and Gautreau A. Synergistic BAR-NPF interactions in actin-driven membrane remodeling. Trends *Cell Biol.,* 22, 141–150, (2012).

234 . Collins A.et al. Structural organization of the actin at sites of clathrin-mediated endocytosis. *Curr Biol*., 21, 1167–1175, (2011).

235. Wu M.et al. Coupling between clathrin-dependent endocytic budding and F-BAR-dependent tubulation in a cell-free system. *Nat Cell Biol.,*12, 902–908, (2010).

236. Schwintzer L.et al. The functions of the actin nucleator Cobl in cellular morphogenesis critically depend on syndapin I. *EMBO J.,* 30, 3147–3159, (2011).

237. Shibata Y.et al. Mechanisms shaping the membranes of cellular organelles. *Annu Rev Cell Dev Biol*., 25, 329–354, (2009).

238. Rothberg K. G.et al. Caveolin a protein component of caveolae membrane coats. *Cell,*68, 673–682, (1992).

239. Hill M. M.et al. PTRF-Cavin, a conserved cytoplasmic protein required for caveola formation and function. *Cell*., 132, 113–124, (2008).

240. Koch D.et al. Ultrastructural freeze-fracture immunolabeling identifies plasma membrane-localized syndapin II as a crucial factor in shaping caveolae. *Histochem Cell Biol.,*138, 215–230, (2012).

241. Senju Y. et al. Essential role of PACSIN2/syndapin- II in caveolae membrane sculpting. *J Cell Sci.,* 124, 2032–2040, (2011).

242. Moren B.et al. EHD2 regulates caveolar dynamics via ATP-driven targeting and oligomerization. *Mol Biol Cell.,* 23, 1316–1329, (2012).

243. Stoeber M.et al. EHD2 confine caveolae to the plasma membrane through association with actin. *EMBO J*, 31, 2350–2364, (2012).

244. Sabharanjak S.et al. GPI-anchored proteins are delivered to recycling endosomes via a distinct cdc42-regulated, clathrin-independent pinocytic pathway. *Dev Cell.,* 2, 411–423, (2002).

245. Lundmark R.et al.The GTPase-activating protein GRAF1 regulates the CLIC/GEEC endocytic pathway. *Curr Biol.,* 18, 1802–1808, (2008).

246. Loisel T. P.et al. Reconstitution of actin-based motility of Listeria and Shigella using pure proteins. *Nature.,* 401, 613–616, (1999).

247. Suetsugu S.et al. The RAC binding domain/IRSp53- MIM homology domain of IRSp53 induces RAC-dependent membrane deformation. *J Biol Chem*., 281, 35347–35358, (2006).

248. Scita G.et al. IRSp53: crossing the road of membrane and actin dynamics in the formation of membrane protrusions. *Trends Cell Biol.,* 18, 52–60, (2008).

249. Ahmed S. et al. I-BAR domains, IRSp53 and filopodium formation. *Semin Cell Dev Biol.,* 21, 350–356, (2010).

250. Foletta V. C. et al.Cloning of rat ARHGAP4/C1, a RhoGAP family member expressed in the nervous system that colocalizes with the Golgi complex and microtubules. *Brain Res.,* 107, 65–79, (2002).

251. Guerrier S. et al.The F-BAR domain of srGAP2 induces membrane protrusions required for neuronal migration and morphogenesis. *Cell.*, 138, 990–1004, (2009).

252. Charrier C. et al. Inhibition of SRGAP2 function by its human-specific paralogs induces neoteny during spine maturation. *Cell.*,149, 923–935, (2012).

253. You J. J.et al. Gas7 functions with N-WASP to regulate the neurite outgrowth of hippocampal neurons. *J Biol Chem*., 285, 11652–11666, (2010).

254. Zhao X.et al. Phosphorylation of the Bin, Amphiphysin, and RSV161/167 (BAR) domain of ACAP4 regulates membrane tubulation. *Proc Natl Acad Sci USA.*, 110, 11023–11028, (2013).

255.Takeda T. et al. Drosophila F-BAR protein Syndapin contributes to coupling the plasma membrane and contractile ring in cytokinesis. *Open Biol.*, 3, 13-81, (2013).

256. Rohatgi R. et al. The interaction between N-WASP and the Arp2/3 complex links Cdc42-dependent signals to actin assembly. *Cell*., 97, 221–231, (1999).

257. Padrick S. B. et al. Regulation of WASP/ WAVE proteins. *Mol Cell.*, 32, 426–438, (2008).

258. Rao Y. et al. Regulation of IRSp53-dependent filopodial dynamics by antagonism between 14–3-3 binding and SH3-mediated localization. *Mol Cell Biol.*, 30, 829–844, (2010).

259. Dombrosky-Ferlan P.Felic.et al. (CIP4b), a novel binding partner with the Src kinase Lyn and Cdc42, localizes to the phagocytic cup.*Blood*., 101, 2804–2809, (2003).

260. Koduru S.et al. Cdc42 interacting protein 4 (CIP4) is essential for integrindependent T-cell trafficking. *Proc Natl Acad Sci USA.*,107, 16252–16256, (2010).

261. Razzaq A. et al. Amphiphysin is necessary for organization of the excitation-contrac-tion coupling machinery of muscles, but not for synaptic vesicle endocytosis in Drosophila. *Genes Dev.*, 15, 2967–2979, (2001).

262. Pendaries C. et al. Phosphoinositide signaling disorders in human diseases. *FEBS Lett.*, 546, 25–31, (2003).

263. Dharmalingam E.et al. F-BAR proteins of the syndapin family shape the plasma membrane and are crucial for neuromorphogenesis. J *Neurosci.*, 29, 13315–13327, (2009).

264. Koch D. et al. Ultrastructural freeze-fracture immunolabeling identifies plasma membrane-localized syndapin II as a crucial factor in shaping caveolae. *Histochem Cell Biol.*, 138, 215–230, (2012).

265. Qualmann B.et al. Syndapin I, a synaptic dynamin-binding protein that associates with the neural Wiskott-Aldrich syndrome protein. *Mol Biol Cell.*, 10, 501–513, (1999).

266. Milosevic I.et al.Recruitment of endophilin to clathrin-coated pit necks is required for efficient vesicle uncoating after fission. *Neuron.*,72, 587–601, (2011).

267. Schuske K. R. et al.Endophilin is required for synaptic vesicle endocytosis by localizing synaptojanin. *Neuron.*, 40, 749–762, (2003).

268. Saengsawang W.et al.The F-BAR protein CIP4 inhibits neurite formation by producing lamellipodial protrusions. *Curr Biol.,* 22, 494–501, (2012).

269. Holbert S. et al.Cdc42-interacting protein 4 binds to huntingtin: neuropathologic and biological evidence for a role in Huntington's disease. *Proc Natl Acad Sci USA.,* 100, 2712–2717, (2003).

270. Endris V. et al.The novel Rho-GTPase activating gene MEGAP/ srGAP3 has a putative role in severe mental retardation. *Proc Natl Acad* Sci USA., 99, 11754–11759, (2002).

271. Carlson B. R.et al.WRP/srGAP3 facilitates the initiation of spine development by an inverse F-BAR domain, and its loss impairs long-term memory. *J Neurosci.,* 31, 2447–2460, (2011).

272. Kim I. H.et al. Disruption of wave-associatedRac GTPase-activating protein (Wrp) leads to abnormal adult neural progenitor migration associated with hydrocephalus. *J Biol Chem.,* 287, 39263–39274, (2012).

273.Waltereit R. et al.Srgap3 mice present a neurodevelopmental disorder with schizophrenia- related intermediate phenotypes. *FASEB J*., 26, 4418–4428, (2012).

278. Charrier C.et al.Inhibition of SRGAP2 function by its human-specific paralogs induces neoteny during spine maturation. *Cell*., 149, 923–935, (2012).

279. Saitsu H.et al. Early infantile epileptic encephalopathy associated with the disrupted gene encoding Slit-Robo Rho GTPase activating protein 2 (SRGAP2). *Am J Med Genet A.,*158, 199–205, (2012).

280. Schuler S.et al.Ciliated sensory hair cell formation and function require the F-BAR protein syndapin I and the WH2 domain-based actin nucleator Cobl. *J Cell Sci.,* 126, 196–208, (2013).

281. Cao H. et al.FCHSD1 and FCHSD2 are expressed in hair cell stereocilia and cuticular plate and regulate actin polymerization in vitro. *PLoS One.,* 8, 56-16, (2013).

282. Bona C. et al. Transfer of antigen from macrophages to lymphocytes. II. Immunological significance of the transfer of lipopolysaccharide. *Immunology,* 5, 831–840, (1973).

283. Mathivanan M. et al.Exosomes: Extracellular organelles important in intercellular communication. J. *Proteom.,* 73, 19-07, (2010).

284. Kalra, H.et al. Comparative proteomics evaluation of plasma exosome isolation techniques and assessment of the stability of exosomes in normal human blood plasma. *Proteomics.,*13, 3354–3364, (2013).

285. Muralidharan-Chari V. et al. ARF6-regulated shedding of tumor cell-derived plasma membrane microvesicles. *Curr. Biol.,*19, 1875–1885, (2009).

286. Wickman G. et al. How apoptotic cells aid in the removal of their own cold dead bodies. *Cell Death Differ.,*19, 735-742, (2012).

287. Orlando K. A. et al. Rho kinase regulates fragmentation and phagocytosis of apoptotic cells. *Exp Cell Res.,*312, 5-15, (2006).

288. Witasp E. et al. Bridge over troubled water: milk fat globule epidermal growth factor 8 promotes human monocyte-derived macrophage clearance of non-blebbing phosphatidylserine-positive target cells.*Cell Death Differ.,* 14, 1063-1065, (2007).

289. Kerr J. F.et al. Apoptosis: a basic biological phenomenon with wide-ranging implications in tissue kinetics. *Br J Cancer*.,26, 239-257, (1972)

290. Gerhart J. et al. Warkany lecture: signaling pathways in development. *Teratology*.,60, 226–239, (1999).

291. Simons M and Raposo G. Exosomes-vesicular carriers for intercellular communication. *Curr. Opin. Cell Biol.*, 21, 575– 1245, (2009).

292. Balaj L. et al. Tumour microvesiclescontain retrotransposon elements and amplified oncogene sequences. *Nat. Commun*., 2, 578-456, (2011).

293. Cossetti C. J. et al. Extracellular vesicles from neural stem cells transfer IFN- via Ifngr1 to activate Stat1 signaling in target cells. *Mol. Cell*., 56, 193–204, (2014).

294. Alonso R. et al. A new role of diacylglycerol kinase α on the secretion of lethal exosomes bearing Fas ligand during activation-induced cell death of T lymphocytes. *Biochimie* 89, 213–21, (2007).

295. Turola E. et al. Microglial microvesicle secretion and intercellular signaling. *Front. Physiol.,* 3, 149-190, (2012).

296. Cocucci E. et al. Shedding microvesicles: artefacts no more. *Trends Cell Biol.,* 19, 43–51, (2009).

397 .Baroni M. et al. Stimulation of P2 (P2X7) receptors in human dendritic cells induces the release of tissue factor-bearing particles. *FASEB J.,* 21, 1926–1033, (2007).

398. Bianco F. et al. Astrocyte-derived ATP induces vesicle shedding and IL-1b release from microglia. *J. Immunol*,. 174, 7268– 7277,(2005).

399. Cocucci E. et al. Enlargeosome traffic: exocytosis triggered by various signals is followed by endocytosis, membrane shedding or both. *Traffic.,* 8, 742–757, (2007).

400. Cocucci E. et al. Enlargeosome traffic: exocytosis triggered by various signals is followed by endocytosis, membrane shedding or both. *Traffic.*,8, 742–757, (2007).

401. Gasser O. et al. Characterisation and properties of ectosomes released by human polymorphonuclear neutrophils. *Exp. Cell Res.,* 285, 243–257, (2003).

402. Li C.J. et al. Novel proteolytic microvesicles released from human macrophages after exposure to tobacco smoke. *Am. J. Pathol*., 182, 1552–1562,(2013).

403. Martinez de Lizarrondo S. et al. Synergistic effect of thrombin and CD40 ligand on endothelial matrix metalloproteinase-10 expression and microparticle generation in vitro and in vivo. Arterioscler. *Thromb. Vasc. Biol.,* 32, 1477–1487, (2012).

404. Del Conde I. et al. Tissue-factor-bearing microvesicles arise from lipid rafts and fuse with activated platelets to initiate coagulation. *Blood.,* 106, 1604–1611, (2015).

405. Heijnen H.F. et al. Activated platelets release two types of membrane vesicles: Microvesicles by surface shedding and exosomes derived from exocytosis of multivesicular bodies and _-granules. *Blood.*,94, 3791–3799, (1994).

406. Falati S. et al. Accumulation of tissue factor into developing thrombi in vivo is dependent upon microparticle P-selectin glycoprotein ligand 1 and platelet P-selectin. *J. Exp. Med.*, 197, 1585–1598, (2003).

407. Mezouar S.et al. Inhibition of platelet activation prevents the P-selectin and integrin-dependent accumulation of cancer cell microparticles and reduces tumor growth and metastasis in vivo. Int. *J. Cancer.*, 136, 462–475, (2015).

408. Al-Nedawi K. et al. Intercellular transfer of the oncogenic receptor EGFRvIII by microvesicles derived from tumour cells. *Nat. Cell Biol.*, 10, 619–624, (2008).

409. Bernimoulin M. et al. Differential stimulation of monocytic cells results in distinct populations of microparticles. *J. Thromb. Haemost.*, 7, 1019–1028, (2009).

410. Elliott J. I.et al .Phosphatidylserine exposure in B lymphocytes: A role for lipid packing. *Blood.*, 108, 1611–1617, (2006).

411. Jimenez J. J. et al . Endothelial cells release phenotypically and quantitatively distinct microparticles in activation and apoptosis. *Thromb.*, 109, 175–180, (2003)

412. Connor D. E. et al . The majority of circulating platelet-derived microparticles fail to bind annexin V, lack phospholipid-dependent procoagulant activity and demonstrate greater expression of glycoprotein Ib. *Thromb. Haemost*., 103, 1044–1052, (2010).

413. Frühbeis C. et al. Neurotransmitter triggered transfer of exosomes mediates oligodendrocyte neuron communication. *PLoS Biol.*, 11, 1001- 604, (2013).

414. Mathivanan S. et al. Extracellular organelles important in intercellular communication. *J Proteomics.*, 73, 1907–1920, (2010).

41. Zhang Y. et al. Secreted monocytic miR- 150 enhances targeted endothelial cell migration. *Mol Cell.*, 39, 133– 144, (2010).

416. Peinado H. et al. Melanoma exosomes educate bone marrow progenitor cells toward a pro- metastatic phenotype through MET. *Nat Med.*, 18, 883–891, (2012).

417. Chivet M. et al. Exosomes as a novel way of interneuronal communication. *Biochem Soc Trans.*, 41, 241–244, (2013).

418. Frühbeis C. et al. Neurotransmitter triggered transfer of exosomes mediates oligodendrocyte neuron communication. *PLoS Biol.*, 11, 1001-604, (2013).

419. Pegtel M. D. et al. Extracellular vesicles as modulators of cell-to-cell communication in the healthy and diseased brain. *Philos Trans R Soc Lond B Biol Sci.*, 369, 1–31, (2014).

420. De Toro J. et al. Emerging roles of exosomes in normal and pathological conditions: new insights for diagnosis and therapeutic applications. *Front Immunol*., 6, 1–12, (2015).

421. Vlassov A.V. et al. Exosomes: current knowledge of their composition, biological functions, and diagnostic and therapeutic potentials. *Biochim Biophys Acta*., 18, 940–948, (2012).

422. Grad L. I. et al. Intercellular propagated misfolding of wild-type Cu/Zn superoxide dismutase occurs via exosome-dependent and -independent mechanisms. *Proc Natl Acad Sci U S A.*, 111, 3620–5, (2014).

423. Witwer K. W. et al. Standardization of sample collection, isolation and analysis methods in extracellular vesicle research. *J Extracell Vesicle.,,* 2: 203-60, (2013).

424. Lacroix R. et al. Overcoming limitations of microparticle measurement by flow cytometry. *Semin Thromb Hemost.*, 36, 807–818, (2010).

424. Buzas E. I. et al. Biological properties of extracellular vesicles and their physiological functions. *J Extracell Vesicles.,*1, 1–60, (2015).

425. Revenfeld A.L. et al. Diagnostic and Prognostic Potential of Extracellular Vesicles in Peripheral Blood. *Clin Ther.*, 36, 830–846, (2014).

426. Nonaka T. et al. Prion-like properties of pathological TDP-43 aggregates from diseased brains. *Cell Rep.*, 4, 124–134, (2013)

427. Grad, L. I. et al. Exosome-dependent and independent mechanisms are involved in prionlike transmission of propagated Cu-Zn superoxide dismutase misfolding. *Prion.*, 5,331–335, (2014).

428. Turner B.J. et al. Impaired extracellular secretion of mutant superoxide dismutase associates with neurotoxicity in familial amyotrophic lateral sclerosis. *J Neurosci.*, 25, 108-17, (2005).

429. Urushitani M. et al. The Endoplasmic Reticulum-Golgi pathway is a target for translocation and aggregation of mutant superoxide dismutase linked to ALS. *FASEB J.*, 22, 2476-87, (2008).

430. Tashiro Y. et al. Motor neuron-specific disruption of proteasomes, but not autophagy, replicates amyotrophic lateral sclerosis. *J Biol Chem.*, 287, 42984-94, (2012).

431. Chen S. et al. Autophagy dysregulation in amyotrophic lateral sclerosis. *Brain Pathol.*, 22, 110-6, (2012).

432. Johnson B.S. et al. TDP-43 is intrinsically aggregation-prone, and amyotrophic lateral sclerosis-linked mutations accelerate aggregation and increase toxicity. *J Biol Chem.*, 284, 20329–20339, (2009).

433. Revenfeld A.L. et al. Diagnostic and Prognostic Potential of Extracellular Vesicles in Peripheral Blood. *Clin Ther.*, 36, 830–846, (2014).

434. Bemis L. T. et al. Standardization of sample collection, isolation and analysis methods in extracellular vesicle research. *J Extracell Vesicles.*, 1, 1–25, (2013).

435. Zachau A. C. et al. Leukocyte-derived microparticles and scanning electron microscopic structures in two fractions of fresh cerebrospinal fluid in amyotrophic lateral sclerosis: a case report. *Journal of Medical Case Reports.*, 6, 274-37, (2012).

436. Fenenberg E. et al. Limited role of free TDP-43 as a diagnostic tool in neurodegenerative diseases. Amyotroph Lateral Sclerosis.*Frontotemporal Degener.*, 5, 1-6, (2014).

437. Grad L. I. et al. From molecule to molecule and cell to cell Prion- like mechanisms in amyotrophic lateral sclerosis. *Neurobiol Dis.*, 77, 257–265, (2015).

438. S. H. Cho, et al. Review Article: Recent advancements in optofluidic flow cytometer. *Biomicrofluidics.*, 4, 430-01,(2010).

439. L. Jiang, et al., Monitoring the progression of cell death and the disassembly of dying cells by flow cytometry.*Nat. Protoc.*,11, 655–663, (2016).

440. O. D. Laerum and T. Farsund. Clinical application of flow cytometry: a review, *Cytometry.*,2, 1–13,(2981).

441. Brooks B. R. Amyotrophic lateral sclerosis clinimetric scales guidelines for administration and scoring. *In: Herndon R, editor, Handbook of clinical neurologic scales, Demos Vermande.*, 67, 27-28, (1997).

442 . Hugel B. et al. Membrane microparticles: two sides of the coin. Physiology. *Physiology.*, 20, 22–27, (2005).

443. Baietti M.F. et al. Syndecan-syntenin-ALIX regulates the biogenesis of exosomes. *Nat Cell Biol.*, 14, 677–685, (2012).

444. Ayers L. et al. Measurement of circulating cell-derived micropartcles by flow cytometry: sources of variability within the essay. *Thromb Res.*, 127, 4-89, (2011).

445. Lacroix R. et al. Standardization of platelet-derived microparticle enumeration by flow cytometry with calibrated beads: results of the International Society on Thrombosis and Haemostasis SSC Collaborative workshop. *J Thromb Haemost.*, 8, 2571-4, (2010).

446. Hein B. et al. Stimulated emission depletion (STED) nanoscopy of a fluorescent protein-labeled organelle inside a living cell. *Proc Natl Acad Sci U S A.*,105, 14271–1427, (2008).

447. Shapiro HM. Practical flow cytometry. *New York: Wiley-Liss.*,56, 678-1234, (2003).

448. Kiessling, V. et al. Domain coupling in asymmetric lipid bilayers. *Biochim Biophys Acta.*, 1788, 64–71, (2009).

449 . Boersma H.H. et al. Past, present, and future of annexin A5: From protein discovery to clinical applications. *J Nucl Med.*, 46, 2035–2050, (2005).

450. Van Engeland M. et al. Annexin V-affinity assay: A review on an apoptosis detection system based on phosphatidylserine exposure.*Cytometry.*, 31, 1–9, (1998).

451. Schellenberger E.A. et al. Optimal modification of annexin V with fluorescent dyes. *Chembiochem.*, 5, 271–274, (2004).

452 . Connor D. E. et al. The majority of circulating platelet-derived microparticles fail to bind annexin V, lack phospholipid-dependent procoagulant activity and demonstrate greater expression of glycoprotein Ib. *Thromb Haemost.*, 5, 1044–1052, (2010).

453. Nardo G. et al. Amyotrophic lateral sclerosis multiprotein biomarkers in peripheral blood mononuclear cells. *PLoS One.*, 6, 255-45, (2011).

454 . Henkel J. S. et al. Regulatory T-lymphocytes mediate amyotrophic lateral sclerosis progression and survival. *EMBO Mol Med.*, 5, 64–79, (2013).

455. Lu C. H. et al. Neurofilament light chain as a prognostic biomarker in amyotrophic lateral sclerosis. *Neurology.*, 84, 2247-2257, (2015).

456. Munch C. et al. Prion-like propagation of mutant superoxide dismutase-1 misfolding in neuronal cells. *Proc Natl Acad Sci U S A.*, 108, 3548–3553, (2011).

457. Montecalvo A. et al. Mechanism of transfer of functional microRNAs between mouse dendritic cells via exosomes. *Blood.*,119, 75-666, (2012).

458. Silverman J. M. et al. Disease Mechanisms in ALS: Misfolded SOD1 Transferred Through Exosome-Dependent and Exosome-Independent Pathways. *Cell Mol Neurobiol.*,3, 377-81, (2016).

459. Liu, H. et al. Targeting of Monomer-Misfolded SOD1 as a Therapeutic Strategy for Amyotrophic Lateral Sclerosis. *J Neurosci.,* 32, 8791–8799, (2012).

460. Zhang Y. J. et al. Aberrant cleavage of TDP-43 enhances aggregation and cellular toxicity. *Proc Natl Acad Sci U S A.,* 5, 106-1234, (2009).

461. Rakhit, R. et al. Monomeric Cu, Zn-superoxide Dismutase Is a Common Misfolding Familial Amyotrophic Lateral Sclerosis. *J Biol Chem.,* 279, 15499–15504, (2004).

462. Zhang R.. et al. MCP-1 chemokine receptor CCR2 is decreased on circulating monocytes in sporadic amyotrophic lateral sclerosis (sALS). *Journal of Neuroimmunology.*,7,87–93, (2006).

463. Zhang, R. et al. Circulating endotoxin and systemic immune activation in sporadic Amyotrophic Lateral Sclerosis (sALS). *Journal of Neuroimmunology.,* 6, 121–124, (2009).

464.Münch C. et al. 3-Prion-like propagation of mutant superoxide dismutase-1 misfolding in neuronal cells. *Pnas.,* 108, 3548–3553, (2014).

465- Leslie I. et al. Intercellular propagated misfolding of wild-type Cu/Zn superoxide dismutase occurs via exosome-dependent and -independent mechanisms.*Pnas.,* 11,3620–3625, (2014).

466. Swarup D. et al. Deregulation of TDP- 43 in amyotrophic lateral sclerosis triggers nuclear factor Bmediated pathogenic pathways.*The Journal of Experimental Medicine.,* 208, 2429–2447, (2011).

467. McCombe P. A and Henderson R.D. The Role of Immune and Inflammatory Mechanisms in ALS. *Molecular Medicine.*,11,1566-5240,(2011)

468. Huang X. et al. CD4+ T cells in the pathobiology of neurodegenerative disorders.*Journal of Neuroimmunology.,* 211, 3–15, (2009).

-469. Beers D. R. et al. CD4+ T cells support glial neuroprotection, slow disease progression, and modify glial morphology in an animal model of inherited ALS. *Proceedings of the National Academy of Sciences of the United States of America.,* 105, 15558–15563, (2008).

470 . Beers D. R. et al. Neuroinflammation modulates distinct regional and temporal clinical responses in ALS mice. *Brain, Behavior, and Immunity.,* 25, 1025–1035, (2011).

471. .Henkel J. S. et al. Microgliain ALS: the good, the bad, and the resting.*Journal of Neuroimmune Pharmacology.*,4, 389–398, (2009).

472 . Beers D. R. et al. Endogenous regulatory T lymphocytes ameliorate amyotrophic lateral sclerosis in mice and correlate with disease progression in patients with amyotrophic lateral sclerosis. *Brain.,* 134, 1293–1314, (2011).

473. Wolfers J. et al. Tumor-derived exosomes are a source of shared tumor rejection antigens for CTL cross-priming. *Nat. Med.*,7, 297–303,(2001).

474. Hsu D. H. et al. Exosomes as a tumor vaccine: enhancing potency through direct loading of antigenic peptides. *J. Immunother.*, 32, 26440–450, (2003).

475. Utsugi-Kobukai S. et al. MHC class I-mediated exogenous antigen presentation by exosomes secreted from immature and mature bone marrow derived dendritic cells. *Immunol. Lett.*, 89, 125–131, (2003).

476. Andreola G. et al. Induction of lymphocyte apoptosis by tumor cell secretion of FasL-bearing microvesicles. J. Exp. Med., 195, 1303–1316, (2002).

477. Szajnik M. et al. Tumor-derived microvesicles induce, expand and up-regulate biological activities of human regulatory T cells (Treg). *PLoS ON.*, 5, 114-69, (2010).

478. Wieckowski E. U. et al. Tumor-derived microvesicles promote regulatory T cell expansion and induce apoptosis in tumor-reactive activated CD8+ T lymphocytes. *J. Immunol.*, 183, 3720–3730, (2009).